Electrochemical and Adsorption Studies of a Carboxylic Acid-modified Aluminium Aminoterephthalate Framework (H$_2$N-MIL-53) with Heterogeneous Catalysis Applications

A dissertation submitted in accordance with the requirements for the degree

Magister Scientiae

in the

Department of Chemistry

Faculty of Natural and Agricultural Sciences

at the

University of the Free State

by

Frederick Hermanus Peens

Supervisor

Dr. E.H.G. Langner

January 2014

Acknowledgements

It is my utmost pleasure to firstly thank God Almighty for the strength, wisdom, perseverance and an unrelenting passion for chemistry He bestows on me every day.

I would like to thank my supervisor, Dr. E.H.G. Langner, for his excellent guidance during this research project. His patients, love for chemistry and helpfulness inspired me every day. Thank you for your exceptional leadership and support as well as your catching enthusiasm towards science. I would also want to thank the head of our physical chemistry group, Prof. J.C. Swarts, for giving me the opportunity to advance my studies and the privilege to be able to work in a technologically advanced laboratory.

To all my friends and colleagues: thank you very much for your support during my studies and the joys we shared together. I also want to thank Dr. M. Rademeyer at the University of Pretoria for PXRD measurements.

I would like to thank my wife, Roné Peens, for her everlasting inspiration, love, joy and support she gave me throughout my studies. You picked me up when I was weak and kept me strong in times of need. I love you my dear.

My thanks go out to my family members especially to my mother, Saartjie Peens and my father, Hansie Peens for raising me with the correct values for life and making me proud to be their son.

Lastly, I would like to thank the National Research Foundation (NRF) for financial support and thus making it possible for me to live out my passion.

Table of Contents

Chapter 4   **89**

Experimental

Chapter 5

Conclusions and Future Perspectives

Appendix

Abstract

Opsomming

List of Abbreviations

MOF	Metal organic framework
MIL	Matériaux de l'Institut Lavoisier
-ht	High temperature
-lt	Low temperature
PSM	Post-synthetic modification
CVD	Chemical vapour deposition
IWI	Incipient wetness impregnation
-as	As-synthesised
-vac	Evacuated
FTIR	Fourier transform infrared spectroscopy
^{1}H NMR	Proton nuclear magnetic resonance spectroscopy
NaOD/D_2O	Deuterated sodium hydroxide in deuterium oxide
PXRD	Powder x-ray diffraction / diffractogram
TGA	Thermogravimetric analysis
wt%	Weight percentage
ASAP	Accelerated surface area and porosity
BET	Brunauer, Emmett and Teller
DFT	Density functional theory
p/p°	Relative pressure
CV	Cyclic voltammetry / voltammogram
i_{pa}	Peak anodic current
i_{pc}	Peak cathodic current
Cp	Cyclopentadienyl
E	Applied potential
$E^{0\prime}$	Formal reduction potential

LIST OF ABBREVIATIONS

E_{pa}	Peak anodic potential
E_{pc}	Peak cathodic potential
ΔE_p	Separation of peak anodic and peak cathodic potentials
Fc	Ferrocene
$[NBu_4][PF_6]$	Tetrabutylammonium hexafluorophosphate
DCM	Dichloromethane
DMF	Dimethylformamide
r.t.	Room temperature
TLC	Thin layer chromatography

1   **Introduction**

1.1 Metal Organic Frameworks

Research in material science is rapidly growing in order to supply the technological demands of the 21st century. Scientists are constantly pushing the frontiers looking for new materials in the establishment of sustainable developments, applications, catalysis, energy storage and healthcare. Porous materials, including metal organic frameworks (MOFs), are increasingly being investigated for application in these scientific advances. [1,2]

MOFs were first regarded as porous molecular sieves with highly regular pore sizes between 1 nm and 2 nm, but this was only the first sign which distinguished them from mesoporous silica materials and inorganic zeolites. Besides the fact that MOFs are porous, some of them have the ability to "breathe" on a nanoscale, due to the flexibility of their organic constituents. MOFs can be one dimensional (1D), two dimensional (2D) or three dimensional (3D) hybrid solids consisting of metal centres, interlinked by organic ligands, to form ordered network structures with high surface areas. With a large number of transition metals and an even longer list of organic linkers available, an almost inexhaustible array of MOFs can be synthesised.[3(a-d)]

MOFs can be chemically altered after the initial synthesis process, which is generally called post-synthetic modification (PSM), and is different to the silanation and cation exchange of zeolites. Even with mesoporous silicates, with their lack of crystallinity, it is difficult to control the surface distribution of the hydroxyls groups.[4] MOFs are crystalline and contain organic components with a high degree of chemical versatility. Chemical vapour deposition (CVD) and incipient wetness impregnation (IWI) are the two main pathways to introduce other molecules (e.g. solvents, reactants, drugs or catalysts) into the pores of a MOF. With these techniques, novel products can be created and is one of the reasons why the research outputs on porous coordination polymers and MOFs are increasing at an exponential rate. In addition to this, every MOF structure is unique, governed by the way the metal centres are connected to the organic linkers and also by the way the structure interacts with guest molecular species.[1,2] Guest molecules introduced to the MOF structure by methods like CVD or IWI can be physically or chemically bound to the structure, depending mainly on the purpose of the final product.

In this study, the MOF of choice is MIL-53 (**M**atériaux de l'**I**nstitut **L**avoisier).[5] The focus will be on the aluminium-containing MIL-53(Al) and its amine-functionalised analogue, amino-MIL-53(Al). MIL-53(Al) and amino-MIL-53(Al) are porous coordination polymers with 1D diamond-shaped channels and terephthalic and 2-aminoterephthalic acid as the respective organic linkers.[6,7] Both MIL-53(Al) and amino-MIL-53(Al) have flexible structures and depending on their host-guest interactions, their pores can expand or contract.[8] The effect of this "breathing" phenomenon (together with the long channels of the MIL-53 derivatives) is still poorly understood when concerned with the migration of guest species into the MOFs. This process needs to be investigated in order to maximise PSM yields. For PSM, the amine groups of amino-MIL-53(Al) provide great chemical versatility,[9] for which amidation is one of the preferred procedures due to an amide's high thermal stability[7] and ease of synthesis.

1.2 Aims of Study

With the above background in mind, the following goals are set for this study:

a) The synthesis of MIL-53(Al) and amino-MIL-53(Al) by hydrothermal and solvothermal methods, followed by characterisation using Fourier Transform Infrared (FTIR) spectroscopy, Powder X-ray Diffraction (PXRD) and Accelerated Surface Area and Porosity (ASAP) analysis.

b) The introduction of guest species (ferrocene as well as a series of alkyl carboxylic acids from formic acid to butyric acid) to MIL-53(Al) and amino-MIL-53(Al), either through a known chemical vapour deposition (CVD) method or a novel incipient wetness impregnation (IWI) method.

c) Investigate an adapted version of IWI in order to quantitatively control the PSM of amino-MIL-53(Al). This will be done by time-resolved intrusion studies on amino-MIL-53(Al) with butyric acid and ferrocenecarboxylic acid, followed by an amidation reaction after each intrusion. The extent of chemical bonding between amino-MIL-53(Al) and the intruded acid will be determined by a combination of Thermogravimetric Analysis (TGA) and Nuclear Magnetic Resonance (NMR) spectroscopy.

d) The electrochemical characterisation of the ferrocene-containing MIL-53(Al) and amino-MIL-53(Al) derivatives using Cyclic Voltammetry (CV). Since the MOFs are insoluble, a special technique will be employed to immobilise the active species on the electrode surface.

1.3 References

1   D. Farrusseng, in *Metal Organic Frameworks-Applications from Catalysis to Gas Storage*, Wiley-VCH Verlag GmbH and Co. KGaA, 2011, ch. 1-2, pp 3-45.

2   M. Schröder, in *Functional Metal Organic Frameworks: Gas Storage, Separation and Catalysis*, Springer-Verlag, Berlin Heidelberg, 2010, ch. 1, pp 1-33.

3   a) M. Eddaoudi, J. Kim, N. Rosi, D. Vodak, J. Wachter, M. O'Keeffe and O. M. Yaghi, *Science*, 2002, **295**, 469-472.

    b) H. K. Chae, D. Y. Siberio-Perez, J. Kim, Y. Go, M. Eddaoudi, A. J. Matzger, M. O'Keeffe and O. M. Yaghi, *Nature*, 2004, **427**, 523-527.

    c) G. Férey, C. Mellot-Draznieks, C. Serre, F. Millange, J. Dutour, S. Surblé and I. Margiolaki, *Science*, 2005, **309**, 2040-2042.

    d) G. Férey, *Chem. Soc. Rev.,* 2008, **37**, 191-214.

4   B. Bonelli, B. Onida, J. D. Chen, A. Galarneau, D. Di Renzo, F. Fajula, E. Garrone, *Micropor. Mesopor. Mater.*, 2004, **67**, 95-106.

5   S. J. Garibay, Z. Wang and S. M. Cohen, *Inorg. Chem*., 2010, **49**, 8086-8091.

6   T. Loiseau, C. Serre, C. Huguenard, G. Fink, F. Taulelle, M. Henry, T. Bataille and G. Férey *Chem. Eur. J.*, 2004, **10**, 1373-1382.

7   T. Ahnfeldt, D. Gunzelmann, T. Loiseau, D. Hirsemann, J. Senker, G. Férey and N. Stock, *Inorg. Chem*., 2009, **48**, 3057-3064.

8   A. U. Ortiz, A. Boutin, A. H. Fuchs and F. Coudert, *PRL*, 2012, **109**, 195502/1-195502/5.

9   P. Horcajada, C. Serre, G. Maurin, N. A. Ramsahye, F. Balas, M. Vallet-Regí, M. Sebban, F. Taulelle and G. Férey, *J. Am. Chem. Soc*., 2008, **130**, 6774-6790.

2   Literature Survey

2.1   Introduction.

Metal organic frameworks (MOFs) became increasingly popular in chemical research since the synthesis of MOF-5 in 1999[1], making it an interesting topic in modern material science. MOFs began to be of interest when more versatile micro- and mesoporous substitutes were needed for zeolites. With zeolites it is difficult to change and control the chemical nature of the internal surface area onto which a certain gas will adsorb. MOFs, on the other hand, make chemical versatility possible because of the vast number of different metal-organic combinations possible. By repeatedly bridging metal centres with organic linkers, it is possible to produce a permeable coordination polymer.

This study is mainly focused on the use of aluminium and terephthalic acid as the metal centre and organic linker respectively. Together they can form a number of different MOFs, solely depending on the synthesis conditions. One of these MOF's is MIL-53(Al) (aluminium terephthalate) and its amine-functionalised derivative, amino-MIL-53(Al) (aluminium 2-aminoterphthalate), which contains one amine group on all the aromatic rings.
The syntheses, characteristics and applications of MIL-53 and amino-MIL-53 will be discussed with emphasis on the post-synthetic modification of the amine groups inside the channels of amino-MIL-53(Al).

2.2   Aluminium Terephthalate (MIL-53(Al))

2.2.1 Synthesis of MIL-53

MIL-53 was first reported by Férey and co-workers in 2002 at the Institute Lavoisier in France (MIL = *Matériaux de l'Institut Lavoisier*). They isolated chromium based MIL-53 as a crystalline solid after a hydrothermal reaction between chromium nitrate and terephthalic acid under mild, autogenous pressure. A simplified reaction is shown in Figure 2.1 (p 6). The as-synthesised product (MIL-53(Cr)-as) contained unreacted terephthalic acid and was purified

through calcination at 300°C for 30 hours to give the activated product (MIL-53(Cr)-ht[†]) as a polycrystalline powder. Activated MIL-53 is highly hygroscopic after cooling to room temperature, giving a new phase after atmospheric water adsorption, (MIL-53(Cr)-lt[‡]). The framework showed structural flexibility in dimensions going from the as-synthesised state to the high temperature, activated state and then to the low temperature, activated state (Scheme 2.1, p 7). The Langmuir surface area of activated MIL-53, MIL-53(Cr)-ht is 1500 m^2g^{-1} and is larger than that of MIL-53(Cr)-lt which has a surface area of 1150 m^2g^{-1}.[2]
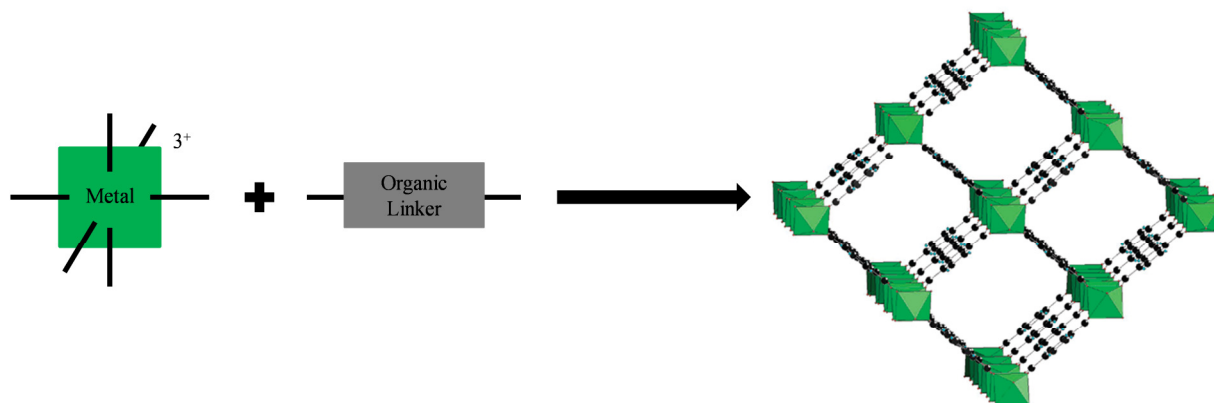

Figure 2.1:   Simplified reaction for the hydrothermal synthesis of MIL-53 with the use of a metal nitrate/chloride and terephthalic acid as the organic linker. Adapted with permission from S. Bauer, C. Serre, T. Devic, P. Horcajada, J. Marrot, G. Férey, N. Stock, *Inorg. Chem.*, 2008, **47**, 7568-7576. Copyright 2013 American Chemical Society.

Cleansing of the MOF's narrow channels was cumbersome, which led to an investigation to purify the structure after synthesis with solvents like acetone, ethanol and DMF. Sorption studies showed that the low temperature form of MIL-53 could not adsorb acetone and ethanol, but DMF was adsorbed, showing that MIL-53 has a strong affinity for DMF molecules.[3]

In 2004 Férey *et al.* produced aluminium based MIL-53 (MIL-53(Al)) from aluminium nitrate and terephthalic acid in a hydrothermal process at 220°C. The MOF is thermally stable up to 500°C and has a Langmuir surface area of 1510 m^2g^{-1}, which is in good agreement with the chromium derivative made previously.[2] MIL-53(Al) can also exist as one of three different forms (as-synthesised), narrow pore (lt) and large pore (ht) with a pore diameter of 8.5 Å for MIL-53(Al)ht.[4,5]

[†] ht = high temperature

[‡] lt = low temperature
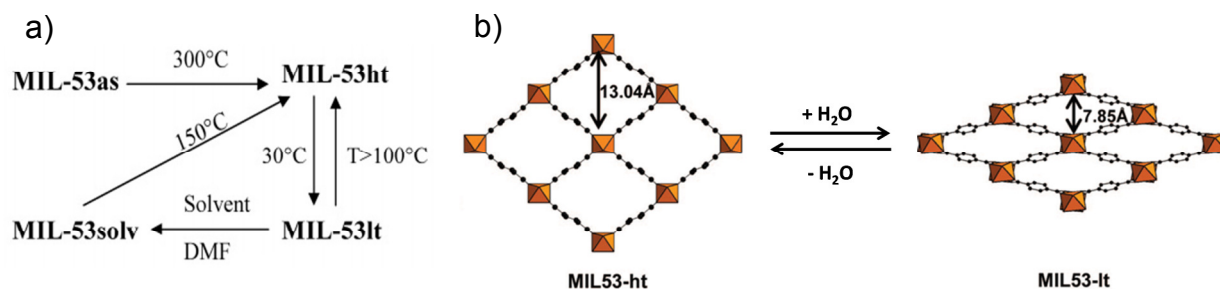
Scheme 2.1: A scheme for the hydration – dehydration (a) of MIL-53(Cr) as well as the adsorption of DMF.[3] The breathing ability (b) of MIL-53(Cr) as a cause of water adsorption during cooling, after activation. Adapted with permission from P. Horcajada, C. Serre, G. Maurin, N. A. Ramsahye, F. Balas, M. Vallet-Regí, M. Sebban, F. Taulelle and G. Férey, *J. Am. Chem. Soc.*, 2008, **130**, 6774-6790 and C. Serre, F. Millange, C. Thouvenot, M. Noguès, G. Marsolier, D. Louër and G. Férey, *J. Am. Chem. Soc.*, 2002, **124**, 13519-13526. Copyright 2013 American Chemical Society.

2.2.2 Structure of MIL-53

2.2.2.1 Structure Layout

In MIL-53, metals such as chromium[2,3] aluminium[4] and iron[6], form corner sharing octahedra with terephthalic acid linkers (Figure 2.2, p 8). The metal ions are bridged with oxygen atoms in the axial direction and form an almost linear chain. The metal ions are coordinated with the carboxylate ligands in the equatorial plane to form a diamond shaped framework with one-dimensional channels.[2,4]
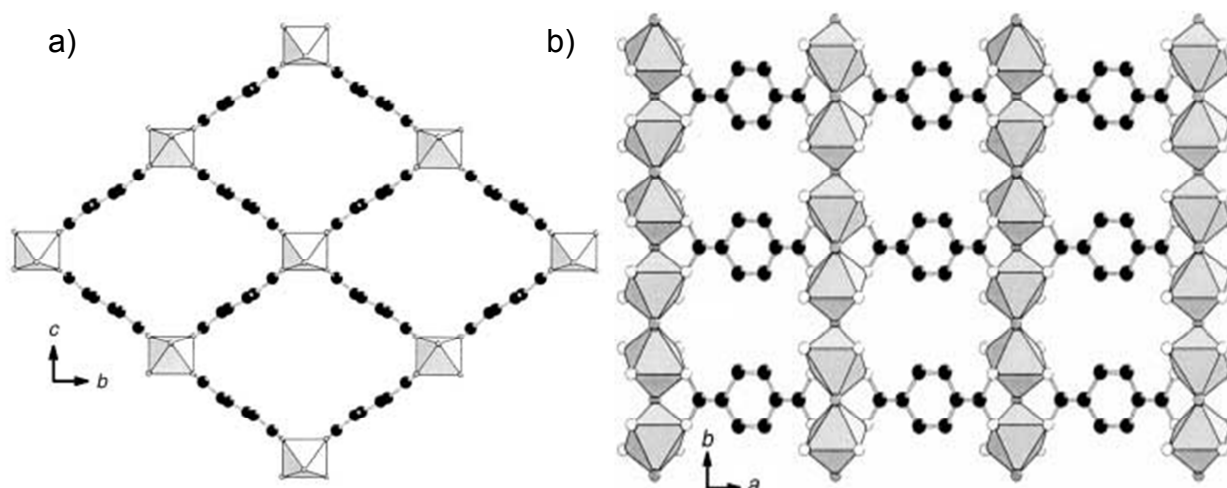
Figure 2.2: Structural representation of MIL-53(Al)-ht (Al(OH)[O_2C-C_6H_4-CO_2]) showing the open pores with diamond-shaped channels (a). The AlO$_4$(OH$_2$) octahedra are shown to line up down the axial position (b). Adapted from T. Loiseau, C. Serre, C. Huguenard, G. Fink, F. Taulelle, M. Henry, T. Bataille and G. Férey *Chem. Eur. J.*, 2004, **10**, 1373-1382 with permission of The Royal Society of Chemistry.

The large breathing ability of the MIL-53 analogues was shown by MIL-53(Cr)-as (Scheme 2.1 (b), p 7). Its pore size increased from 12.18 Å to 13.04 Å during the removal of uncoordinated terephthalic acid at 300°C, but as is cools down, hydration occurs and the structure shrinks dramatically to 7.85 Å. Upon cooling, hydrogen bonds between the carboxyl oxygen atoms and adsorbed water molecules forced the diameter of the pores to decrease to 7.85 Å, giving more than 5 Å in flexibility.[3] This flexibility is one of the special abilities of MOFs, distinguishing them from zeolites which have rigid structures.[7]

2.2.2.2 Fourier Transform Infrared Spectroscopy (FTIR)

Fourier transform infrared spectroscopy is an efficient way to characterise MOFs containing carbonyl groups, since results are easily obtained stepwise or *in situ*. Férey *et al.* used FTIR as a characterisation method to show the differences between the as-synthesised MIL-53(Al)-as and the calcined form, MIL-53(Al)-lt Figure 2.3 (p 9). Unreacted terephthalic acid in MIL-53(Al)-as shows a clear stretching frequency at 1669 cm^{-1} for the carbonyl group, as well as a sharp and broad peak around 3500 cm^{-1}, indicating the presence of water and OH groups from the free acid. In MIL-53(Al)-lt, free terephthalic acid is absent and the hydration during cooling is

confirmed by the bending and stretching frequencies at 1632 cm^{-1} and 3500-3600 cm^{-1} respectively (Figure 2.3 (b), p 9).[4]

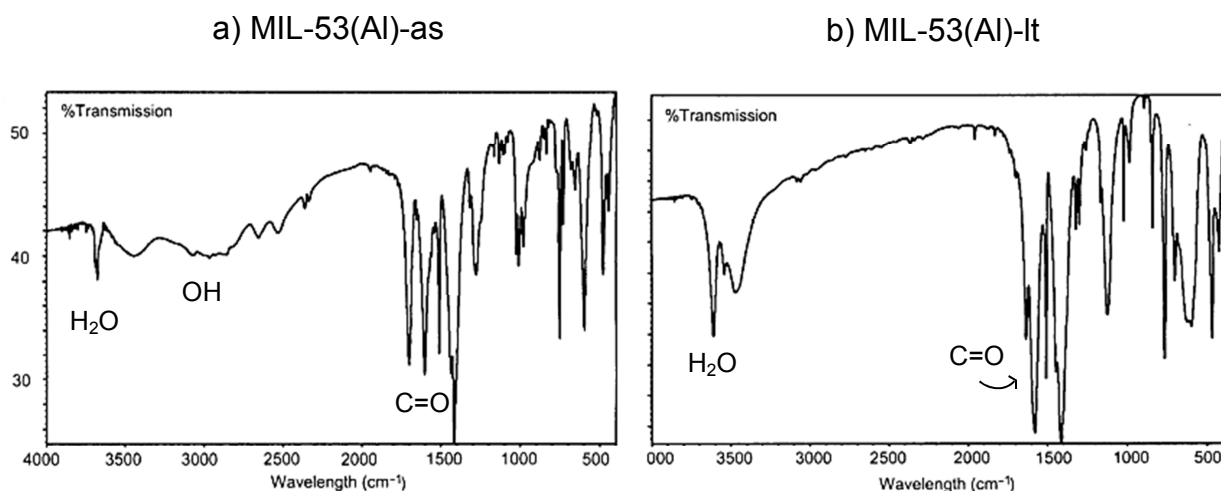### a) MIL-53(Al)-as   b) MIL-53(Al)-lt

Figure 2.3:   Fourier transform infrared spectroscopy of MIL-53(Al)-as (a) and MIL-53(Al)-lt (b). A clear difference is seen in the adsorbed water at 3000 cm^{-1} between the as-synthesised and the activated form.   Adapted from T. Loiseau, C. Serre, C. Huguenard, G. Fink, F. Taulelle, M. Henry, T. Bataille and G. Férey *Chem. Eur. J.*, 2004, **10**, 1373-1382 with permission of The Royal Society of Chemistry.

2.2.2.3 Thermogravimetric Analysis (TGA)

Férey *et al.* showed that the thermal stability of MIL-53(Al) is quite remarkable for its class. In Figure 2.4 (a) (p 10), it can be seen that the free unreacted terephthalic acid is leaving the channels of MIL-53(Al)-as between 275°C and 420°C in two stages: a loss of 0.37 equivalents (19%) up to 300°C followed by a loss of 0.33 equivalents (17%). After a 7% water loss between 25°C and 100°C, MIL-53(Al)-lt is thermally stable up to 500°C in air (this class of MOFs are usually stable up to 400°C) before the organic linkers start to separate from the metal centres, leaving only Al$_2$O$_3$ (Figure 2.4 (b), p 10). MIL-53(Al) has a thermal stability of 150°C higher than that of the chromium[3] and vanadium[8] analogues.[4]
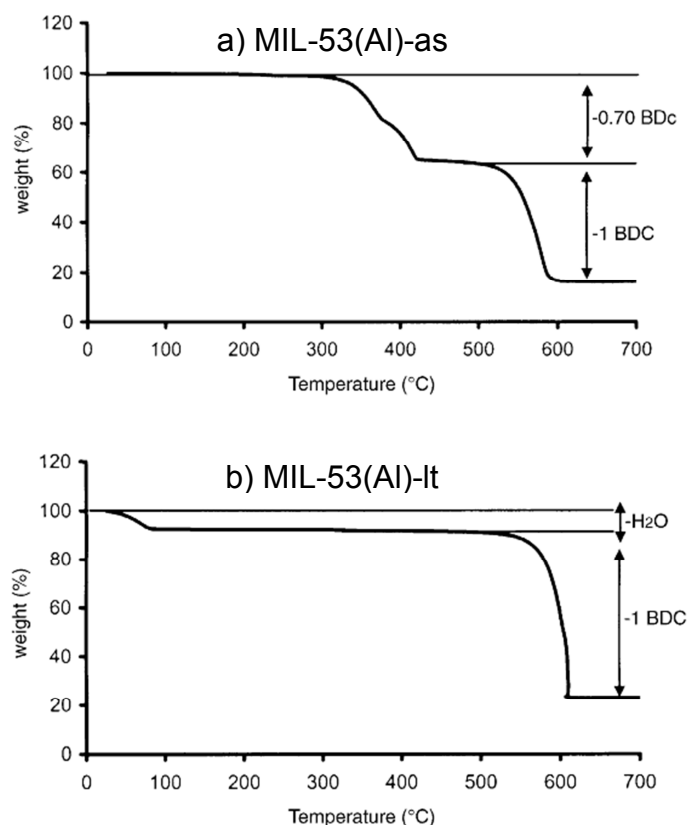
Figure 2.4: TGA in air of a) MIL-53(Al)-as and b) MIL-53(Al)-lt.[4] BDc = benzenedicarboxylic acid and BDC = benzenedicarboxylate. Adapted from T. Loiseau, C. Serre, C. Huguenard, G. Fink, F. Taulelle, M. Henry, T. Bataille and G. Férey *Chem. Eur. J*., 2004, **10**, 1373-1382 with permission of The Royal Society of Chemistry.

2.2.2.4 Magic Angle Spinning (MAS) – Nuclear Magnetic Resonance (NMR) Spectroscopy

Due to the general insolubility of MOFs, solid state NMR has to be used for characterisation. Figure 2.5 (p 11), displays the ^{1}H MAS NMR of MIL-53(Al)-lt, MIL-53(Al)-ht and MIL-53(Al)-as, as reported by Férey *et al*.[4] The ^{1}H spectrum displays three signals at 2.9, 7.2 and 12.5 ppm which can be assigned to the metal-bridging hydroxides, phenyl and carboxylic acid protons respectively.[4]

Figure 2.5:   ^{1}H MAS NMR of MIL-53(Al)-lt, MIL-53(Al)-ht and MIL-53(Al)-as. Figure style was changed. Adapted from T. Loiseau, C. Serre, C. Huguenard, G. Fink, F. Taulelle, M. Henry, T. Bataille and G. Férey *Chem. Eur. J.*, 2004, **10**, 1373-1382 with permission of The Royal Society of Chemistry.
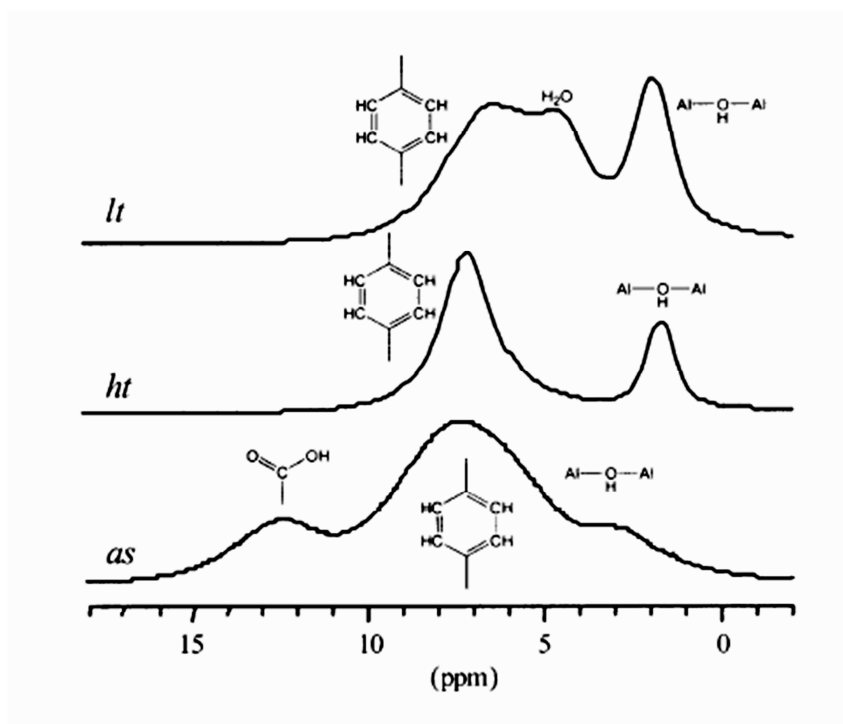
Through solid state NMR, it was proven that hydrogen bonding occurred between the carboxylate groups and atmospheric water vapour, but no bonding occurred to the oxygen atoms bridging the aluminium atoms.[4]

2.2.2.5 Accelerated Surface Area and Porosity (ASAP) Analysis

MIL-53(Al)-lt displays a type I isotherm, typical for microporous materials (Figure 2.6 (a), p 12). As reported by Férey *et al.,* the MOF does not show any hysteresis during desorption, giving a BET surface area of 1140(39) m^2g^{-1} and a Langmuir surface area of 1590(1) m^2g^{-1}, using nitrogen adsorption-desorption isotherms at 77 K.[4] A gas adsorption study at 303 K on MIL-53(Al) using gases like methane, carbon dioxide, carbon monoxide, oxygen, nitrogen and argon (Figure 2.6 (b), p 12) showed that the absolute adsorption ability of this MOF was found to be $CO_2 > CH_4 > CO > N_2 > Ar > O_2$, proving the high affinity of MIL-53(Al) for carbon dioxide. Since the adsorption of CO_2 is so highly selective for this MOF, as well as having a low heat of adsorption (26.4 kJ mol^{-1} for CO_2), it can be separated from gas mixtures.[9]

During the physisorption of gases such as CO_2, the MOF's structure transforms from the large pore form (just after thermal evacuation) to the narrow pore form. Afterwards, it goes back to the large pore form, if the partial pressure is high enough.[10]

a)   b)
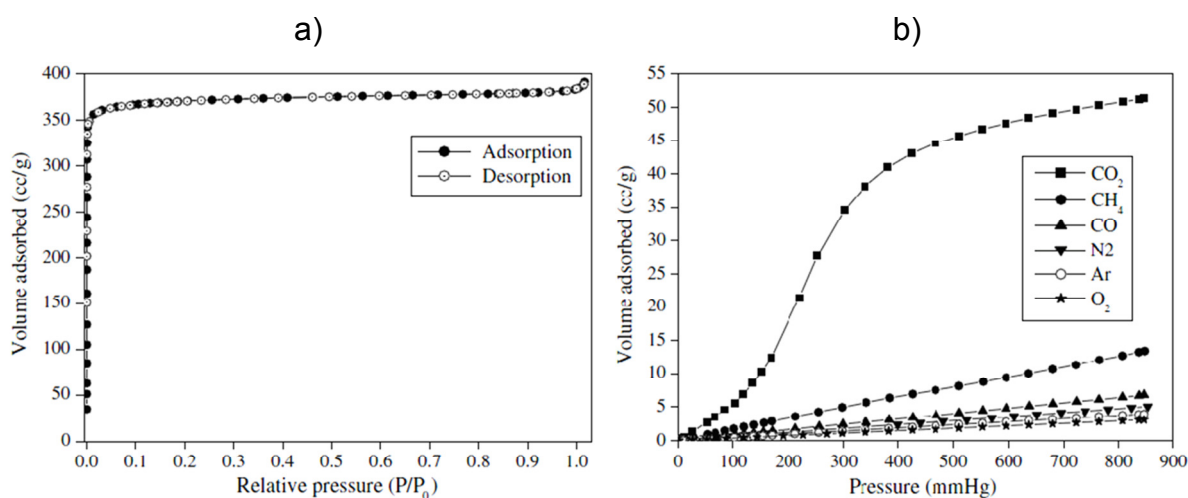
Figure 2.6:   The N_2 adsortion and desorption isotherms of MIL-53(Al)-ht at 77 K (a) and the adsorption isotherms of six different gases in MIL-53(Al)-ht at 303 K (b). Adapted from P. Rallapalli, K. P. Prasanth, D. Patil, R. S. Somani, R. V. Jasra and H. C. Bajaj, *J. Porous. Mater.*, 2011, **18**, 205-210 with permission of Springer.

2.2.2.6 Powder X-ray Diffraction (PXRD)

Suitable single crystals for MIL-53(Al) cannot be obtained, thus making powder X-ray diffraction an appropriate method for structure and phase determination of the MOF in its different thermal and experimental stages. In 2004, Loiseau *et al.* characterised MIL-53(Al) with PXRD, based on the chromium analogue synthesised by Millange *et al* [2], and was able to obtain the crystal data of the three different forms of the MOF with the help of Rietveld refinement. The three different chemical formulas are as follows: a) MIL-53(Al)-as: $Al(OH)[O_2C-C_6H_4-CO_2]\cdot[HO_2C-C_6H_4-CO_2H]_{0.70}$,   b)   MIL-53(Al)-lt: $Al(OH)[O_2C-C_6H_4-CO_2]\cdot H_2O$ and c) MIL-53(Al)-ht: $Al(OH)[O_2C-C_6H_4-CO_2]$.[4]
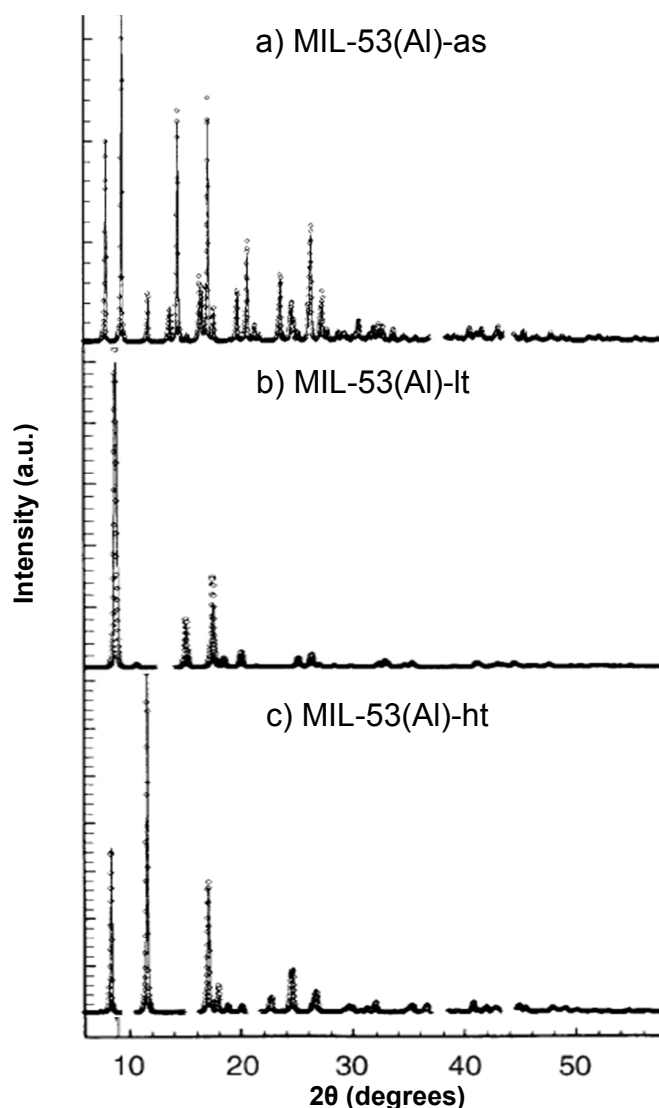
Figure 2.7:   Powder X-ray diffractograms of a) MIL-53(Al)-as, b) MIL-53(Al)-lt and c) MIL-53(Al)-ht.   Figure style was changed.   Adapted from T. Loiseau, C. Serre, C. Huguenard, G. Fink, F. Taulelle, M. Henry, T. Bataille and G. Férey *Chem. Eur. J.*, 2004, **10**, 1373-1382 with permission of The Royal Society of Chemistry.

2.3   Amino-MIL-53(Al)

2.3.1 Synthesis of Amino-MIL-53

In 2008, Arstad *et al.* synthesised a MOF, USO-1-Al-A, analogous to MIL-53(Al), but only with amine groups on the benzene rings.   They showed that these amine-functionalised MOFs have better CO_2 adsorption than their unfunctionalised analogues.[11]   Using the isosteric method introduced by Rouquerol *et al.* in 1999,[12] the differential heat of adsorption of CO_2 was calculated to be 50 kJ mol^{-1} for USO-1-Al-A which was 20 kJ mol^{-1} higher than for the

unfunctionalised analogue, due to stronger van der Waals interactions with the amine groups as the CO_2 molecules intrude into the MOF channels.[11]

Tim Ahnfeldt and co-workers synthesised the same amine-functionalised structure, amino-MIL-53(Al), in 2009, but were able to characterise it with better clarity than Arstad *et al.* Of three different Al-containing reagents, $Al(NO_3)_3 \cdot 9H_2O$, $AlCl_3 \cdot 6H_2O$ and $Al(ClO_4)_3 \cdot 9H_2O$ tested, $AlCl_3 \cdot 6H_2O$ was most suitable for the synthesis. After testing solvents such as DMF, H_2O, MeOH and CH_3CN, water proved to be the best. With a molar ratio of 1:1 for Al^{3+} and aminoterephthalic acid at 150 °C, the reaction may run for 5 hours under autogeneous pressure to deliver amino-MIL-53(Al) which can then be filtered and washed with water to give the as-synthesised form of the MOF.[13]

Despite many attempts, using high-throughput technology and research, it is still a challenge to fully understand how the framework is assembled, seeing that product formation is influenced by aspects like the reaction temperature, different solvents and ratios, reactant molar ratios, pH, and reaction time. Kapteijn *et al.* performed a study on the crystallisation of amino-MIL-53(Al) and amino-MIL-101-(Al) with the use of *in situ*, small angle and wide angle X-ray scattering techniques. By varying the solvent volume ratio between DMF and water, the crystallisation of amino-MIL-53(Al) can be controlled. The key here is the dissolution of the 2-aminoterephthalic acid linker unit which dissolves very poorly in water and results in amino-MIL-101(Al) formation. They found that when a solvent ratio of DMF:water = 1:9 is used, a three-fold increase in yield of amino-MIL-53(Al) is obtained when compared to pure water. The presence of water in this solvothermal reaction also ensures the formation of amino-MIL-53(Al).[14]

During initial PXRD and TG analyses it was found that thermal evacuation alone was not sufficient for the removal of free 2-aminoterephthalic acid captured inside the structure's channels. Thus, the MOF was first dispersed in DMF in an autoclave and heated to 150°C, followed by thermal evacuation at 130°C to give amino-MIL-53(Al)-lt upon cooling. The framework showed slightly lower thermal stability (up to 450°C) than MIL-53(Al) (up to 500°C) while the amine groups had no effect on the flexibility and breathing behaviour of the MOF, compared to MIL-53(Al).[13]

After evacuation, the active sites inside the channels of amino-MIL-53(Al) are now ready for post-synthetic modification (PSM), e.g. by reacting the amine functionalities with formic acid.[13] A more detailed discussion about PSM follows in section 2.4, p 22.

2.3.2 Structure of Amino-MIL-53(Al)

2.3.2.1 Structure Layout

Amino-MIL-53(Al) has a similar framework structure to unfunctionalised MIL-53(Al) (Figure 2.8, p 15). It consists of $[AlO_4(\mu\text{-}OH)_2]$ corner-sharing octahedra, interconnected by 2-aminoterephthalate anions to complete the framework. Hydroxyl groups form the bridging ligands between the organic linkers and the metal nodes, resulting in a porous coordination polymer with one-dimensional channels. The amine groups may facilitate post-synthetic modification of the framework structure. [4,13,15]

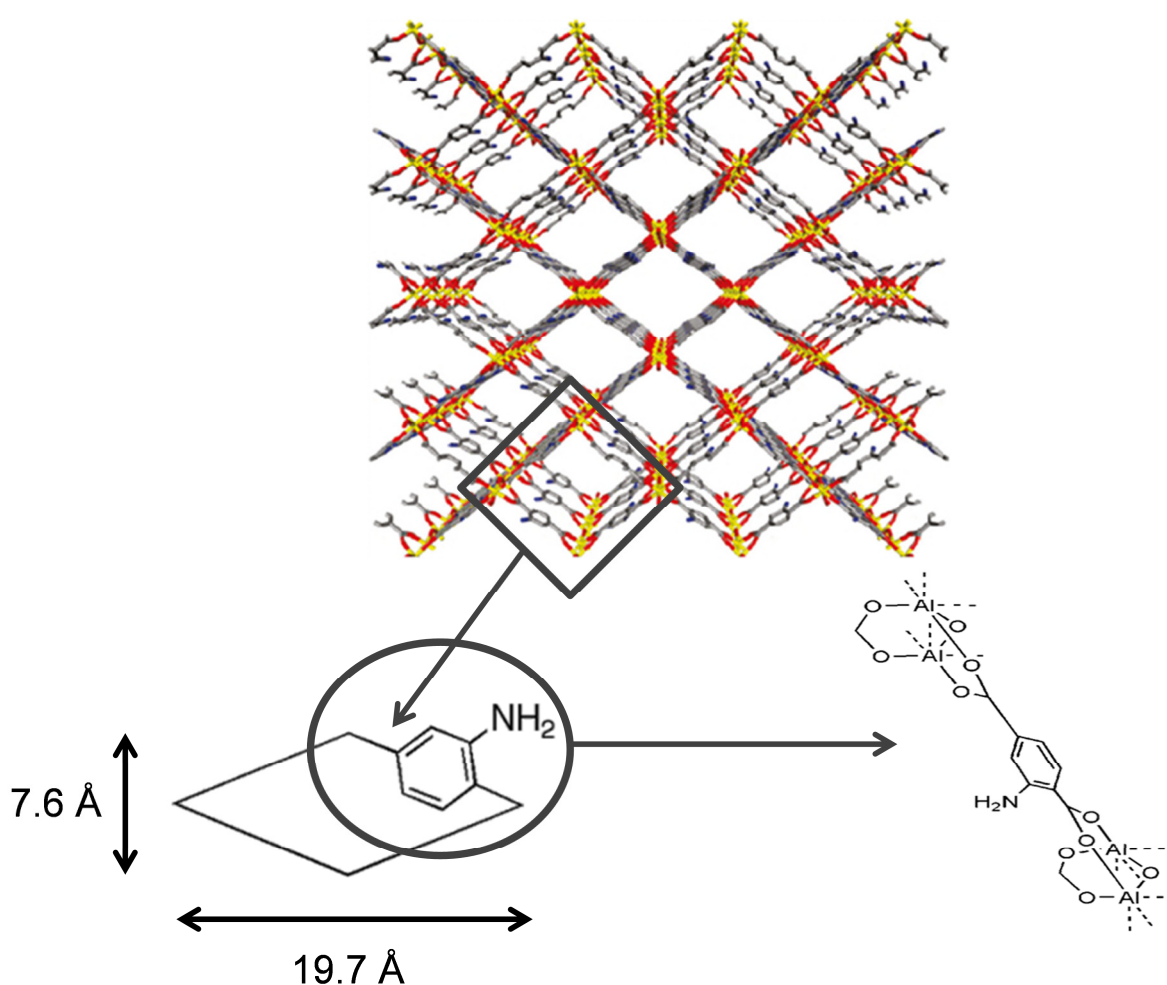Figure 2.8: Framework structure of amino-MIL-53(Al). The diamond shaped channels of the MOF as well as the bidendate coordination of the 2-aminoterephthalate towards the Al^{3+} metal centres are shown. Unit dimension are that of amino-MIL-53(Al)-lt. Adapted with permission from S. J. Garibay, Z. Wang and S. M. Cohen, *Inorg. Chem.*, 2010, **49**, 8086-8091. Copyright 2013 American Chemical Society.

2.3.2.2 Infrared Spectroscopy (IR)

Infrared spectroscopy provides critical data in terms of the residual starting material and solvents in the MOF structure by following every stage during the synthesis procedure. The most important phase of amino-MIL-53(Al) is the low temperature (lt) phase to which the MOF returns after activation. Stock *et al.* reported that the free 2-aminoterephthalic acid in the MOF channels may not be removed simply by thermal activation, but that the MOF has to be re-dispersed in DMF first to dissolve the free acid in the pores. Figure 2.9 (p 17), displays the infrared spectra of the three different stages after synthesis, starting with amino-MIL-53(Al)-as (a) then amino-MIL-53(Al)-DMF (b) and finally amino-MIL-53(Al)-lt (c). For amino-MIL-53(Al)-lt, the C-N vibrations, found at 1338 cm^{-1} and 1261 cm^{-1}, correlate with that of amino-MIL-53(Al)-DMF (Figure 2.9 (b), p 17). The N-H_2 vibrations are found as a doublet at 3497 cm^{-1} and 3385 cm^{-1}. The small peak at 3656 cm^{-1} as well as the broad signal between 2500 cm^{-1} and 3000 cm^{-1} is due to the bridging O-H groups. In the fingerprint areas of the IR spectra between 1200 cm^{-1} and 1700 cm^{-1}, the typical vibrational bands of the carbonyl groups are most prominent.

In Figure 2.9 (a) (p 17), it can be seen that the asymmetric stretching frequencies of the carbonyl groups bound to the aluminium metals, are found at 1583 cm^{-1} and 1497 cm^{-1} while their symmetric stretching frequencies are found lower at 1438 cm^{-1} and 1400 cm^{-1}.[4] Free amino-terephthalic acid inside amino-MIL-53(Al)-as has a carbonyl stretching frequency at 1687 cm^{-1}. This peak is absent in amino-MIL-53(Al)-DMF and a new peak appears at 1670 cm^{-1}, correlating to the carbonyl stretching of DMF (Figure 2.9 (b), p 17). With amino-MIL-53(Al)-lt, the DMF and unreacted acid peaks are absent, showing an evacuated framework (Figure 2.9 (c), 17).[13]
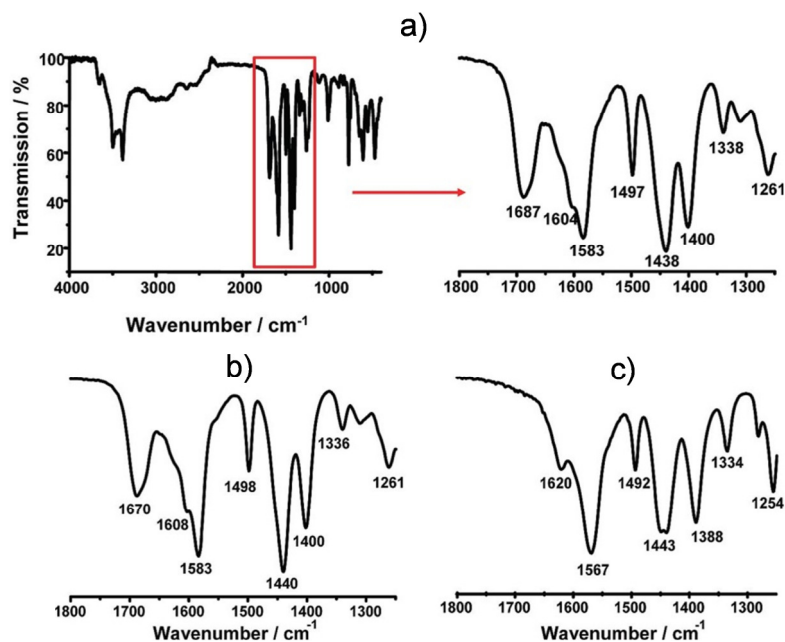
Figure 2.9:   IR spectra of amino-MIL-53(Al)-as (a), amino-MIL-53(Al)-DMF (b) and amino-MIL-53(Al)-lt-(c). Adapted with permission from T. Ahnfeldt, D. Gunzelmann, T. Loiseau, D. Hirsemann, J. Senker, G. Férey and N. Stock, *Inorg. Chem*., 2009, **48**, 3057-3064. Copyright 2013 American Chemical Society.

2.3.2.3 Thermogravimetric Analysis

Thermogravimetric analyses of MOFs are mainly used to determine the thermal stability of the MOF. Figure 2.10 (p 18), shows the different stages in activation after synthesis: a) amino-MIL-53(Al)-as: free 2-aminoterephthalic acid is released from 220°C. The acid loss amounts up to 20% of the structure's weight or 0.3 moles per formula unit of the MOF.

b) With amino-MIL-53(Al)-DMF, DMF molecules are released up to 320°C, giving a mass loss of 23% or 0.95 equivalents.

c) Water is released from amino-MIL-53(Al)-lt at about 100°C. The thermal stability of the MOF compare well in all three stages giving structural decomposition from about 400°C, with the breakdown of the metal-organic bonds and the release of remnants of the organic linkers, leaving alumina (Al_2O_3) behind.[13]
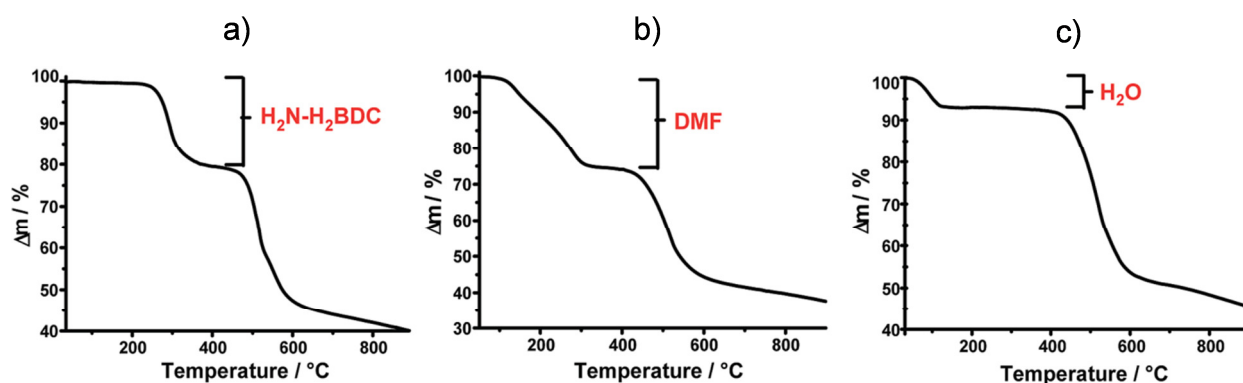
Figure 2.10   TGA of amino-MIL-53(Al)-as (a), amino-MIL-53(Al)-DMF (b) and amino-MIL-53(Al)-lt (c).   BDC = benzenedicarboxylate   Adapted with permission from T. Ahnfeldt, D. Gunzelmann, T. Loiseau, D. Hirsemann, J. Senker, G. Férey and N. Stock, *Inorg. Chem.*, 2009, **48**, 3057-3064.   Copyright 2013 American Chemical Society.

2.3.2.4 MAS-NMR

Stock *et al.* characterised amino-MIL-53(Al) also with solid state MAS NMR (^{1}H and ^{15}N) (Figure 2.11, p 19).   The ^{1}H spectra (i): with amino-MIL-53(Al)-as (a), three peaks are of importance: the bridging hydroxide groups at 2.3 ppm, the phenyl protons at 6.4 ppm and the carbonyl protons from the unreacted 2-aminoterephthalic acid at 12.2 ppm.   Amino-MIL-53(Al)-DMF (b) also displays three peaks: the DMF methyl protons at 1.5 ppm, obscuring the bridging hydroxide groups at 2.3 ppm and again the aromatic protons at 7.3 ppm.   Since DMF replaced the unreacted acid inside the channels of the framework, the acid's peak is not observed. Amino-MIL-53(Al)-lt (c) displays peaks at 2.6, 4.5 and 6.4 ppm which can be assigned to the bridging hydroxide groups, adsorbed water (upon cooling to room temperature) and the aromatic protons respectively.[13]   The ^{15}N spectra (ii) show the nitrogen peak (-NH$_2$) between -300 and -325 ppm for all three synthesis stages, as well as the peak for the DMF nitrogen in (b) at -270 ppm.
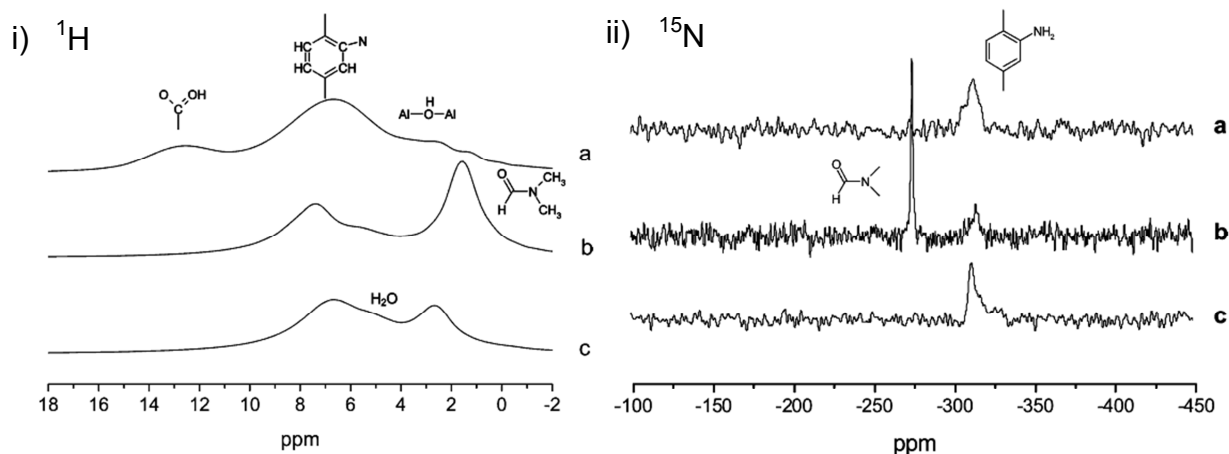
Figure 2.11: ^{1}H (i) and ^{15}N (ii) MAS NMRs of amino-MIL-53(Al)-as (a), amino-MIL-53(Al)-DMF (b) and amino-MIL-53(Al)-lt (c) respectively. Adapted with permission from T. Ahnfeldt, D. Gunzelmann, T. Loiseau, D. Hirsemann, J. Senker, G. Férey and N. Stock, *Inorg. Chem.*, 2009, **48**, 3057-3064. Copyright 2013 American Chemical Society.

2.3.2.5 Physisorption Analysis

Due to the breathing behaviour or flexibility of amino-MIL-53(Al), sorption studies, especially with nitrogen as the adsorbent, becomes challenging. Stock *et al.* found a prominent hysteresis between repeated adsorption and desorption of nitrogen-sorption studies (Figure 2.12, p 20). Amino-MIL-53(Al)-lt was heated under vacuum for 3 hours at 130°C before each analysis. This procedure was run four times and an increase in adsorption was found after every run. The effect of the hysteresis became less prominent after the third analysis.[13]

Gascon *et al.* measured the BET surface area and micropore volume of amino-MIL-53(Al) to be 675 m^2g^{-1} and 0.22 cm^3g^{-1} respectively. This specific measurements was performed on amino-MIL-53(Al) which was synthesised with the use of DMF as the only solvent and $Al(NO_3)_3 \cdot 9H_2O$ as the metal salt.[16] These values were improved by Guo *et al.* who achieved a BET surface area of 1882 m^2g^{-1} and a micropore volume of 0.83 cm^3g^{-1}. This was achieved by the use of $AlCl_3 \cdot 6H_2O$ as the metal salt and a mixture of water and DMF as the solvent.[17]

Amino-MIL-53(Al) has a high affinity towards carbon dioxide.[18] This is due to the free standing amino groups and open metal sites throughout the MOF structure which providing areas for CO_2 molecules to latch onto. Amino-MIL-53(Al) adsorption capabilities was also tested with various other gasses such as CO, H_2, and CH_4, and in all cases their adsorption was lower than that of

CO_2 (Figure 2.13, p 20).[19] This makes amino-MIL-53(Al) a highly capable CO_2 separator which can be of aid in the rising search for materials that can sequestrate CO_2 from polluting gas mixtures.[10,20]
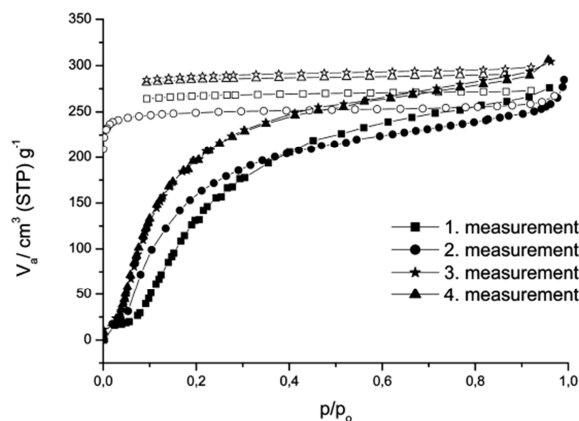

Figure 2.12: N_2 sorption isotherms of amino-MIL-53(Al) at 77 K. Black symbols denote adsorption while empty symbols denote desorption. Four consecutive adsorption-desorption cycles were performed. Adapted with permission from T. Ahnfeldt, D. Gunzelmann, T. Loiseau, D. Hirsemann, J. Senker, G. Férey and N. Stock, *Inorg. Chem.*, 2009, **48**, 3057-3064. Copyright 2013 American Chemical Society.
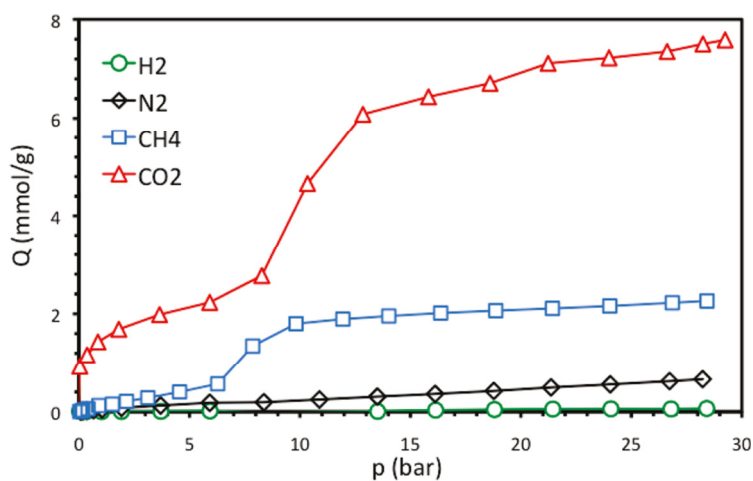

Figure 2.13: High pressure adsorption isotherms of H_2, N_2, CH_4 and CO_2 performed on amino-MIL-53(Al) showing the highest affinity towards CO_2. Adapted with permission from E. Stavitski, E. Pidko, S. Couck, T. Remy, E. Hensen, B. Weckhuysen, J. F. M. Denayer, J. Gascon and F. Kapteijn, *Langmuir*, 2011, **27**, 3970-3976. Copyright 2013 American Chemical Society.

20

Amino-MIL-53(Al) was first thought to have the same breathing capabilities as the non-functionalised MIL-53(Al). Results found by Gascon *et al.* showed that this is indeed the opposite: amino-MIL-53(Al) behaves more like its iron analogue, MIL-53(Fe). After activation it stays in the narrow pore phase and only move to a large pore phase when the partial pressure of the adsorbent is high enough.[21,19] This is due to the amine groups forming strong hydrogen bonds with the u_2-hydroxo groups situated at the metal nodes. This also enables amino-MIL-53(Al) to behave like an optical switch.[22]

2.3.2.6 Powder X-Ray Diffraction

Ahnfeldt *et al.* compared the PXRD scans of amino-MIL-53(Al) and MIL-53(Al) and saw that the amine groups changed the structure very little (Figure 2.14, p 21) resulting in an orthorhombic system. After dissolution of the internal free acid with DMF (amino-MIL-53(Al)-DMF), the structure stayed the same and only changed to a monoclinic system after thermal evacuation (amino-MIL-53(Al)-lt).
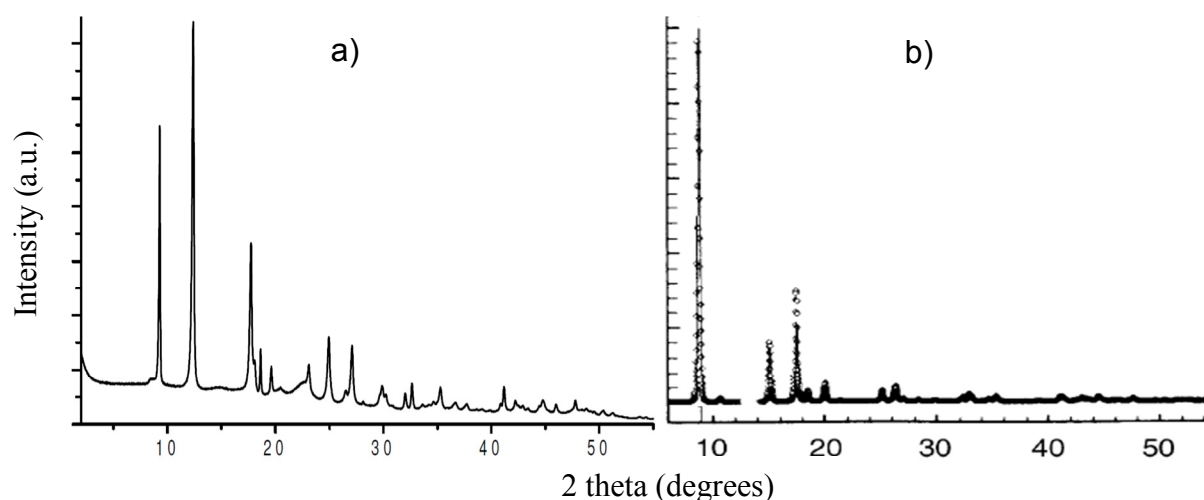
Figure 2.14: PXRD comparison between amino-MIL-53(Al)-lt (a) and MIL-53(Al)-lt (b). Figure style was changed. Adapted with permission from T. Ahnfeldt, D. Gunzelmann, T. Loiseau, D. Hirsemann, J. Senker, G. Férey and N. Stock, *Inorg. Chem.*, 2009, **48**, 3057-3064 and T. Loiseau, C. Serre, C. Huguenard, G. Fink, F. Taulelle, M. Henry, T. Bataille and G. Férey *Chem. Eur. J.*, 2004, **10**, 1373-1382. Copyright 2013 American Chemical Society and The Royal Society of Chemistry.

In this study, PXRD is used for identification of synthesised products and verification of their crystalline phases. Unit cell dimensions were not calculated.

2.4 Post-Synthetic Modification (PSM) of Amino-MIL-53(Al)

2.4.1 General

MOFs like amino-MIL-53(Al), with amine groups distributed throughout the structure, has a wide applicability in terms of post-synthetic modification, which often results in amide bond formation. Amongst acyl chlorides, acid anhydrides, esters and amides, the latter is the most stable bond. This is because of the strong electron withdrawing nature of the C-O bond and the delocalisation of the lone pair of electrons on the nitrogen atom over the C-N bond, which creates a partial double bond, strengthening the amide function (Figure 2.15, p 22). This resonance is also the cause for the rigidity of the amide bond due to the restriction of free rotation around the C=N bond.
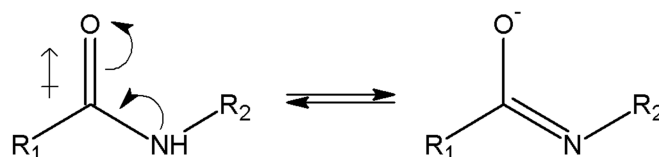

Figure 2.15: General amide resonance structures.

Carboxylic acids react with amines to form amide or peptide bonds through a condensation reaction with or without a catalyst. The formation of robust amide bonds is important in terms of purification after PSM. MOFs cannot be extracted as with general organic reactions to purify the product. Instead, MOFs have to be evacuated either with or without vacuum at medium to high temperatures (130°C-350°C). In some cases the unreacted reagents need to be extracted by solvent before thermal cleansing can commence.[13]

2.4.2 Amidation of Amino-MIL-53(Al)

MOFs are usually synthesised using hydrothermal or solvothermal conditions with high temperatures and pressures, making it difficult to functionalise the organic linkers prior to the formation of the MOF lattice. The selected inorganic salts such as metal nitrates and chlorides produce concentrated acid as side products during these syntheses, thus limiting the scope of pre-synthetic functionalisation. Robson *et al.* suggested in 1990 that if certain species can be allowed to migrate throughout the whole lattice unhindered, it would be possible for chemical functionalisation after initial formation of the lattice.[23] Cohen *et al.* started to develop strategies

for post-synthetic modification of MOF's almost 18 years later, using IRMOF-3, also an amine-functionalised framework (Scheme 2.2, p 23). [24]
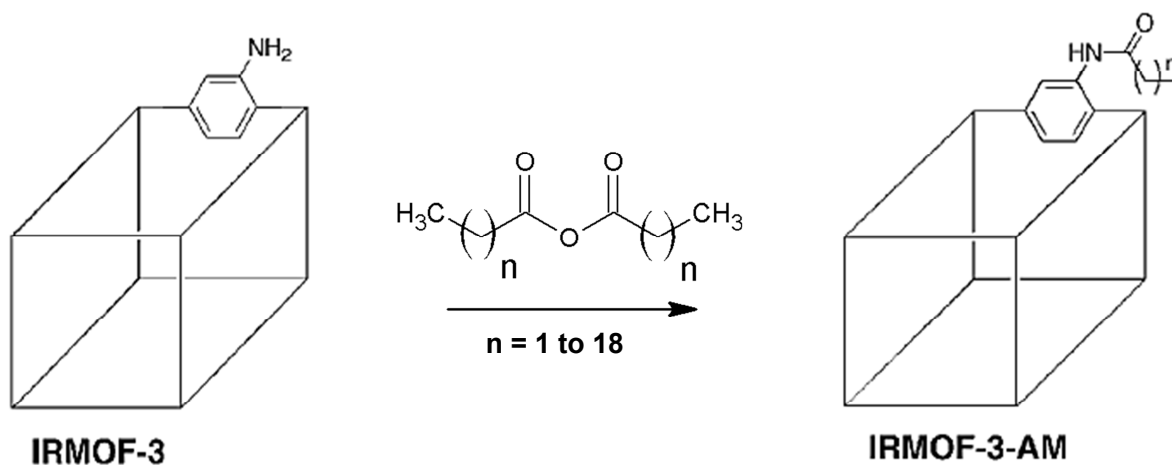
Scheme 2.2: General reaction scheme for the amidation of IRMOF-3 with a series of aliphatic, straight chain, acid anhydrides. Adapted with permission from K. K. Tanabe, Z. Wang, and S. M. Cohen, *J. Am. Chem. Soc.*, 2008, **130**, 8508-8517. Copyright 2013 American Chemical Society.

The goal was to fully investigate the solid state reactivity towards alkylation of the amino groups inside the lattice with 10 aliphatic, straight chain, acid anhydrides (formula $O(CO(CH_2)_nCH_3)_2$ with $n = 1$ to 18). The MOF was prepared prior to post-synthetic modification in two ways: a) A dry method where the MOF was dried at 75°C under a vacuum and then suspended and stored in $CHCl_3$. After re-suspension in $CDCl_3$, the anhydrides were added. b) A wet method where the MOF was used as is without prior drying. After digesting the products in a mixture of d^6-DMSO, DCl and D_2O, liquid ^{1}H-NMR spectroscopy showed full conversion with method a) after 5 days with the anhydrides ($n \leq 5$). With $n > 5$, only partial modification occurred, decreasing as the chain-length increases. The wet method showed similar results but, because of the wet conditions, a lower amount of modification occurred where $n > 5$.[24]

Stock *et al.* reacted amino-MIL-53(Al) with formic acid to produce MIL-53(Al)-NHCHO (Figure 2.16, p 24). Since formic acid is the smallest, saturated aliphatic acid, it is a quite suitable reagent, considering the small pore diameter (~6 Å)[25] of amino-MIL-53(Al).[13]
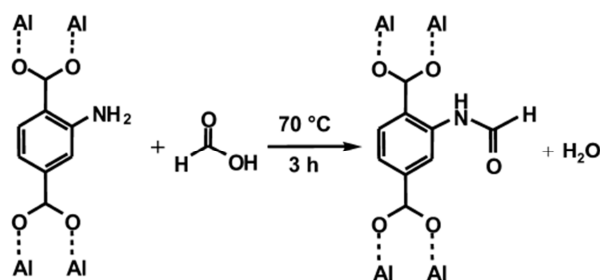
Figure 2.16: Amide condensation of amino-MIL-53(Al) with formic acid. Adapted with permission from T. Ahnfeldt, D. Gunzelmann, T. Loiseau, D. Hirsemann, J. Senker, G. Férey and N. Stock, *Inorg. Chem.*, 2009, **48**, 3057-3064. Copyright 2013 American Chemical Society.

Only partial modification was seen with the use of IR (Figure 2.17, p 24) due to the decreased presence of C-N vibrations at 1334 and 1254 cm^{-1} which comes from the unmodified amino groups. Another signal arose at 1690 cm^{-1} due to the C=O stretching vibrations of the amide. Also the NH$_2$ vibrations were overshadowed (usually at ~3400-3500 cm^{-1}) by one large band possibly due to water presence which is indicated in the compound's TG analysis (Figure 2. 18, p 25).[13]
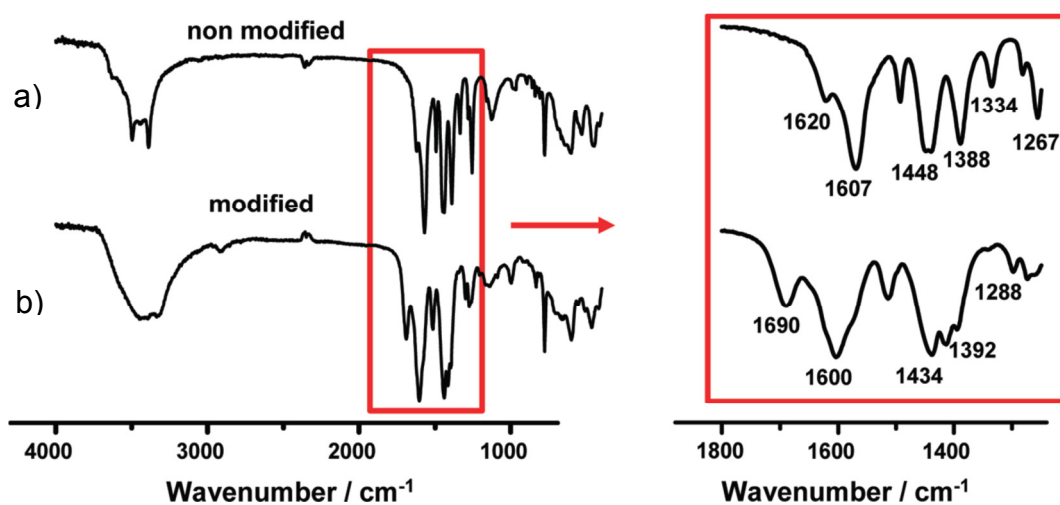

Figure 2.17: Infrared spectra of amino-MIL-53(Al)-lt (a) and after its reaction with formic acid (b). Adapted with permission from T. Ahnfeldt, D. Gunzelmann, T. Loiseau, D. Hirsemann, J. Senker, G. Férey and N. Stock, *Inorg. Chem.*, 2009, **48**, 3057-3064. Copyright 2013 American Chemical Society.
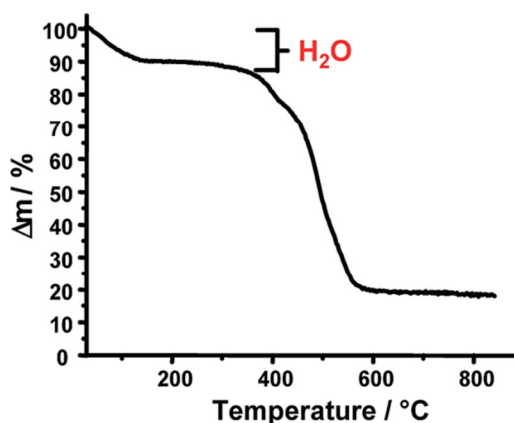
Figure 2. 18: TG analysis of MIL-53(Al)-NHCHO showing the mass loss of water up about 150°C.

As previously described, the MOF's crystal lattice goes from orthorhombic to monoclinic upon thermal activation. During post-synthetic modification of the NH_2 groups with formic acid, the lattice goes back to orthorhombic, due to hydrogen bonds formed between the carboxylic groups in the framework and water released during the reaction.

The PXRD patterns of MIL-53(Al)-NHCHO and MIL-53-NH_2(lt) (Figure 2.19, p 25) thus appears to be similar with the exception of a few peaks. In this study, these patterns will be used for the confirmation of structures after synthesis.

Figure 2.19: PXRD pattern of MIL-53(Al)-NHCHO (a) compared to that of MIL-53-NH_2(lt) (b). Adapted with permission from T. Ahnfeldt, D. Gunzelmann, T. Loiseau, D. Hirsemann, J. Senker, G. Férey and N. Stock, *Inorg. Chem.*, 2009, **48**, 3057-3064. Copyright 2013 American Chemical Society.
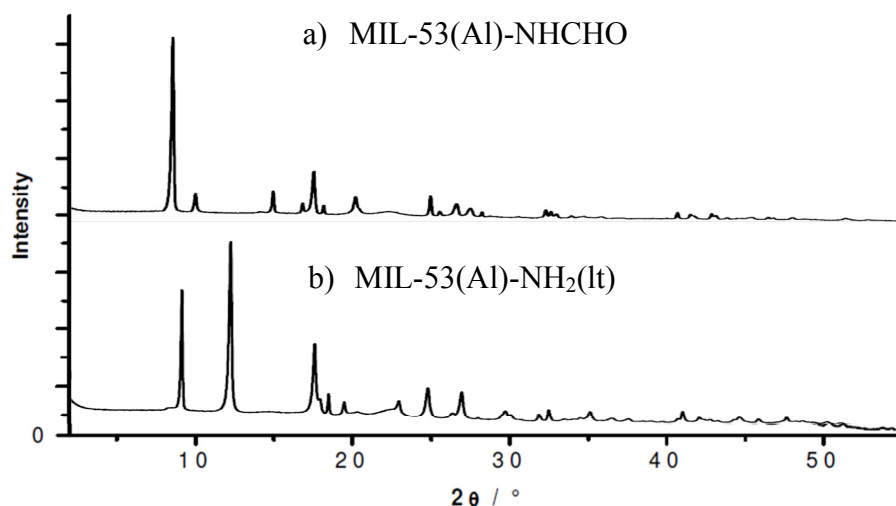
To improve the hydrophobicity of amino-MIL-53(Al), Cohen *et al.* investigated alkylation by producing straight chain aliphatic amides.[26] Amino-MIL-53(Al) underwent amidation with alkyl anhydrides ($O(CO(CH_2)_nCH_3)_2$ where n = 0, 3 and 5). Measurements showed that the surface contact angle where n = 0 (acetic anhydride) was 0° showing no change in hydrophobicity, but in the case where n = 3 and 5, the angles were found to be greater than 150°, an indication of superhydrophobicity.[27,28,29]

2.5 Ferrocene in Amino-MIL-53(Al)

2.5.1 Introduction

Ferrocene ((η^5-$C_5H_5)_2$Fe) is an organometallic compound consisting of two cyclopetadienyl rings bound to iron (II). Ferrocene derivatives are well-known for their key roles in anti-cancer research[30] and acting as redox catalysts.[31] The covalent binding of these complexes onto supports such as silica has also been widely researched.[32]. Recently investigations into the binding of ferrocene to a suitable substrate started to focus on MOFs, simply because they can offer a versatile support system with good chemical and thermal stability, as well as ease of work-up.

2.5.2 Synthesis and Characterisation

Prior to 2009, little research on the incorporation of metallocenes inside Porous Coordination Polymers (PCPs) was performed.[33,34] Fischer *et al.* investigated the physical integration between ferrocene and unfunctionalised MIL-53(Al), by using chemical vapour deposition (CVD) where ferrocene and MIL-53(Al) were subjected to a high vacuum (1 x 10^{-3} mbar) at static conditions just above the sublimation temperature of ferrocene. This was motivated by another report stating that ferrocene was able to fit easily (65 molecules per formula unit) into [Tb(tatb)] (tatb=triazine-1,3,5-tribenzoate), a mesoporous complex with large cages (3.9 by 4.7 nm).[35] MIL-53(Al) is a microporous complex with uniform channels up to a maximum of 1.3 nm in size. To quantify the adsorbed ferrocene inside the MOF's structure, Rietveld refinement was applied to the PXRD of the product, and showed that the ferrocene molecules align themselves in a straight line in the middle of the MOF's channels with an occupancy of 50% as shown in Figure 2.20, p 27.[36]

In 2009, Fischer *et al.* made use of the bridging hydroxyl groups between the aluminium metal atoms in MIL-53(Al) to form covalent bonds with 1,1′-ferrocenediyl-dimethylsilane which is

highly reactive towards surface hydroxyl groups (Figure 2.21, p 27). Unfortunately the ferrocenediyl-dimethylsilane was bound to only 25% of the available hydroxyl groups, because of steric hindrance and the way it aligns itself in the channels of the MOF. After MIL-53(Al) was loaded with ferrocenyl groups, it still adsorbed benzene molecules up to a maximum of 13 wt%. The MOF's ability to selectively oxidise the adsorbed benzene to the appropriate phenol was tested and although the reaction was not optimised, a successful conversion of ~15% was achieved.[31]
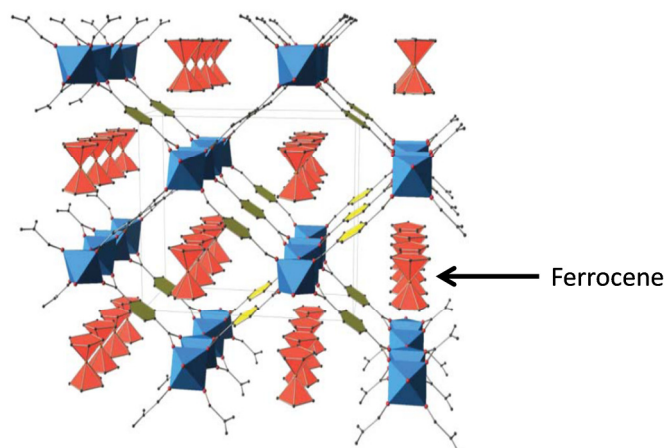
Figure 2.20: Structure of Fc@MIL-53(Al) showing physisorbed ferrocene molecules in the channels of MIL-53(Al). Adapted from M. Meilikhov, K. Yusenko and R. A. Fischer, *Dalton Trans*., 2009, 600–602 with permission of The Royal Society of Chemistry.
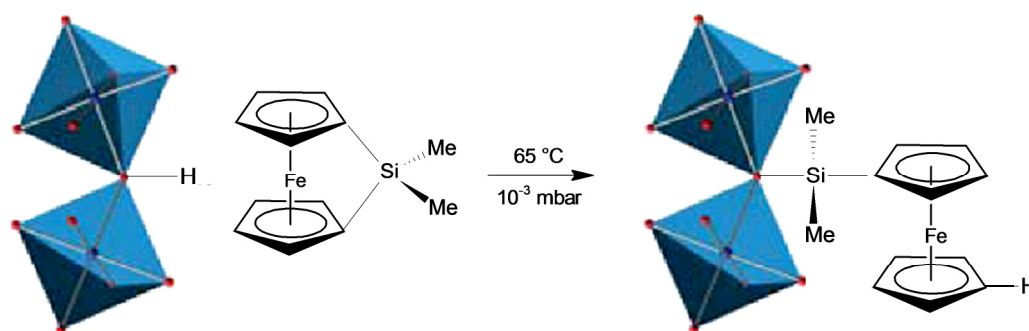
Figure 2.21: Reaction between the bridging O-H groups of MIL-53(Al) and 1,1′-ferrocenediyl-dimethylsilane. Adapted with permission from M. Meilikhov, K. Yusenko and R.A. Fischer, *J. Am. Chem. Soc*., 2009, **131**, 9644-9645. Copyright 2013 American Chemical Society.

Fischer *et al.* investigated the incorporation of different ferrocene derivatives into MIL-53(Al): 1-formylferrocene$_{0.33}$@MIL-53(Al), 1,1'-dimethylferrocene$_{0.33}$@MIL-53(Al), 1,1'-diformyl-ferrocene$_{0.5}$@MIL-53(Al), 1,1'-diethylferrocene$_{0.33}$@MIL-53(Al) and cobaltocene$_{0.25}$@ MIL-53(Al).** In addition to these compounds, cobaltocene and ferrocene was also incorporated in the vanadium analogue, MIL-53(V). The rigidity of MIL-53(V) is in contrast with the flexibility of MIL-53(Al). The bridging O-H groups connecting the Al centres of MIL-53(Al), provide better flexibility than the O^{2-} anions connecting vanadium centres in MIL-53(V). Another fact leading to this unique breathing ability of MIL-53(Al) is the orientation of metallocene molecules occupied inside the channels of the MOF. In the case of MIL-53(V), the inserted ferrocene molecules were tilted so that they entered the pores of the MOF "head first", whereas with MIL-53(Al), the ferrocene molecules were aligned upright. Since stronger intra-molecular interaction exists between MIL-53(Al) and ferrocene, the occupancy of ferrocene inside MIL-53(V) was half that of MIL-53(Al).[37]

Little is known about post-synthetic modification of amino-MIL-53(Al) with ferrocene since most were done using organic attachments[14] and other metal complexes.[38] Recently, Marken *et al.* performed post-synthetic modification of amino-MIL-53(Al), as well as three other amine containing MOFs, with ferrocene, through amidation with ferrocenecarboxylic anhydride (Figure 2.22, p 29). The best conversions were obtained by refluxing the reagent in CHCl$_3$ for three days. To determine the amide conversion percentage, the MOFs were digested in NaOD/D$_2$O, but unfortunately the amide bond was hydrolysed before the conversion could be measured. Therefore proof of amidation was achieved with negative mode ESI mass spectroscopy, finding a maximum conversion of 5% for the zinc-based IRMOF-3 which is constructed out of the same organic linkers as amino-MIL-53(Al).[39]

** The subscript values denote the occupancy of the molecules inside the MOF
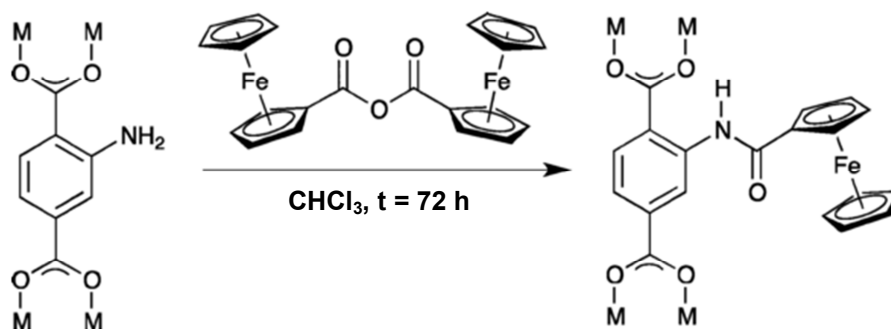
Figure 2.22   Reaction between the amine groups on the terephthalate linkers of IRMOF-3 and ferrocenecarboxylic anhydride to form a post-synthetically modified amide. The reaction was performed at either room temperature or reflux temperature. Adapted from J. E. Halls, A. Hernán-Gómez, A.D. Burrows and F. Marken, *Dalton Trans.*, 2012, **41**, 1475-1480 with permission of The Royal Society of Chemistry.

2.6   Electrochemistry in the Solid State

2.6.1 Introduction

Electrochemistry is the study of the change in current when a substance or compound is subjected to an applied potential. This change can either indicate an oxidation or a reduction process. The potential program used in this study is called Cyclic Voltammetry (CV).

Since conventional electrochemistry is usually performed on dissolved compounds and amino-MIL-53(Al) is an insoluble material, the electrochemistry thereof is quite challenging.
Of the many methods for solid state electrochemistry, the one where particles immobilised on an electrode surface will be used for the insoluble MOFs in this study. A typical three phase electrode is used as shown in Figure 2.23 (p 30).

The analyte is fixated onto the working electrode either by grafting or adhesion *via* a conductive material. The latter method can be achieved by spin coating a thin film on the electrode. In a setup like this, the three electrodes are in very close proximity of each other. The working electrode, analyte and electrolyte have to be in contact with each other to ensure good ion-transfer between the analyte and the electrolyte, and electron transfer between the working electrode and analyte. [40]
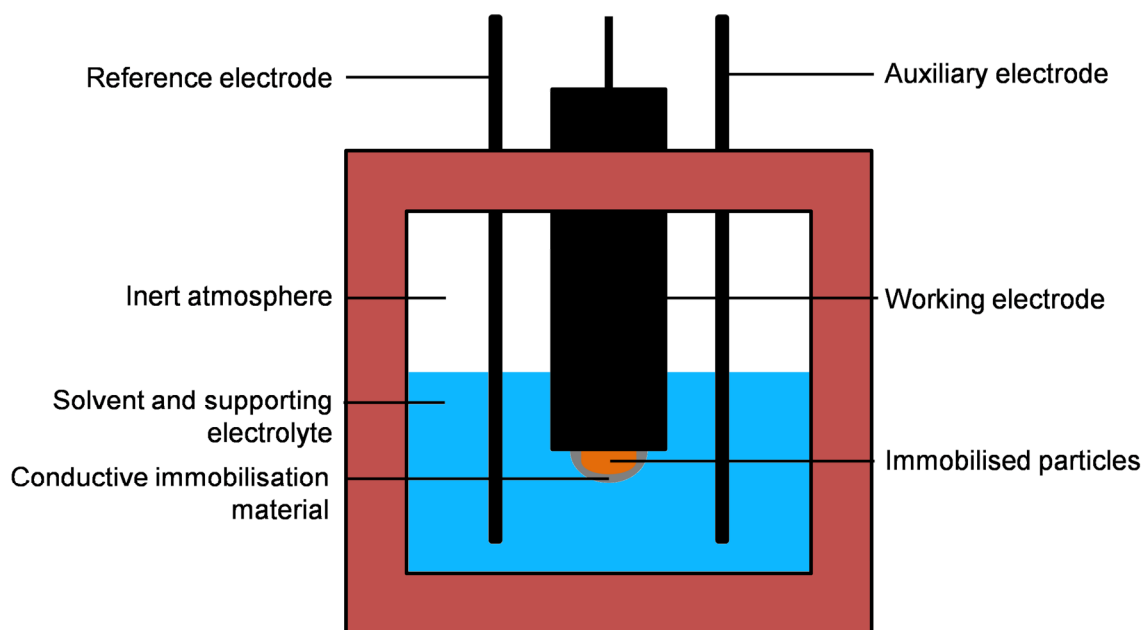
Figure 2.23: Simplified representation of a typical electrode setup where insoluble particles are immobilised on the surface of the working electrode.

2.6.2 Electrochemistry of MIL-53(Al) and Amino-MIL-53(Al)

After the attachment of 1,1′-ferrocenediyl-dimethylsilane to MIL-53(Al), Fischer *et al.* tested the product's redox activity. They used an electrochemical cell with a Ag/AgCl/KCl (3 M) reference electrode, a platinum auxiliary electrode and a graphite (3.05 mm diameter) working electrode. After suspending the product in an ethanol-Nafion (5%) solution and depositing the mixture on the electrode surface, they performed cyclic as well as differential pulse voltammetry in a potential window between – 50 mV and 400 mV. The product appeared stable during five consecutive scan cycles without decomposition or decreasing of the redox peak heights. Electrochemical reversibility was shown as ΔE_p = 60 mV (Figure 2.24, p 31). With proof that this inorganically functionalised MOF can act as redox active MOF, they suggested that reducing the ferrocenyl groups in the channels of the MOF can allow for the motion of the species inside the MOF to improve.[31]
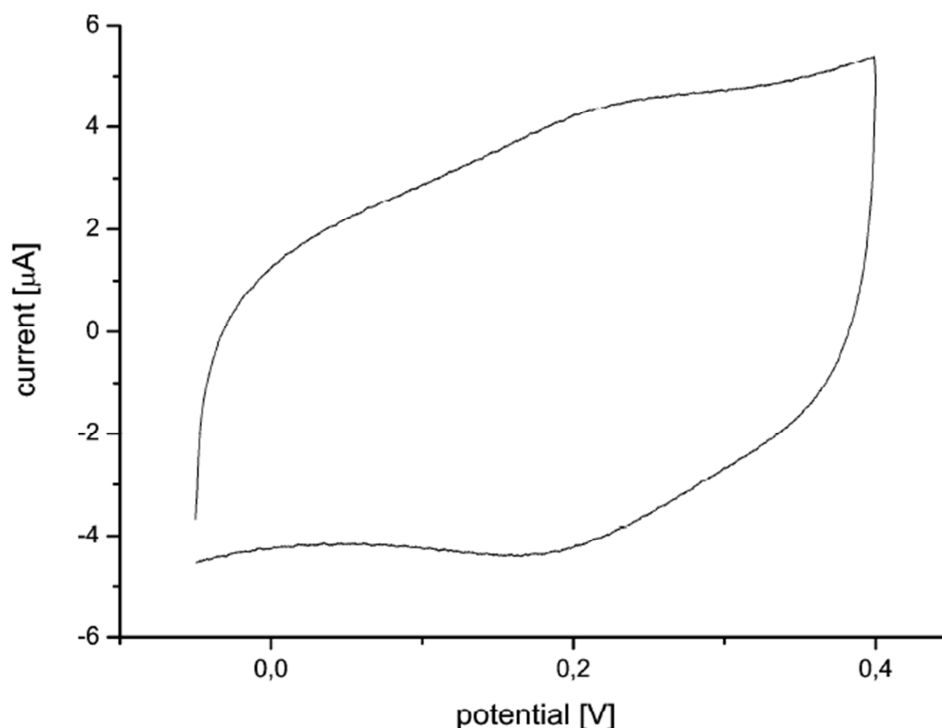
Figure 2.24: Cyclic voltammogram of 1,1′-ferrocenediyl-dimethylsilane linked to MIL-53(Al). Adapted with permission from M. Meilikhov, K. Yusenko and R.A. Fischer, *J. Am. Chem. Soc*., 2009, **131**, 9644-9645. Copyright 2013 American Chemical Society.

Marken *et al.* investigated the redox characteristics of amino-MIL-53(Al) after it was post-synthetically modified with ferrocenecarboxylic anhydride (Figure 2.22, p 29). Electrochemistry of the ferrocenyl-modified amino-MIL-53(Al) was done in both organic and aqueous conditions, as well as at different pH levels (pH = 5, 7 and 9). The general setup consisted of a saturated calomel electrode (SCE) as the reference electrode, platinum (1 mm) as the auxiliary electrode and a basal plane pyrolytic graphite (BPPG) electrode (4.9 mm diameter) as the working electrode. Ground MOF powder was transferred to the working electrode by gently rubbing the electrode over the powder on filter paper.

In the case where dichloroethane with 0.1 M [NBu$_4$][PF$_6$] as supporting electrolyte was used, one redox couple was seen at (E_{pa} + E_{pc})/2 = 680 mV *vs.* SCE (Figure 2.25 (a), p 32) with ΔE_p = 120 mV. This is an electrochemically irreversible process, which also appeared to be independent from the scan rate, an indication of a fast electron transfer influenced by a limited diffusion of ions.

In the case where an aqueous medium was used (Figure 2.25 (b), p 32), two redox processes were observed, but due to a quick decay of the redox peaks during consecutive cycles (i-iv), the voltammetric responses were less clear. A first reversible process appeared at around 400 mV

and a second irreversible process at about 700 mV. The rapid decay was an indication of surface oxidation on the MOF.

The studies done in an aqueous medium suggested that the MOF underwent partial decomposition. The ferrocene inside the MOF's channels produce protons upon oxidation which in turn, produce hydroxyl groups that can attack and break down the structure's outer layer (Figure 2.26, p 32). This effect was not seen in the organic medium studies.[39]
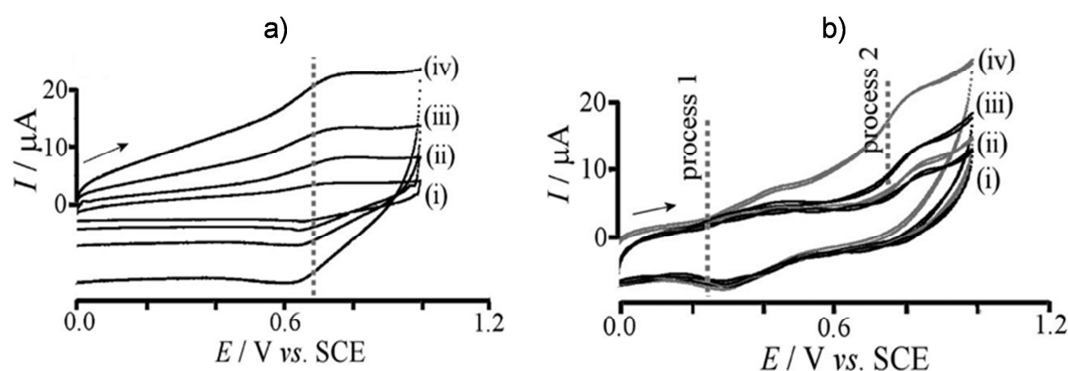
Figure 2.25: Cyclic voltammograms of FcCONH-MIL-53(Al) with scanned speeds: i) 10 mV s^{-1}, ii) 20 mV s^{-1}, iii) 50 mV s^{-1} and iv) 100 mV s^{-1} in dichloroethane (a) and aqueous medium (b). Adapted from J. E. Halls, A. Hernán-Gómez, A.D. Burrows and F. Marken, *Dalton Trans*., 2012, **41**, 1475-1480 with permission of The Royal Society of Chemistry.

Figure 2.26: Electrochemical behaviour of FcCONH-MIL-53(Al) on the electrode surface in an organic medium (a) and in an aqueous medium (b). Adapted from J. E. Halls, A. Hernán-Gómez, A.D. Burrows and F. Marken, *Dalton Trans*., 2012, **41**, 1475-1480 with permission of The Royal Society of Chemistry.

2.7   References

1   H. Li, M. Eddaoudi, M. O'Keeffe and O. M. Yaghi, *Nature*,1999, **402,** 276-279.

2   F. Millange, C. Serre and G. Férey, *Chem. Commun.*,2002, 822-823.
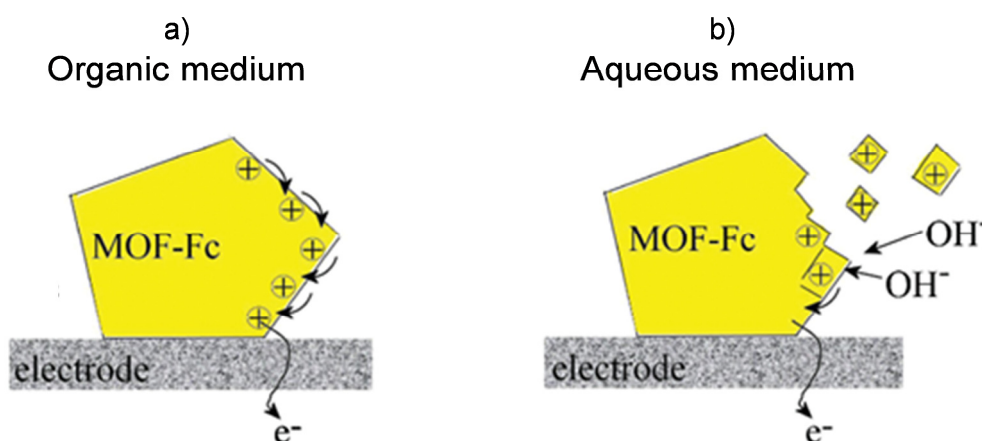
3   C. Serre, F. Millange, C. Thouvenot, M. Noguès, G. Marsolier, D. Louër and G. Férey, *J. Am. Chem. Soc.*, 2002, **124**, 13519-13526.

4   T. Loiseau, C. Serre, C. Huguenard, G. Fink, F. Taulelle, M. Henry, T. Bataille and G. Férey *Chem. Eur. J.*, 2004, **10**, 1373-1382.

5   P. Horcajada, C. Serre, G. Maurin, N. A. Ramsahye, F. Balas, M. Vallet-Regí, M. Sebban, F. Taulelle and G. Férey, *J. Am. Chem. Soc.*, 2008, **130**, 6774-6790.

6   G. Férey, F. Millange, M. Morcrette, C. Serre, M. L. Doublet, J. M. Grenèche and J. M. Tarascon, *Angew. Chem. Int. Ed.*, 2007, **46**, 3259-3263.

7   D. Peralta, G. Chaplais, A. Simon-Masseron, K. Barthelet, C. Chizallet, A. Quoineaud and G. D. Pirngruber, *J. Am. Chem. Soc.*, 2012, **134**, 8115-8126.

8 a) K. Barthelet, J. Marrot, D. Riou and G. Férey, *Angew. Chem.*, 2002, **114**, 291-294; b) K. Barthelet, J. Marrot, D. Riou and G. Férey *Angew. Chem. Int. Ed.*, 2002, **41**, 281-284.

9   P. Rallapalli, K. P. Prasanth, D. Patil, R. S. Somani, R. V. Jasra and H. C. Bajaj, *J. Porous. Mater.*, 2011, **18**, 205-210.

10   P. Serra-Crespo, E. Gobechiya, E. V. Ramos-Fernandez, J. Juan-Alcañiz, A. Martinez-Joaristi, E. Stavitski, C. E. A. Kirschhock, J. A. Martens, F. Kapteijn and J. Gascon, *Langmuir*, 2012, **28**, 12916-12922.

11   B. Arstad, H. Fjellvåg, K. O. Kongshaug, O. Swang and R. Blom, *Adsorption*, 2008, **14**, 755-762.

12   F. Rouquerol, in *Adsorption by Powders and Porous Solids*, J. Rouquerol and K. Sing, Academic Press, WILEY-VCH Verlag GmbH & Co. KGaA, Weinheim, 3rd issue, 1999,.vol. 11, pp 191.

13   T. Ahnfeldt, D. Gunzelmann, T. Loiseau, D. Hirsemann, J. Senker, G. Férey and N. Stock, *Inorg. Chem.*, 2009, **48**, 3057-3064.

14   E. Stavitski, M. Goesten, J. Juan-Alcañiz, A. Martinez-Joaristi, P. Serra-Crespo, A. V. Petukhov, J. Gascon, and F. Kapteijn, *Angew. Chem. Int. Ed.*, 2011, **50**, 9624–9628.

15   S. J. Garibay, Z. Wang and S. M. Cohen, *Inorg. Chem.*, 2010, **49**, 8086-8091.

16   J. Gascon, U. Aktay, M. D. Hernandez-Alanso, G. P. M. van Klink, F. Kapteijn, *J. Catal.*, 2009, **261**, 75-87.

17   X. Cheng, A. Zhang, K. Hou, M. Liu, Y. Wang, C. Song, G. Zhang and X. Guo, *Dalton Trans.*, 2013, **42**, 13698-13705.

18   J. Kim, W. Y. Kim and W. Ahn, *Fuel*, 2012, **102**, 574-579.

19   E. Stavitski, E. Pidko, S. Couck, T. Remy, E. Hensen, B. Weckhuysen, J. F. M. Denayer, J. Gascon and F. Kapteijn, *Langmuir*, 2011, **27**, 3970-3976.

20   A. Boutin, S. Couck, F. Coudert, P. Serra-Crespo, J. Gascon, F. Kapteijn, A. H. Fuchs and J. F. M. Denayer, Microporous Mesoporous Mater. 2011, **140**, 108-113.

21   S. Couck, E. Gobechiya, C. E. A. Kirschhock, P. Serra-Crespo, J. Juan-Alcañiz, A. Martinez-Joaristi, E. Stavitski, J. Gascon, F. Kapteijn, G.V. Baron and J. F. M. Denayer, *Chem .Sus. Chem.*, 2012, **5**, 740-750.

22   P. Serra-Crespo, M. A. van der Veen, E. Gobechiya, K. Houthoofd, Y. Filinchuk, C. E. A. Kirschhock, J. A. Martens, B. F. Sels, D. E. De Vos, F. Kapteijn and J. Gascon, *J. Am.Chem. Soc.*, 2012, **134**, 8314-8317.

23   B. F. Hoskins, R. Robson,. *J. Am. Chem. Soc.*, 1990, **112**, 1546-1554.

24   K. K. Tanabe, Z. Wang, and S. M. Cohen, *J. Am. Chem. Soc.*, 2008, **130**, 8508-8517.

25   S. Couck, T. Rémy, G. V. Baron, J. Gascon and F. Kapteijn, *Phys. Chem. Chem. Phys.*, 2010, **12**, 9413-9418.

26   G. J. Nguyen and S. M. Cohen, *J. Am. Chem. Soc.*, 2010, **132**, 4560-4561.

27   S. Hausdorf, J. Wagler, R Mossig and F. O. R. L. Mertens, *J. Phys. Chem.* A, 2008, **112**, 7567-7576.

28   S. S. Kaye, A. Dailly, O. M. Yaghi and J. R. Long, *J. Am. Chem. Soc.*, 2007, **129**, 14176-14177.

29   Y. Li and R. T. Yang, *Langmuir*, 2007, **23**, 12937-12944.

30   B. Zhou, J. Li, B. Feng, Y. Ouyang, Y. Liu and F. Zhou, *J. Inorg. Biochem.*, 2012, **116**, 19-25.

31   M. Meilikhov, K. Yusenko and R.A. Fischer, *J. Am. Chem. Soc.*, 2009, **131**, 9644-

9645.

32   M. Tanaka,T. Sawaguchi, M. Kuwahara and O. Niwa, *Langmuir*, 2013, **29**, 6361−6368.

33   M. J. Ingleson, J. P. Barrio, J. B. Guilbaud, Y. Z. Khimyak and M. J. Rosseinsky, *Chem. Commun*., 2008, **23**, 2680-2682.

34   S. S. Kaye and J. R. Long, *J. Am. Chem. Soc.,* 2008, **130**, 806-807.

35   Y. K. Park, S. B. Choi, H. Kim, K. Kim, B. H. Won, K. Choi, J. S. Choi, W. S. Ahn, N. Won, S. Kim, D. H. Jung, S. H. Choi, G. H. Kim, S. S. Cha, Y. H. Jhon, J. K. Yang and J. Kim, *Angew. Chem., Int. Ed.*, 2007, **46**, 8230-8233.

36   M. Meilikhov, K. Yusenko and R. A. Fischer, *Dalton Trans*., 2009, 600–602.

37   M. Meilikhov, K. Yusenko and R. A. Fischer, *Dalton Trans.,* 2010, **39**, 10990–10999.

38   Y. Huang, Z. Zheng, T. Liu, J. Lü, Z. Lin, H. Li and R. Cao, *Catal. Commun*., 2011, **11**, 27-31.

39   J. E. Halls, A. Hernán-Gómez, A.D. Burrows and F. Marken, *Dalton Trans*., 2012, **41**, 1475-1480.

40   F. Scholz, in *Electrochemistry of Immobilised Particles*, U. Schröder and R. Gulaboski, Springer – Verlag, Berlin Heidelberg, 2005, ch. 1-3, pp 1-29.

3 Results & Discussion

3.1. Introduction

In this chapter the synthesis and characterisation of MIL-53(Al) and amino-MIL-53(Al) metal organic frameworks (MOFs) will be described. Thereafter, the post-synthetic modification (PSM) of these two MOFs with organic carboxylic acids, HCOOH and $CH_3(CH_2)_nCOOH$ (n = 0, 1, 2) as well as ferrocenecarboxylic acid, $(C_5H_5)Fe(C_5H_4COOH)$, will be discussed. Lastly, a novel solid state electrochemical study of MIL-53(Al) and amino-MIL-53(Al), containing ferrocene moieties will be discussed.

For this study, the detailed structure of MIL-53(Al) and amino-MIL-53(Al) will be simplified for use in diagrams and reaction schemes as depicted in Figure 3.1.
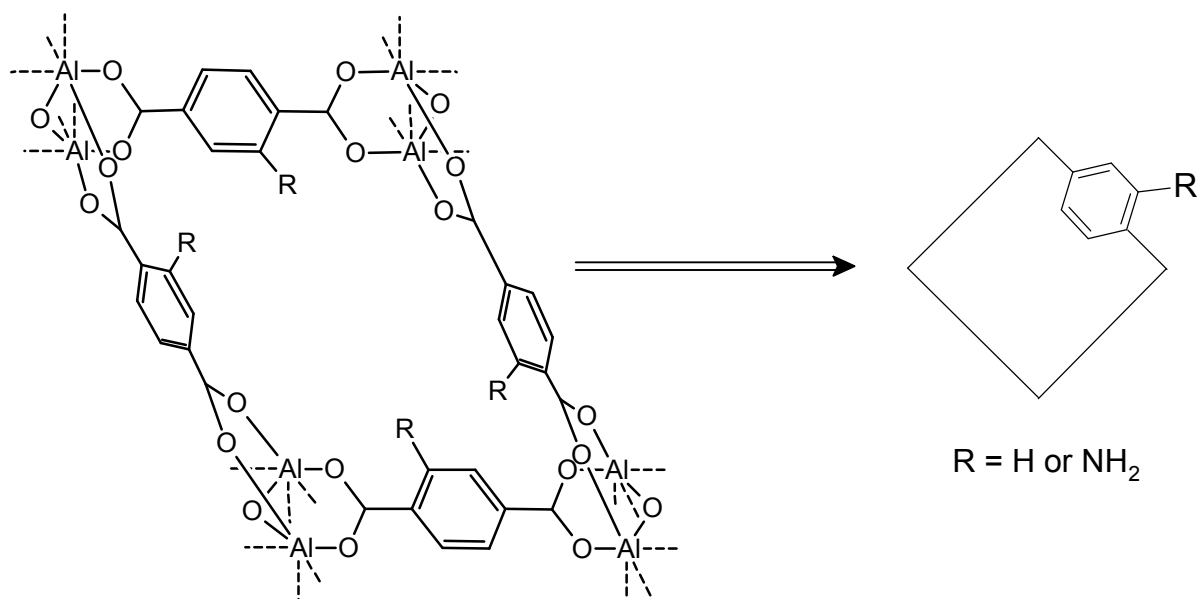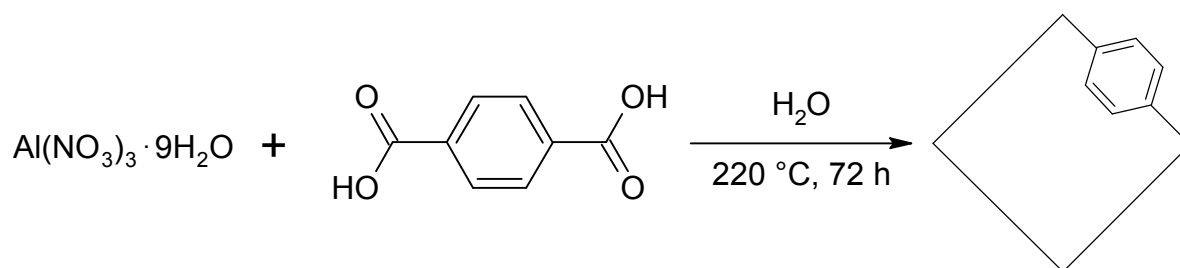

Figure 3.1:   Simplification of the structure of MIL-53(Al) (R = H) or amino-MIL-53(Al) (R = NH_2) to emphasise the phenyl functional group of the organic linker.

3.2. Synthesis

3.2.1. Al(OH)[O$_2$C-C$_6$H$_4$-CO$_2$] (MIL-53(Al))

3.2.1.1. Synthesis Routes

MIL-53(Al) was synthesised to be a reference material during this study[1]. Two synthesis procedures were used.
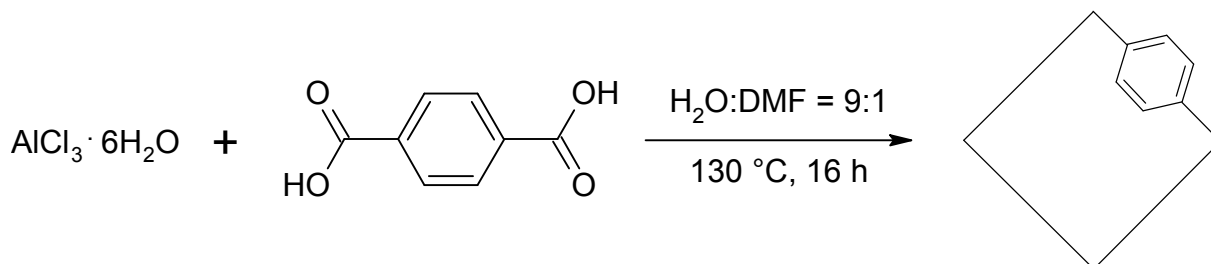

Scheme 3.1: Synthesis of MIL-53(Al) with the use of aluminium nitrate nonahydrate as the metal salt precursor and terephthalic acid as the organic linker.

The first procedure to synthesise MIL-53(Al) followed a method by Férey *et al* (Scheme 3.1, p 38).[1]   The as-synthesised (crude) product, MIL-53(Al)-as, was formed through a one-pot, hydrothermal synthesis procedure, and contained unreacted terephthalic acid as well as nitric acid as a by-product. Centrifugation was used as an effective method to isolate and wash the product with little loss, although it does not remove the free molecules (mostly terephthalic acid) inside the channels. Therefore, the MOF is subjected to thermal activation under a nitrogen stream at 330°C for 72 hours to yield the activated (evacuated) product, MIL-53(Al)-ht, which upon cooling, attracts atmospheric water and undergoes a phase change to MIL-53(Al)-lt. With this method a yield of 57% was achieved.

For the second method to produce MIL-53(Al), aluminium chloride hexahydrate (AlCl$_3$·6H$_2$O) was used as the metal salt precursor (Scheme 3.2, p 39) and the solvent changed to water:DMF = 9:1, since this ratio has already been proven to be crucial for MIL-53 formation, avoiding the formation of a MIL-101 intermediate.[2] Aluminium chloride is a more reactive precursor than the aluminium nitrate, reducing the synthesis time to 16 hours. After this synthesis, a two-step solvent purification procedure was applied before thermal activation. MIL-53(Al)-as was transferred to a bomb reactor and heated with DMF at 150°C for 16 hours, to facilitate the removal of the trapped terephthalic acid inside the channels of the MOF, and replace it with

DMF molecules. Thereafter, the MOF was refluxed with methanol overnight to exchange the high boiling DMF with the more volatile methanol. Thermal activation of the MOF at 350°C under N_2 flow for 72 hours completed the process to obtain MIL-53(Al)-lt (after cooling). The difference between this method and the previous is that the solvent purification ensures removal of free terephthalic acid trapped in the inner channels of the MOF. The second difference is that the thermal activation of the MOF after solvent purification is a much cleaner process.

Scheme 3.2: Synthesis of MIL-53(Al) with aluminium chloride hexahydrate as the metal salt precursor and terephthalic acid as the organic linker.

3.2.1.2.   Characterisation
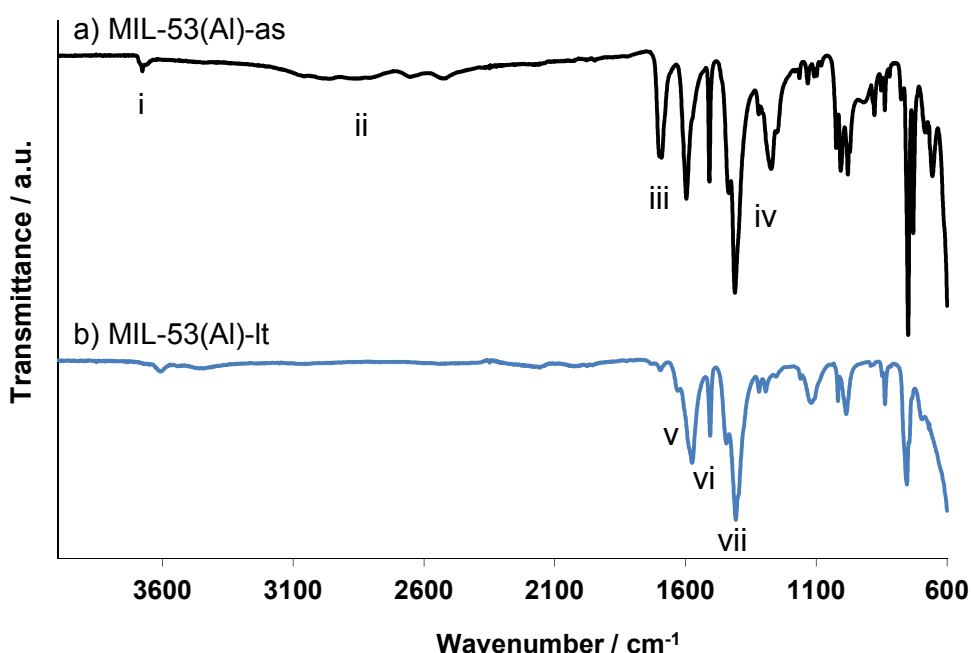
Figure 3.2: FTIR spectra of MIL-53(Al)-as (a) and MIL-53(Al)-lt (b).

Figure 3.2 (p 39) displays the Fourier transformed infrared (FTIR) spectrum of MIL-53(Al)-as (a), obtained directly after synthesis and MIL-53(Al)lt (b), obtained after activation. The broad band between 3000 cm^{-1} and 2500 cm^{-1} (scan a, ii) is due to the hydroxyl groups from free terephthalic acid present in the channels of MIL-53(Al)-as, which also displays two extra bands

between 1800 and 1400 cm^{-1}. The peak at 1702 cm^{-1} (scan a, iii) represents the C=O stretching of the free terephthalic acid. Both bands (ii and iii) are absent in MIL-53(Al)-lt. For MIL-53(Al)-as, the peak at 3686 cm^{-1} (scan a, i), attributed to the stretching frequency of water, is shifted by 50 cm^{-1} to the right (3636 cm^{-1}, scan b) when water from the reaction leave the pores and only adsorbed water vapour from the atmosphere are present in MIL-53(Al)-lt. The bending frequency of water is seen as a shoulder peak at 1637 cm^{-1} (scan b, v). The FTIR spectrum of MIL-53(Al)-lt (scan b) with the prominent peaks at 1577/1506 cm^{-1} (vi) and 1446/1409 cm^{-1} (vii), representing the anti-symmetric and symmetric carbonyl stretching frequencies respectively, is in excellent agreement with literature results.[1]

The FTIR spectra for the second synthesis method for MIL-53(Al) (Scheme 3.2, p 39) are shown in Figure 3.3 (p 40).
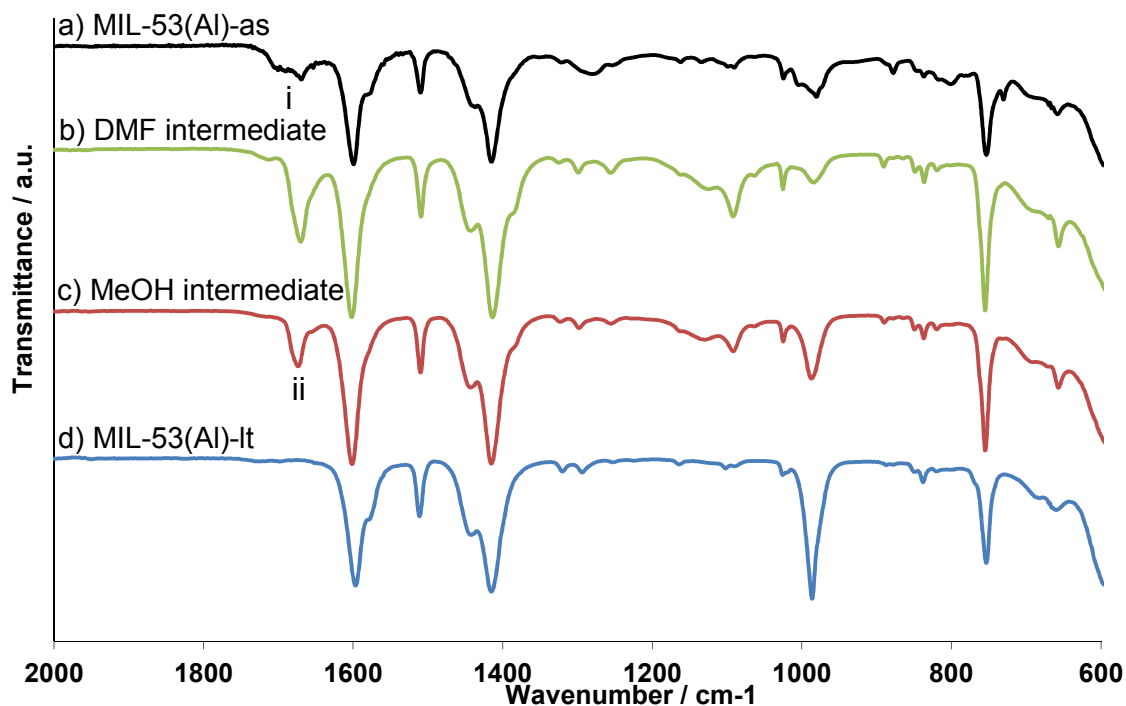

Figure 3.3:   FTIR of MIL-53(Al): a) after synthesis in H$_2$O:DMF = 9:1; b) after heating in DMF (150°C, 16 h); c) after reflux in methanol for 16 hours and d) after thermal activation at 350°C under N$_2$ flow for 72 hours.

MIL-53(Al)-as (Figure 3.3 a) has two overlapping C=O bands at 1700 cm^{-1} (i) from the free terephthalic acid and DMF left in the channels of the MOF after synthesis. For the MOF structure, the same C=O asymmetric and symmetric stretching bands are seen in all four scans between 1600 cm^{-1} and 1400 cm^{-1} as previously reported. After heating MIL-53(Al)-as in DMF, MIL-53(Al)-DMF (Figure 3.3 b) displays a strong carbonyl stretching peak from DMF at 1674

cm^{-1} (ii). In the next scan (Figure 3.3 c), the C=O peak of DMF appears much smaller after refluxing the MOF in methanol. No peak related to DMF or free terephthalic acid is observed in the last scan (MIL-53(Al)-lt) (Figure 3.3 d), taken after thermal activation of the MOF.

Thermogravimetric analysis (TGA) was performed on MIL-53(Al)-as and MIL-53(Al)-lt for both syntheses, Scheme 3.1 (p 38) and Scheme 3.2 (p 39) as seen in Figure 3.4 (p 42). Both as-synthesised structures (a and c) show a loss of water between 65 and 200°C (steps 1a and 1c). When the as-synthesised structures are heated between 200 and 450°C, the free terephthalic acid trapped inside the structure is released as seen in TGA traces a) and c). MIL-53(Al) synthesised in water (Scheme 3.1, p 38) shows a small loss (step 2a) followed by a 22.55% mass loss (step 3a), which could be attributed to a minority of free terephthalic acid closer to the crystal surface being released first, followed by a larger quantity from deeper inside the MIL-53(Al) structure. This is possible due to the restricted movement of molecules through the small channels ranging between 8 Å and 13 Å in diameter (depending on the breathing behaviour).[3]

The as-synthesised MIL-53(Al) from the H$_2$O:DMF = 9:1 synthesis (Scheme 3.2, p 39) has a much smaller loss of free terephthalic acid (step 2c) starting at 260°C. In the latter case (step 1c), the process is extended to about 260°C, which can be attributed to a mixture of water and DMF leaving the channels of the MOF. MIL-53(Al)-as thus contained much less free terephthalic acid than its counterpart synthesised in water only. This may be due to the presence of DMF which could dissolve the free terephthalic acid much better than water during workup. Both activated products are thermally stable up to ~450°C as seen from traces b) and d) correlating with commercial MIL-53(Al)-lt (See Appendix, Spectrum 12a, A-10). After the breakdown and release of the bound terephthalic linkers, Al$_2$O$_3$ remains.

a) MIL-53(Al)-as (synthesised in H₂O)

Step 1a   -0.27 %   Step 2a   -1.13 %   Step 3a   -22.55 %
Onset   68.7 °C   Onset   218.8 °C   Onset   281.8 °C
Endset   90.8 °C   Endset   281.5 °C   Endset   486.7 °C

b) MIL-53(Al)-lt

Step 4a   -35.50 %
Onset   486.7 °C
Endset   796.9 °C

Step 1b   -54.22 %
Onset   384.1 °C
Endset   797.4 °C

Mass loss 50 %

c) MIL-53(Al)-as (synthesised in H₂O:DMF = 9:1)

Step 1c   -3.47 %   Step 2c   -3.85 %
Onset   65.6 °C   Onset   261.1 °C
Endset   261.1 °C   Endset   417.7 °C

Step 3c   -47.12 %
Onset   417.8 °C
Endset   790.9 °C

d) MIL-53(Al)-lt

Step 1d   -6.68 %
Onset   57.1 °C
Endset   419.1 °C

Step 2d   -53.74 %
Onset   419.5 °C
Endset   791.9 °C

100 150 200 250 300 350 400 450 500 550 600 650 700 750 °C
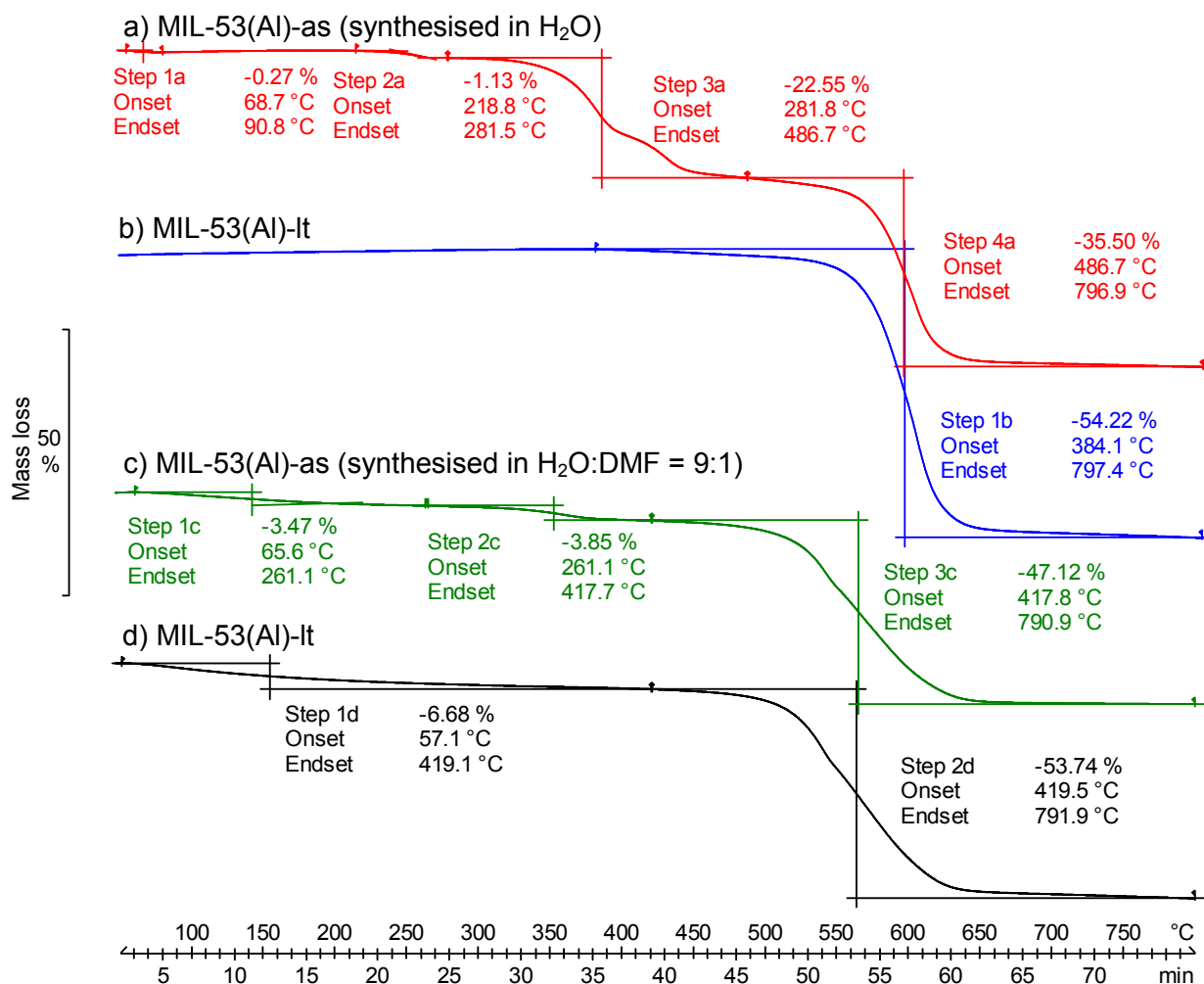5   10   15   20   25   30   35   40   45   50   55   60   65   70   min

Figure 3.4:   TGA thermograms (under Ar) of MIL-53(Al) from synthesis in water (as-synthesised, a); activated, b); as well as the synthesis in H₂O:DMF = 9:1 (as-synthesised, c); activated, d).

Accelerated Surface Area and Porosity (ASAP) measurements performed on MIL-53(Al)-lt (Graph 3.1, p 43), synthesised in H_2O:DMF = 9:1 resulted in a type I isotherm (also observed for all the other MIL-53(Al) batches, see Spectra 21 and 22, A-14) with a monolayer or Langmuir layer formed below 0.01 p/p°. The MIL-53(Al) synthesised in this study compared favourably to the commercial product in terms of surface area and pore width as shown in Table 3.1 (p 43). The ASAP results confirmed the exceptional microporosity of MIL-53(Al)-lt. It sets the stage for the post-synthetic modification of this material, which rests heavily on the successful evacuation and availability of the pores.

42
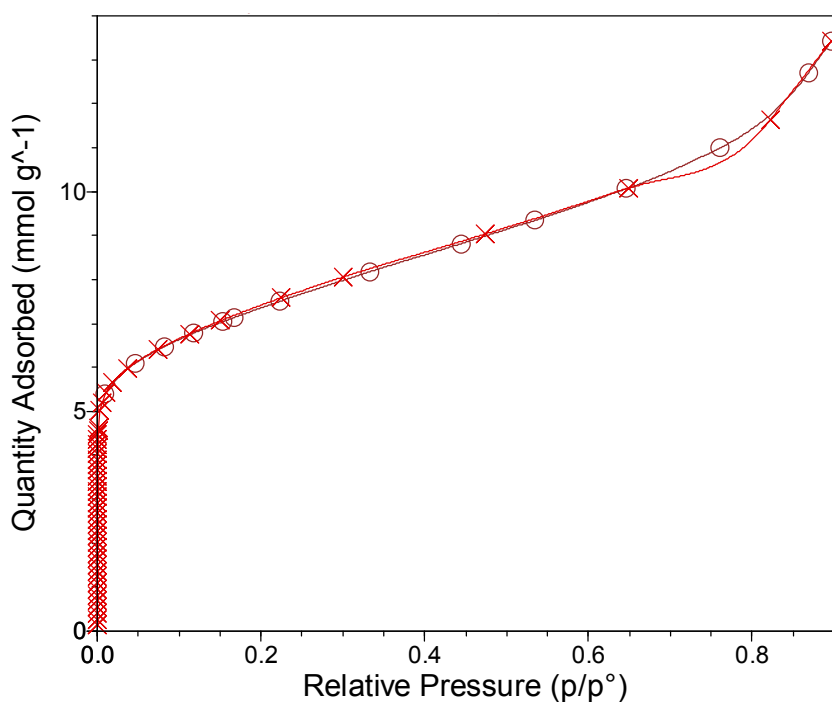
Graph 3.1: Nitrogen adsorption (crosses) and desorption (circles) isotherms of MIL-53-ht synthesised in $H_2O:DMF = 9:1$ at 77 K.

Table 3.1: Porosity measurement results of MIL-53(Al)-ht synthesised in $H_2O:DMF = 9:1$ compared to that of the commercial MIL-53(Al).

MIL-53(Al)-ht	Langmuir Surface Area (m^2g^{-1})	BET Surface Area (m^2g^{-1})	T-plot micropore volume (cm^3g^{-1})	DFT Pore size (Å)
MIL-53(Al) synthesised	901 ± 16	590 ± 1	0.14	9.8
MIL53-(Al) commercial	1044 ± 20	775 ± 1	0.25	9.8

As mentioned before, in this study PXRD analyses are mainly used for identification of the MIL-53(Al) structure. The activated batches of MIL-53(Al) were analysed with PXRD. In Figure 3.5 (p 44) it can be seen that the peak positions of the synthesised MIL-53(Al)-lt (a) correspond very well with those of the commercial MIL-53(Al)-lt (b). The differences in peak intensities may stem from preferred orientation effects as well as sample size and preparation.
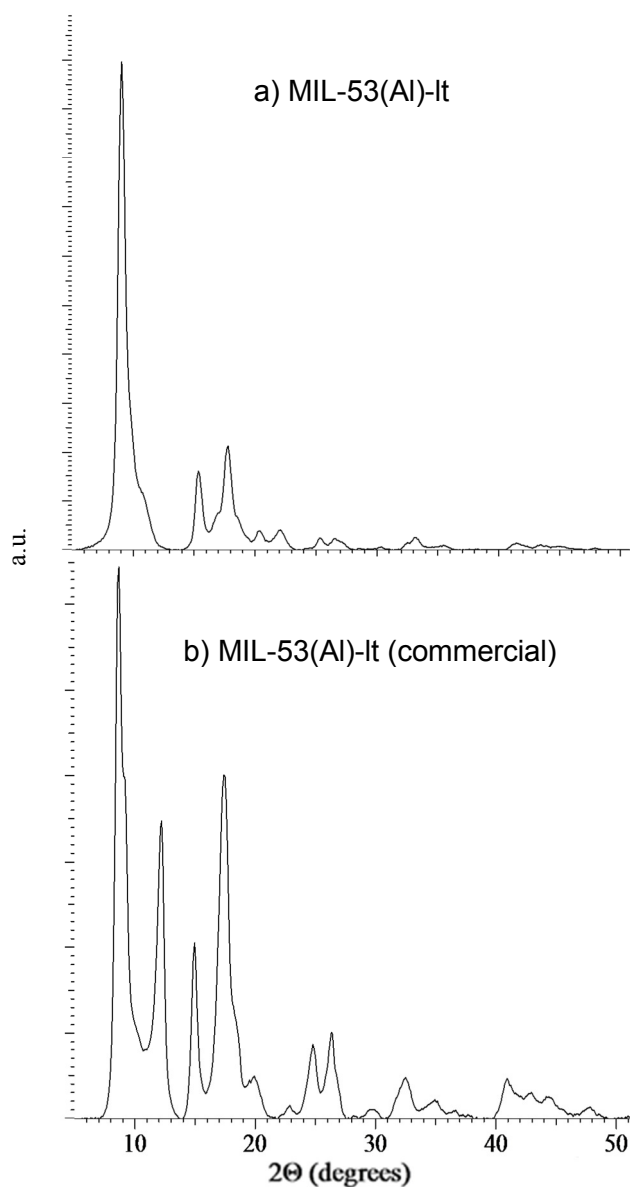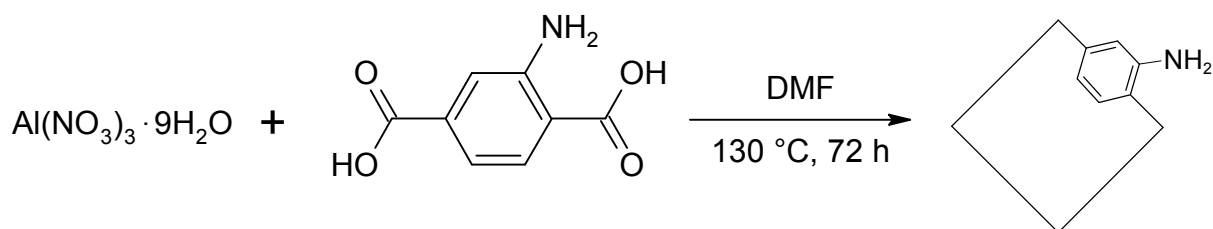
Figure 3.5: PXRD of MIL-53(Al)-lt (a) and the commercially available MIL-53(Al)-lt (b).

3.2.2. Al(OH)[O$_2$C-C$_6$H$_3$NH$_2$-CO$_2$] (Amino-MIL-53(Al))

3.2.2.1. Synthetic Routes

The first method was adapted from Denayer *et al.*,[4] using Al(NO$_3$)$_3$·9H$_2$O and 2-aminoterephthalic acid as precursors and DMF as the solvent (Scheme 3.3, p 45).

Scheme 3.3: Solvothermal synthesis of amino-MIL-53(Al) with $Al(NO_3)_3 \cdot 9H_2O$ and 2-aminoterephthalic acid as precursors and DMF as solvent.

The product (amino-MIL-53(Al)-as) was refluxed with methanol for 72 hours to extract the free terephthalic acid trapped inside the MOF's channels, followed by thermal activation at 300°C under nitrogen flow for 72 hours.

The second reaction was adapted from Kapteijn *et al.*[2] using $AlCl_3 \cdot 6H_2O$ as the metal precursor with 2-aminoterephthalic acid and a water:DMF (9:1) mixture as solvent (Scheme 3.4, p 45). Immediately after adding an aqueous solution of $AlCl_3 \cdot 6H_2O$ to a lukewarm solution of 2-aminoterephthalic acid in DMF, a yellow suspension formed. This can be the intermediate product, NH_2-MOF-235, formed in the early stages of the synthesis.[5] After the as-synthesised product was obtained, it went through a similar 2-step cleaning process before thermal activation as with MIL-53(Al), synthesised in the same solvent system. Amino-MIL-53(Al)-as was transferred to a bomb reactor and heated with DMF at 150°C for 16 hours, to facilitate the removal of the trapped terephthalic acid inside the channels of the MOF, and replace it with DMF molecules. Thereafter, the MOF was refluxed with methanol overnight to exchange the high boiling DMF with the more volatile methanol. Thermal activation was performed at 300°C for 72 hours to obtain amino-MIL-53(Al)-lt (after cooling).
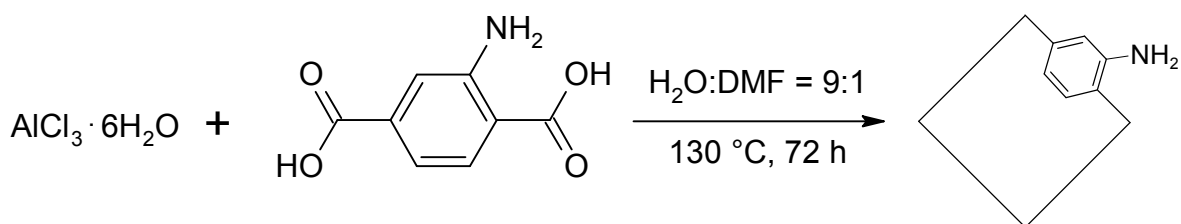
Scheme 3.4: Solvothermal synthesis of amino-MIL-53(Al) with the use of $AlCl_3 \cdot 6H_2O$ and 2-aminoterephthalic acid incorporating a solvent mixture to improve product formation.

3.2.2.2. Characterisation

Amino-MIL-53(Al) synthesised with DMF as solvent (Scheme 3.3, p 45) was characterised in two steps, with the FTIR spectra of the as-synthesised and activated products shown in Figure 3.6 (p 46).

Since water was not used during this synthesis, both FTIR spectra lack hydroxyl bands between 3000 cm^{-1} and 2500 cm^{-1}. For the as-synthesised product, the C=O stretching frequency of DMF is seen at 1662 cm^{-1} (i), but is absent for the activated product (b).
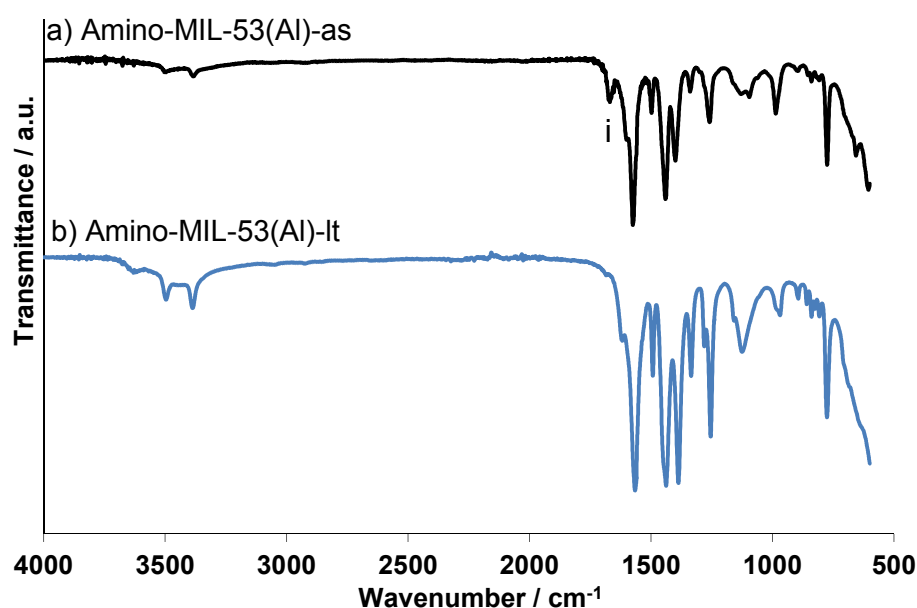

Figure 3.6:   FTIR spectra of amino-MIL-53(Al) from synthesis in DMF in its as-synthesised (a) and activated (b) form.

The FTIR spectra of amino-MIL-53(Al), synthesised using a H_2O:DMF ratio of 9:1 (Figure 3.7, p 47), represents the four stages from its synthesis to the activated amino-MIL-53(Al)-lt.

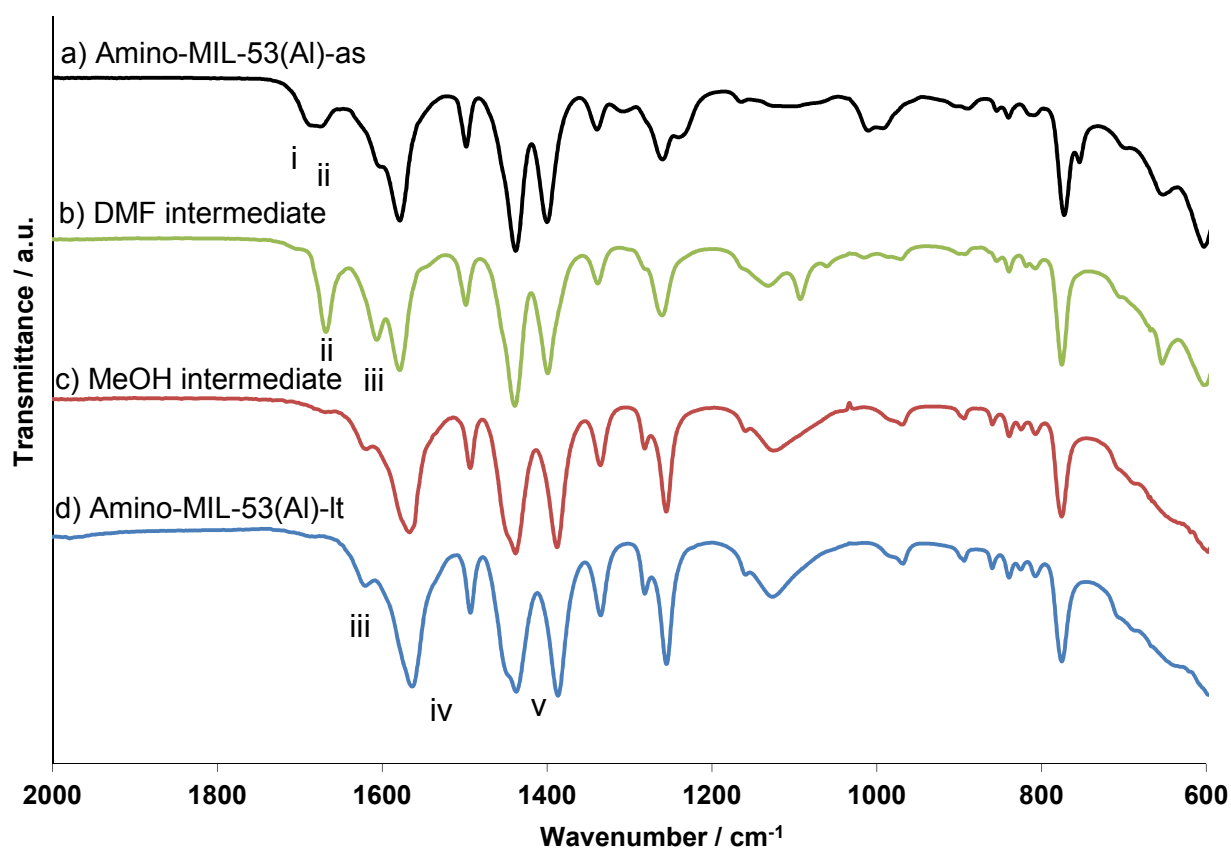Figure 3.7:   FTIR spectra of amino-MIL-53(Al): a) after synthesis in H_2O:DMF = 9:1; b) after heating in DMF (150°C, 16 h); c) after reflux in methanol for 16 hours and d) after thermal activation at 300°C under N_2 flow for 72 hours.

The FTIR spectrum of amino-MIL-53(Al) (a) displays a broad peak at 1700 cm^{-1} (i and ii) representing the overlapping carbonyl stretching frequencies of DMF and free terephthalic acid. After heating the as-synthesised product with only DMF, a single band remains at 1670 cm^{-1} (b, ii) which is attributed to DMF. This band is absent in spectrum c), after the DMF was exchanged with methanol. In the final stage, the material was activated under N_2 flow at 300°C for 72 hours. The bending frequency of water (iii) is seen in spectrum a) and b) at 1610 cm^{-1}, after which it shifts 20 cm^{-1} (1630 cm^{-1}) in spectrum c) and d). In all four spectra, the asymmetric and symmetric stretching frequencies of the carbonyl groups bound to the MOF structure is given at 1570/1500 cm^{-1} (iv) and 1440/1390 cm^{-1} (v).

Metal organic frameworks such as amino-MIL-53(Al) are insoluble materials and to be able to perform liquid nuclear magnetic resonance (NMR) studies, these frameworks need to be digested. Amino-MIL-53(Al) can be digested with NaOD/D_2O since the Al-O bonds that keep the framework together are sensitive to strong basic conditions. The carboxylate anions formed

47

after digestion, allow NMR observation of the organic fragments in the aqueous medium (Scheme 3.5, p 48).

R = NH$_2$, organic or organometallic ligands
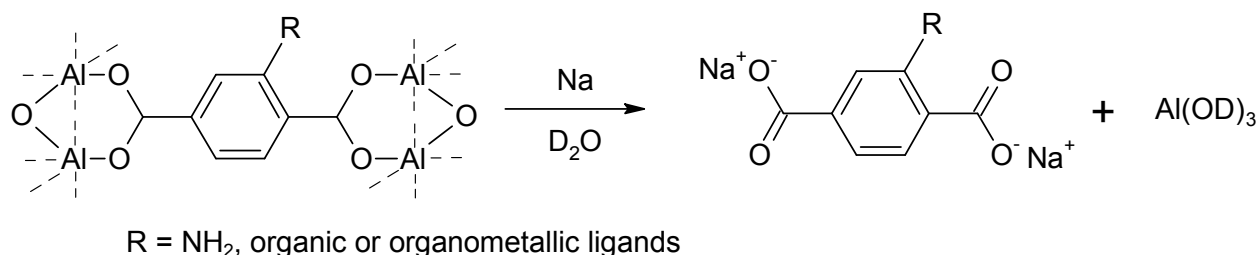
Scheme 3.5:   Digestion of amino-MIL-53(Al) or its post-synthetically modified derivatives for liquid NMR studies.

Since the benzene rings of amino-MIL-53(Al) are asymmetrically substituted with the single amine group in the 2-position, NMR spectroscopy can be used to identify all the protons on the benzene ring individually (Figure 3.8, p 48).
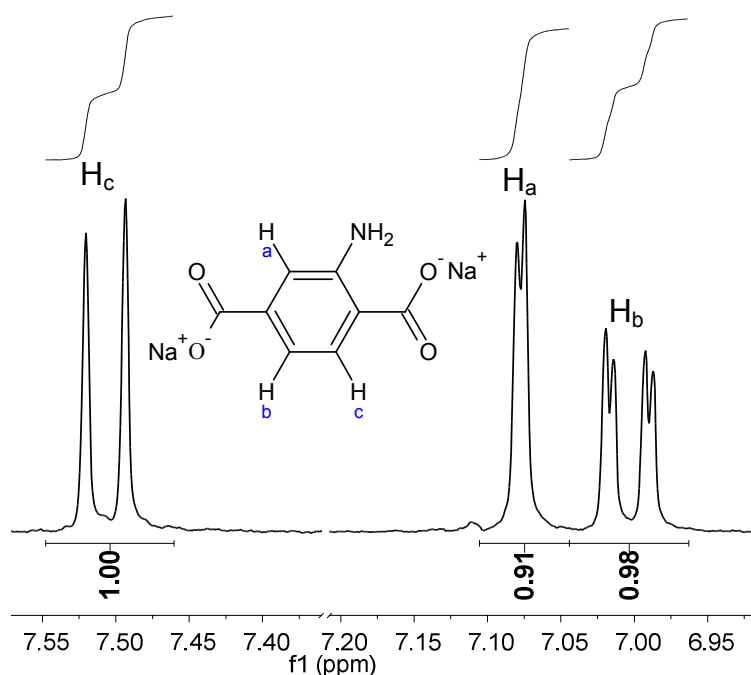

Figure 3.8:   Liquid ^{1}H NMR spectrum of amino-MIL-53(Al), digested in NaOD/D$_2$O showing the position of the three different protons on the phenyl rings of the organic linker.

Starting from the left in Figure 3.8 (p 48), H$_c$ gives a doublet at 7.5 ppm coupling with H$_b$ (J^1 = 8.1 Hz). H$_a$ gives a doublet at 7.08 ppm with a small coupling constant to H$_b$ (J^2 = 1.6 Hz). H$_b$ at 7 ppm has both primary and secondary coupling with H$_c$ and H$_a$ respectively giving a doublet of doublets.

TG analyses of the as-synthesised and activated products of amino-MIL-53(Al) (from two different synthesis methods) are shown in Figure 3.9 (p 49). All four thermograms show a first mass loss after 50°C (i), due to evaporation of adsorped water in the case of a), b) and d), as well as residual water in the case of c). Amino-MIL-53(Al)-as from the H_2O/DMF (9:1) synthesis is the only compound which had contact with liquid water, resulting in a prolonged mass loss step (c, i). This mass loss would also include DMF leaving the channels of the MOF. Amino-MIL-53(Al)-as from the DMF synthesis (Scheme 3.3, p 45) loses DMF together with the free 2-aminoterephthalic acid after 138°C (a, ii). DMF could act as a solvent, assisting the free acid's movement.
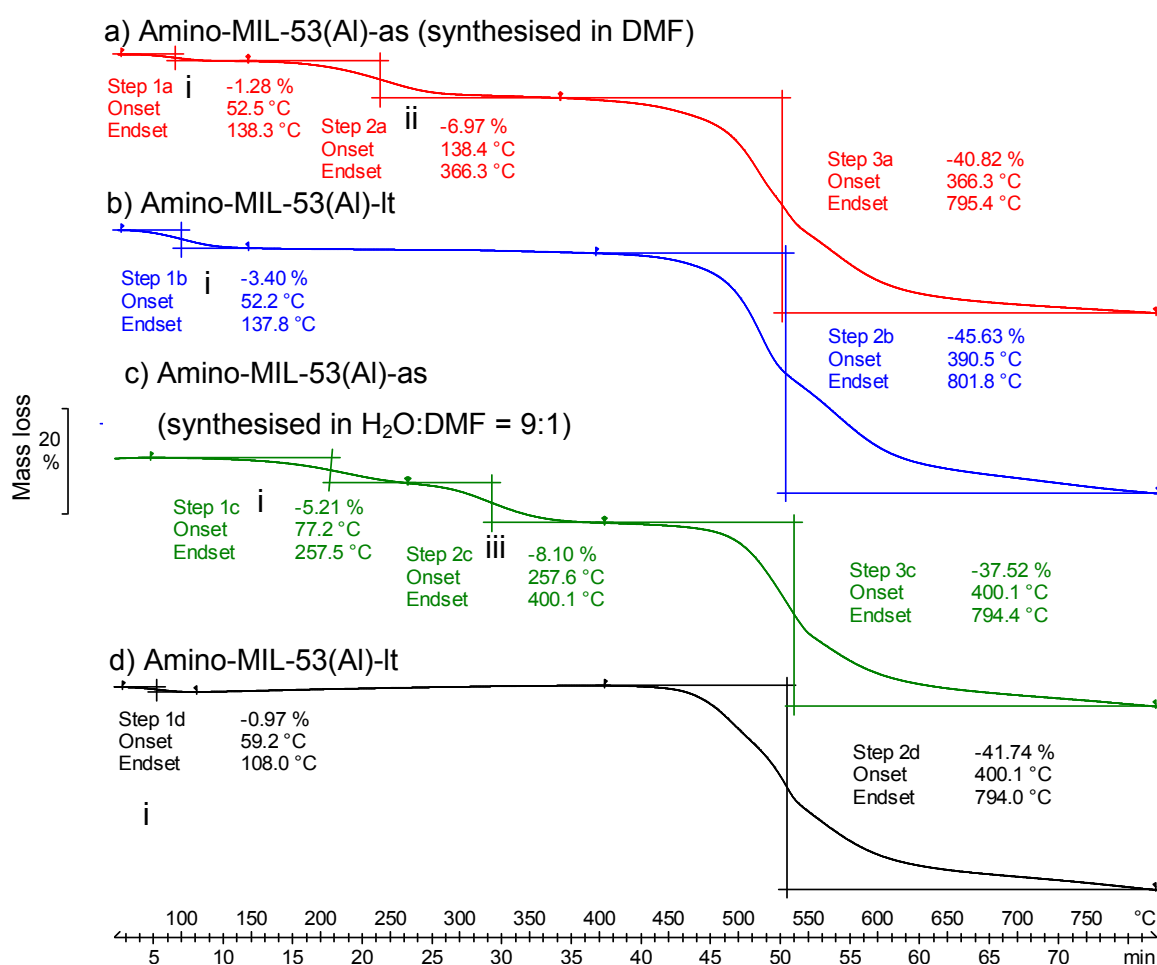

Figure 3.9: TGA thermograms (under Ar) for amino-MIL-53(Al)-as (a) and amino-MIL-53(Al)-lt (b) from the DMF synthesis, as well as for amino-MIL-53(Al)-as (c) and amino-MIL-53(Al)-lt (d) from the H_2O:DMF = 9:1 synthesis.

The second mass loss of amino-MIL-53(Al)-as (synthesised in H_2O:DMF = 9:1) (Figure 3.9, (c) iii, p 49) after 250°C, represents the leaving of free 2-aminoterephthalic acid. All four amino-MIL-53(Al) structures were stable up to 400°C after which structural decomposition started.

Porosity measurements on the activated amino-MIL-53(Al)-ht (synthesised with two different methods) gave a type II isotherm (Graph 3.2, p 50) with little adsorption in the low pressure Langmuir range where p/p° < 0.1. The results are summarised in Table 3.2 (p 50).
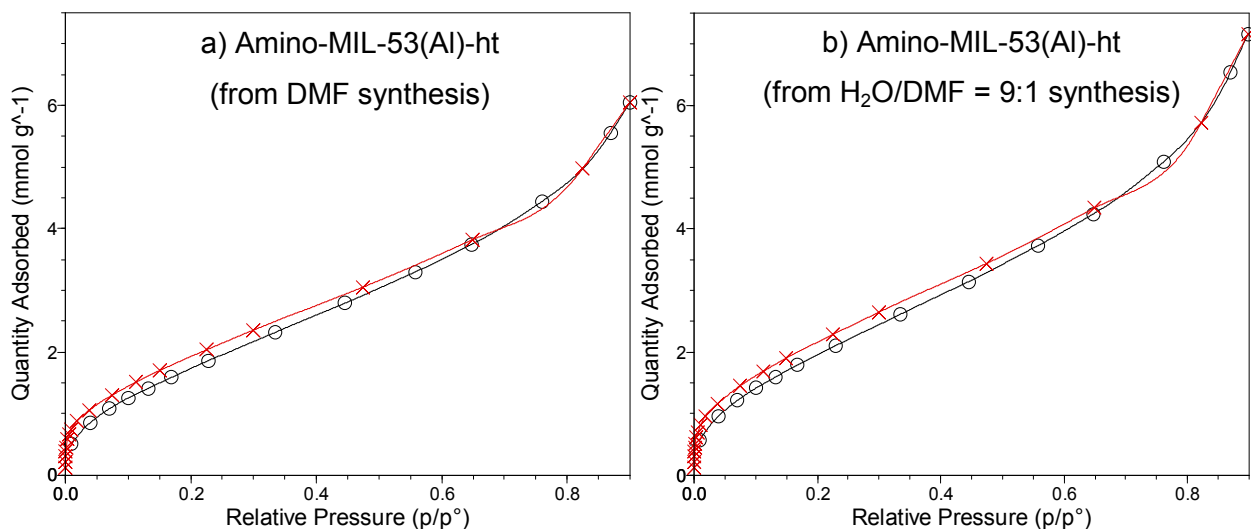
Graph 3.2: N_2 adsorption (red crosses) and desorption (black circles) at 77 K of amino-MIL-53(Al)-ht: from synthesis with DMF as solvent (a) and from synthesis with H_2O/DMF = 9:1 as solvent (b).

Table 3.2: N_2 porosity measurement results for amino-MIL-53(Al)-ht done at 77 K.

Amino-MIL-53(Al)-ht	Langmuir Surface Area (m^2g^{-1})	BET Surface Area (m^2g^{-1})	Pore volume (cm^3g^{-1})
Synthesised in DMF	627 ± 54	201 ± 0.9	0.25
Synthesised in H_2O:DMF = 9:1	551 ± 48	178 ± 0.8	0.21

PXRD analysis of the two amino-MIL(Al)-lt products gave identical patterns with five prominent peaks in the range $8° < 2\theta < 30°$. These identical PXRD spectra are representative of the amino-MIL-53(Al)-lt which was first produced by Stock *et al.*[6] Regular crystallinity is portrayed by the sharp peaks on the graphs. The PXRD of amino-MIL-53(Al)-lt (synthesised in H_2O:DMF = 9:1) is shown as a representative sample in Figure 3.10 (p 51). See Appendix, Spectrum 24 (A-15) for the PXRD of amino-MIL-53(Al)-lt (synthesised in DMF).
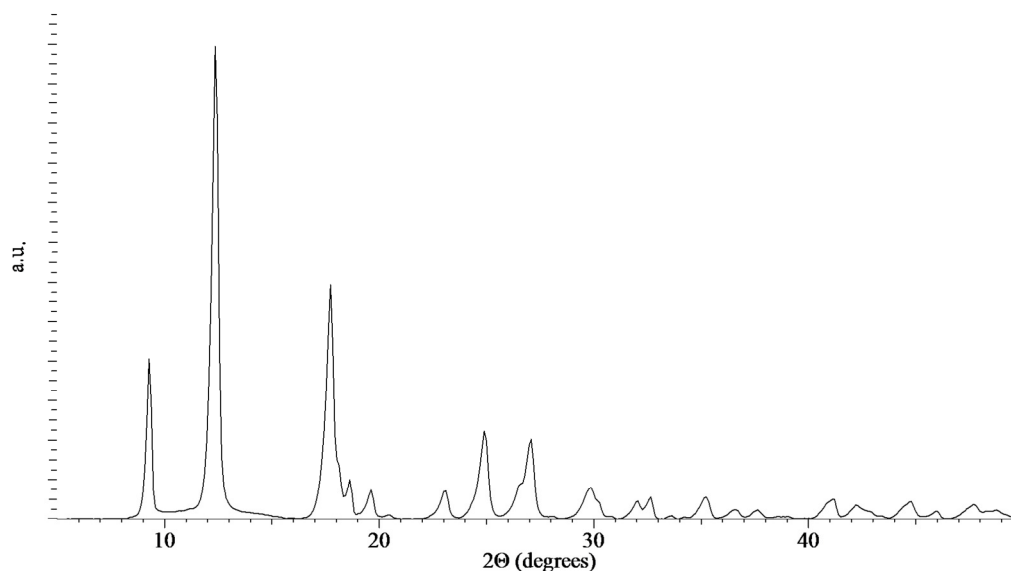

Figure 3.10:   PXRD of amino-MIL-53(Al)-lt (synthesised in H_2O:DMF = 9:1).

3.3. Post-Synthetic Modification (PSM)

PSM was applied on both MIL-53(Al) and amino-MIL-53(Al). A series of short-chain, aliphatic acids (RCOOH, with R = H and R = $CH_3(CH_2)_n$ with n = 0, 1, 2) as well as ferrocene (Fc) were employed as probe molecules to be intruded into the microporous channels of the MOFs. In the case of amino-MIL-53(Al), the aliphatic acids as well as ferrocene carboxylic acid were not only intruded into the channels of the structure, but also reacted with the amine groups on the linkers. From nitrogen adsorption studies, it was already determined that the migration of molecules through the MOF structure is restricted by the size of the small channels making up the frameworks of MIL-53(Al) and amino-MIL-53(Al).[6] This migration through the frameworks will also have an influence on the maximum chemical conversion that can be achieved in the case of amino-MIL-53(Al). An aim of this study is to establish whether the intrusion period before the chemical reaction is crucial for the success of linking the intruded acid to the framework structure *via* an amide bond.
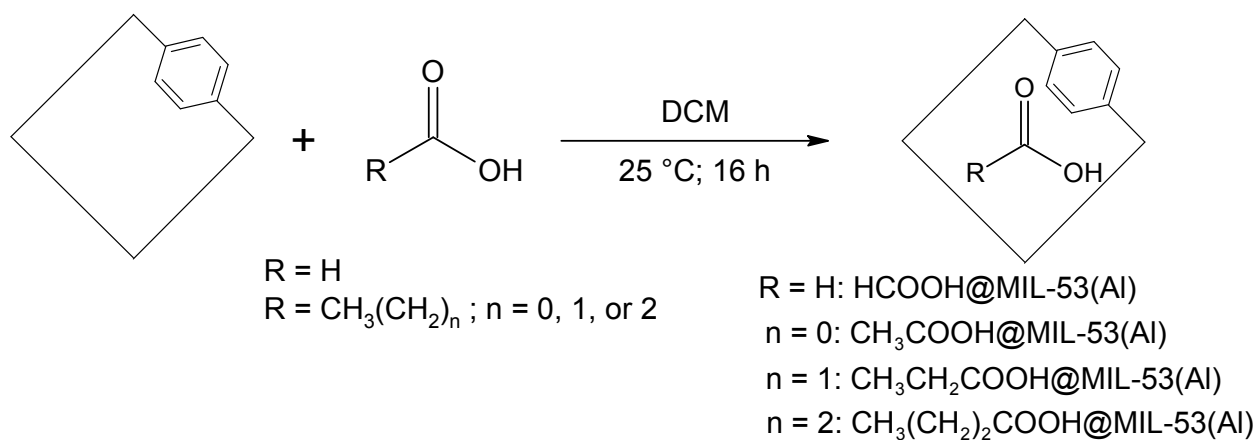
In this study, a well-known intrusion method, Incipient Wetness Impregnation (IWI), was adapted and implemented on MIL-53(Al) as well as amino-MIL-53(Al). Knowing that

evacuated MIL-53(Al) and amino-MIL-53(Al) (called the ht-form) are hygroscopic and that the presence of hydrogen-bonded water molecules will shrink the channels to their minimum diameter, the MOFs were activated at 150°C overnight under high vacuum, prior to PSM. To start the intrusion, the activated MOF was kept under vacuum while introducing and covering the MOF with the reagent (probe material) either dissolved in an appropriate, anhydrous solvent or used as is (if it is a liquid). With the use of this modified IWI method, the internal migration of molecules inside the MOF channels could be studied and quantified using proton Nuclear Magnetic Resonance spectroscopy (^{1}H NMR) and Thermogravimetric Analyses (TGA).

3.3.1. Loading of Aliphatic Acids in MIL-53(Al) Derivatives

3.3.1.1. MIL-53(Al)

Only PSM by physisorption of a series of four aliphatic carboxylic acids (RCOOH where R = H and R = $CH_3(CH_2)_n$ with n = 0, 1 or 2) were performed on MIL-53(Al)-ht as shown in Scheme 3.6 (p 52).

R = H
R = $CH_3(CH_2)_n$; n = 0, 1, or 2

R = H: HCOOH@MIL-53(Al)
n = 0: CH_3COOH@MIL-53(Al)
n = 1: CH_3CH_2COOH@MIL-53(Al)
n = 2: $CH_3(CH_2)_2COOH$@MIL-53(Al)

Scheme 3.6:   Reaction scheme for the physisorption of four aliphatic, carboxylic acids into MIL-53(Al)-ht (anhydrous) done at room temperature.

HCOOH@MIL-53(Al)[*] was the first product obtained. One equivalence (towards the terephthalate linkers in the MOF) of formic acid dissolved in dry DCM was intruded (16 hours) into the MOF structure, followed by thorough washing of the powder with DCM in order to

---

[*] In this context and throughout the research protect, the "@" sign indicates molecules intruded into the framework of the MOF without any covalent bonding.

remove all molecules not intruded into the pores. This was done as quickly as possible, using centrifugation to isolate the powder and minimize leaching of the intruded reagent from the microporous channels. $CH_3COOH@MIL-53(Al)$, $CH_3CH_2COOH@MIL-53(Al)$ and $CH_3(CH_2)_2COOH@MIL-53(Al)$ were all produced in the same manner as for $HCOOH@MIL-53(Al)$. All four products are light-grey in colour.

After digestion of the aliphatic acid-loaded MIL-53 samples in $NaOD/D_2O$, the ^1H NMR spectra of $RCOOH@MIL-53(Al)$ (R=H, $CH_3(CH_2)_n$ with n = 0,1,2) showed the presence of the different carboxylic acids as seen in Figure 3.11 (p 54). With $HCOOH@MIL-53(Al)$ (a), the singlet from the C-H proton of formic acid is observed at 8.30 ppm. $CH_3COOH@MIL-53(Al)$ (b) shows a singlet for the $-CH_3$ protons at 1.77 ppm. These $-CH_3$ protons are observed as triplets below 1 ppm for $CH_3CH_2COOH@MIL-53(Al)$ (c) and $CH_3(CH_2)_2COOH@MIL-53(Al)$ (d). The methylene protons of $CH_3CH_2COOH@MIL-53(Al)$ (c) and $CH_3(CH_2)_2COOH@MIL-53(Al)$ (d) are represented by peaks between 2.1 and 1.3 ppm.

The amount of aliphatic acid intruded into MIL-53(Al) could also be established by comparing the relative integration of the aliphatic protons to that of the aromatic protons of the terephthalate fragments (7.75 ppm; Figure 3.11, p 54). Since these carboxylic acids were physisorbed, their quantity is expressed relative to the unit cell of the MIL-53(Al) structure as seen in Table 3.3 (p 54). With $HCOOH@MIL-53(Al)$, 80% of the MIL-53(Al) unit cells each contains a molecule of formic acid. In the case of $CH_3COOH@MIL-53(Al)$, the amount of physisorbed acetic acid (0.63) was determined from the $-CH_3$ signal (Figure 3.11 b, p 54) after subtracting the amount of residual water obscured by the $-CH_3$ signal in (b), at an average of 3.3% (calculated from (a), (c) and (d) with 2.5, 3.5 and 4.0% respectively). The physisorption ratio of propionic acid and butyric acid in MIL-53(Al) was calculated to be 0.55 and 0.39 respectively. This decrease in the physisorption yield with an increase in carbon chain length of the carboxylic acids could be caused by a decrease in mobility of the molecules through the microporous material as the carbon chain length increases.

Table 3.3: Relative amounts of aliphatic acids (RCOOH@MIL-53(Al)) (R=H, $CH_3(CH_2)_n$ with n = 0,1,2) physisorbed in MIL-53(Al) after 16 hours of Incipient Wetness Impregnation (IWI), as analysed by ^1H NMR in $NaOD/D_2O$.

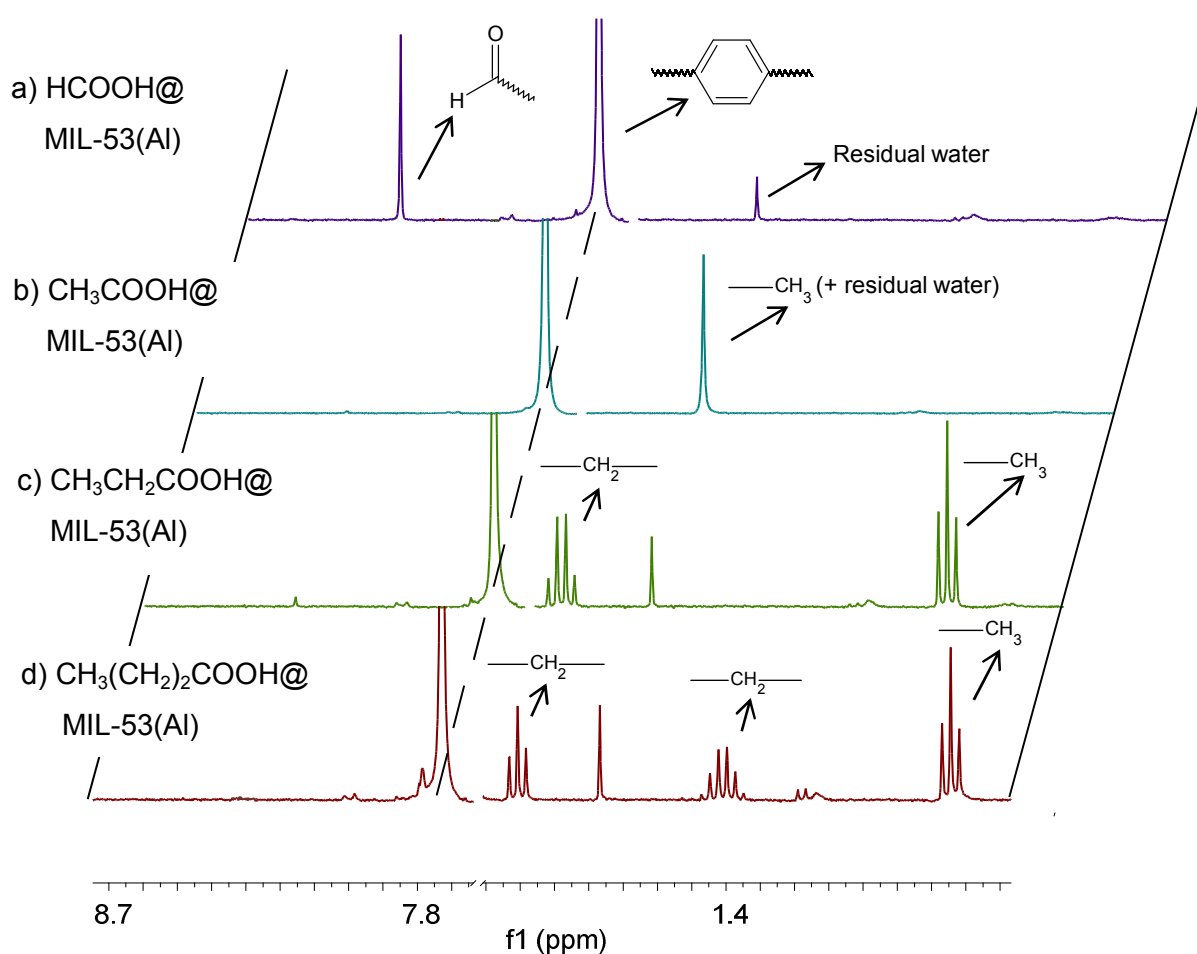| Carboxylic acid in MIL-53(Al)	NMR Integration				Intrusion ratio (molecules per unit cell)
	Ar-H	-CH$_2$	-CH$_2$-	-H (Formic acid) or -CH$_3$	
HCOOH	4	-	-	0.20	0.80
CH$_3$COOH	4	-	-	0.57	0.63
CH$_3$CH$_2$COOH	4	-	0.28	0.41	0.55
CH$_3$(CH$_2$)$_2$COOH	4	0.19	0.18	0.32	0.39

Figure 3.11: 3D Stacked ^1H NMR spectra of HCOOH@MIL-53(Al) (a, purple), CH$_3$COOH@MIL-53(Al) (b, blue), CH$_3$CH$_2$COOH@MIL-53(Al) (c, green) and CH$_3$(CH$_2$)$_2$COOH@MIL-53(Al) (d, red) showing the resonance peaks from the different aliphatic carboxylic acid protons as well as the prominent singlet from the aromatic protons at 7.75 ppm in each spectrum.

RESULTS & DISCUSSION

TG analyses of the four aliphatic acid-impregnated MIL-53(Al) compounds are shown in Figure 3.12 (p 55), each displaying three mass loss steps. The first step in each thermogram (Step 1(a-d)) can be assigned to the loss of solvent (DCM), as well as adsorbed water vapour trapped inside the channels of the MOF and is less than 0.6% for all four products. The second step for each compound is attributed towards the specific carboxylic acid intruded into MIL-53(Al)-ht. When the mass losses of step 2(a-d) are expressed in terms of molecules leaving per unit cell (see Table 3.4, p 56), the values do not correlate to the molecular load obtained during ^{1}H NMR analyses (Table 3.3, p 54). These lower values could result from carbonisation of the aliphatic carboxylic acid molecules inside the channels of MIL-53(Al) during the TGA procedure. After 450°C, all four compounds show identical structural breakdown (step 3(a-d)), as found for MIL-53(Al) in section 3.2.1.2 (p 42).
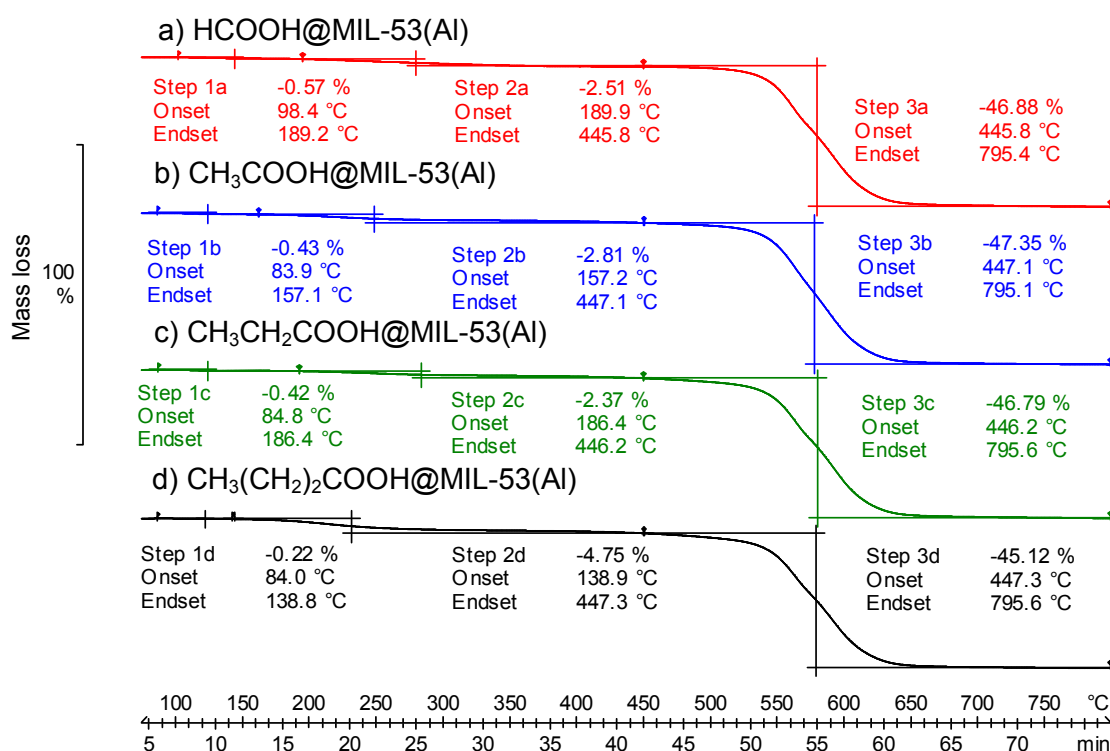

Figure 3.12: TG thermograms of HCOOH@MIL-53(Al) (a) CH$_3$COOH@MIL-53(Al) (b), CH$_3$CH$_2$COOH@MIL-53(Al) (c) and CH$_3$(CH$_2$)$_2$COOH@MIL-53(Al) (d) displaying three mass loss steps. TGA was performed in Argon atmosphere.

Table 3.4: Results of TG analyses showing the relative loss of impregnated carboxylic acids from RCOOH@MIL-53(Al) (R=H, $CH_3(CH_2)_n$ with n = 0,1,2).

Carboxylic acid in MIL-53(Al)	Mass loss (wt%)	Mass loss (molecules per unit cell)
HCOOH	2.51	0.46
CH_3COOH	2.81	0.40
CH_3CH_2COOH	2.37	0.27
$CH_3(CH_2)_2COOH$	4.75	0.45

The FTIR spectra of all the acid-containing MIL-53 products (except for $CH_3(CH_2)_2COOH@MIL-53(Al)$) are displayed in Appendix, Spectrum 3 (A-1). Since less than 5 wt% of carboxylic acid compounds were present in the MOF structures, only a small C=O peak around 1670 cm^{-1} (i) is visible in Figure 3.13 (p 56). The alkane CH_3 and CH_2 stretching frequencies usually found the region 3000 to 2850 cm^{-1} could not be detected.
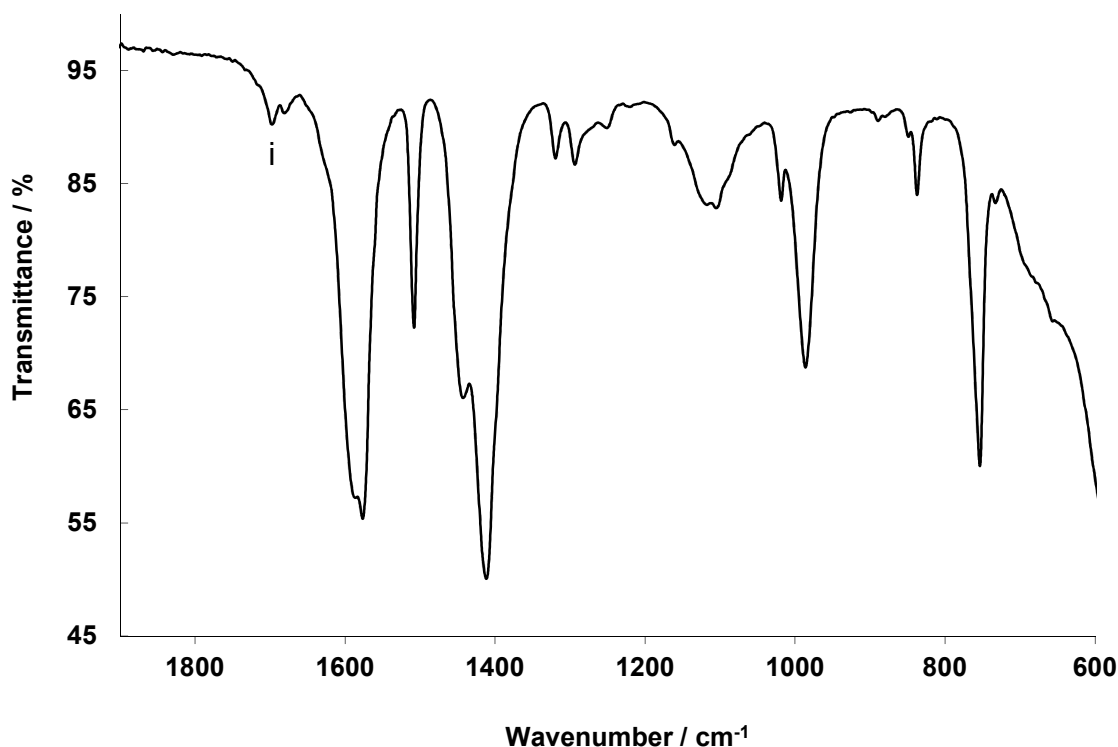

Figure 3.13: FTIR spectrum of $CH_3(CH_2)_2COOH@MIL-53(Al)$.

PXRD analyses of the four aliphatic acid loaded MIL-53(Al) compounds displayed similar spectra up to 2θ = 50°, compared to the PXRD pattern of commercial MIL-53(Al)-lt, as seen in Figure 3.14 (p 57). Differences in peak intensities can be attributed to slight differences in

sample preparation and sample size. This means that no structural changes to MIL-53(Al) occurred during the impregnation process.
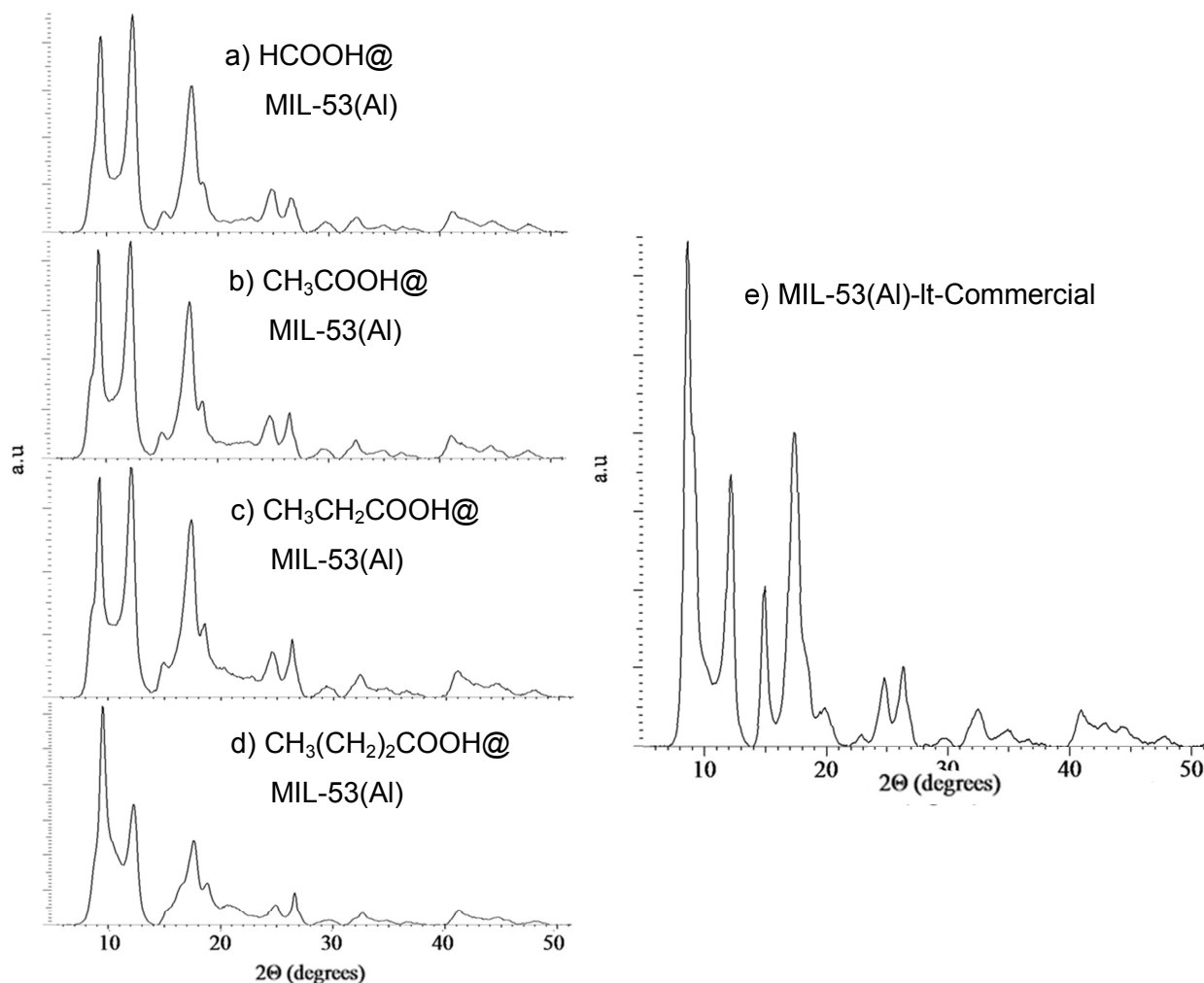

Figure 3.14: PXRD scans of HCOOH@MIL-53(Al) (a), CH₃COOH@MIL-53(Al) (b), CH₃CH₂COOH@MIL-53(Al) (c) and CH₃(CH₂)₂COOH@MIL-53(Al) (d) compared to MIL-53(Al)-lt (e) as reference. All the acid-containing products were exposed to the atmosphere and are in the lt-form.

3.3.1.2. Amino-MIL-53(Al)

With amino-MIL-53(Al), the same four carboxylic acids as used in section 3.3.1.1 (p 52), were intruded into the framework followed by chemical bonding to the amine-functionalised terephthalate linkers, as shown in Scheme 3.7 (p 58).
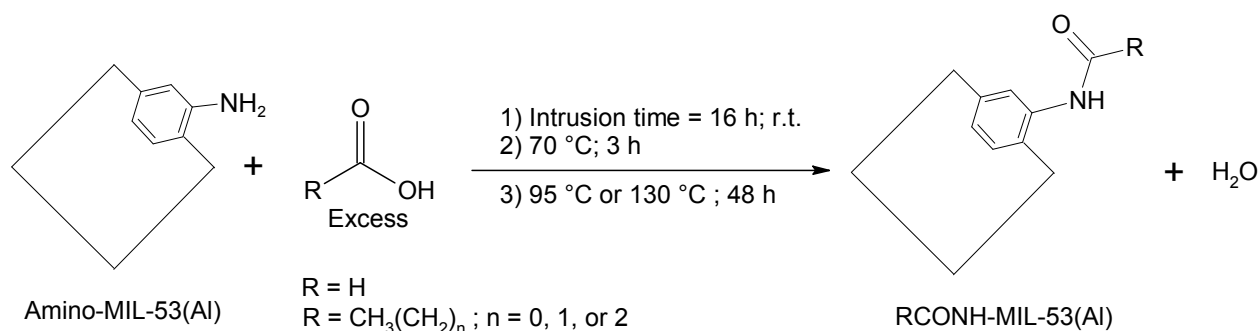
Scheme 3.7: Reaction scheme for the chemical binding of four aliphatic, carboxylic acids (RCOOH (R=H, $CH_3(CH_2)_n$ with n = 0,1,2)) to amino-MIL-53(Al)-ht through amidation.

In this study, the Incipient Wetness Impregnation (IWI) method used by Stock *et al.*[6] to synthesise HCONH-MIL-53(Al) was improved in order to eliminate the presence of atmospheric vapour, before the intrusion of the acid reagents. This was done by keeping the amino-MIL-53(Al) powder under vacuum until covering it with the acid (liquid). Using the carboxylic acid as a liquid ensured a maximum concentration of the molecules to be intruded. Intrusion of the acid molecules into the framework was performed at room temperature to maximise loading without chemical bonding. After an intrusion of 16 hours, the carboxylic acid was allowed to react with the amine groups at 70°C for three hours before removing unreacted acid by washing with water. The amidation reaction was then recommenced at 95°C (for HCOOH) or 130°C (for the other three acids) for two days, before extracting water (a reaction by-product) and free acid from the channels of the MOF at 80°C under high vacuum overnight. As determined by FTIR, the 130°C (used in the case of the higher boiling acids) creates too harsh conditions for formic acid. The unbound acid from $CH_3CONH-MIL-53(Al)$, $CH_3CH_2CONH-MIL-53(Al)$ and $CH_3(CH_2)_2CONH-MIL-53(Al)$ were removed at 100°C, 120°C and 150°C respectively

The FTIR spectra of the RCONH-MIL-53(Al) products are shown in Figure 3.15 (p 59), but only in the case of HCONH-MIL-53(Al), peaks from the amide bond are clearly seen. The two NH_2 stretching frequencies usually found between 3500 and 3400 cm^{-1}, are now a single peak at 3307 cm^{-1} (i) for the N-H bond. The amide bond's C=O stretching frequency is found at 1685 cm^{-1} (ii), with the C-N stretching frequency of the amide at 1270 cm^{-1} (iii). When comparing the peak at 1414 cm^{-1} (iv) with the spectrum of amino-MIL-53(Al) (Figure 3.7 d, p 47), it is clear that the two symmetric stretching frequencies of the carboxyl groups coordinated to Al are influenced by possible hydrogen bonding from the formamido groups, causing further splitting of these peaks.
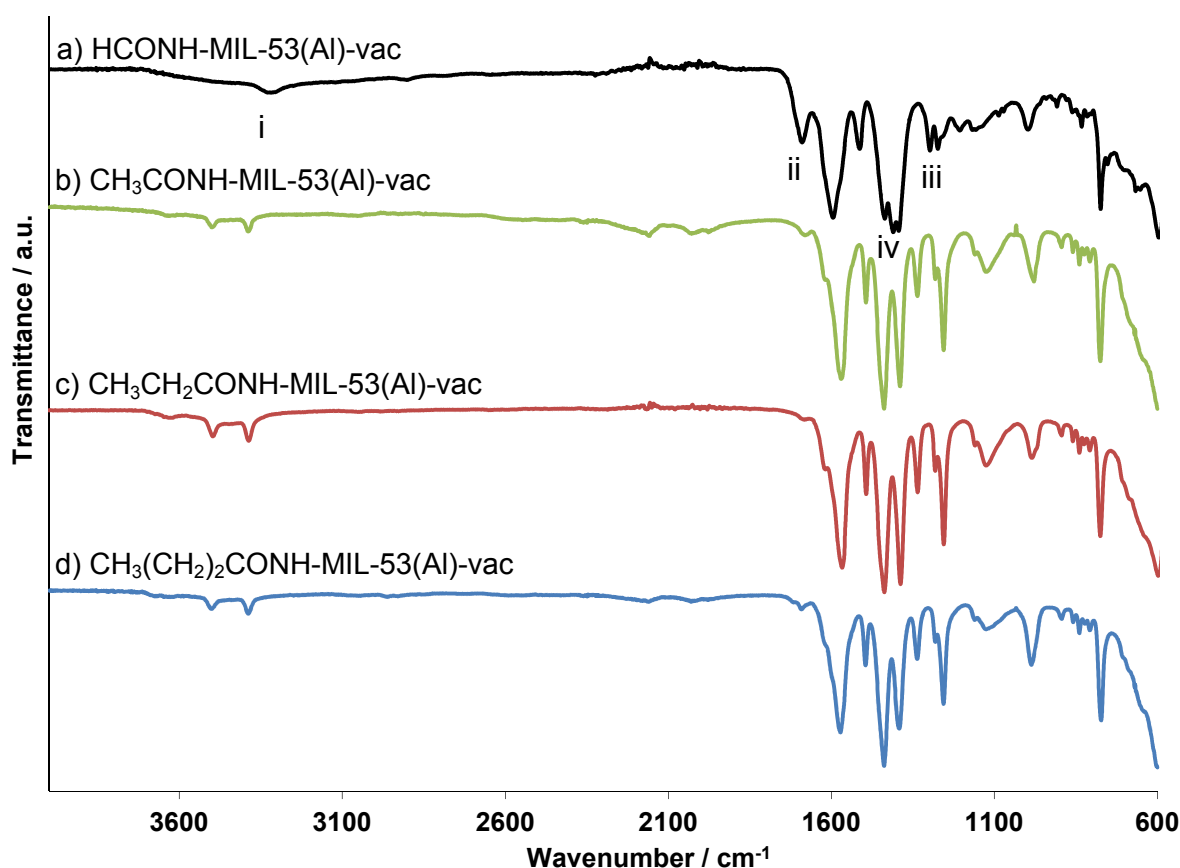
Figure 3.15: FTIR spectra of HCONH-MIL-53(Al)-vac (a, black), CH_3CONH-MIL-53(Al)-vac (b, green), CH_3CH_2CONH-MIL-53(Al)-vac (c, red) and $CH_3(CH_2)_2CONH$-MIL-53(Al)-vac (after a 16 hours intrusion time) (d, blue).

In the case of CH_3CONH-MIL-53(Al)-vac (Figure 3.15 b, p 59), CH_3CH_2CONH-MIL-53(Al)-vac (c) and $CH_3(CH_2)_2CONH$-MIL-53(Al)-vac (d), no significant peaks due to amidation could be observed since the degree of amidation was too low to be detected by FTIR.

For ^{1}H NMR studies, the RCONH-MIL-53(Al) products had to be digested in $NaOD/D_2O$ prior to measurement. During the digestion of HCONH-MIL-53(Al)-vac, hydrolysis of the amide bond occurred, leading to unreliable results. Only the ^{1}H NMR spectra of the digested CH_3CONH-MIL-53(Al)-vac and CH_3CH_2CONH-MIL-53(Al)-vac are shown in Figure 3.16 (p 60) since the spectra of the $CH_3(CH_2)_2CONH$-MIL-53(Al)-vac products will be discussed in detail in section 3.3.2 (p 63) (See Appendix, Spectrum 7, A-5 for the ^{1}H-NMR analysis of the as-synthesised products). The success of chemically binding the aliphatic acids to the amino-MIL-53(Al) framework can be determined by ^{1}H NMR and will be expressed as a conversion percentage based on the total number of NH_2 groups available for amidation. The three aromatic protons of the terephthalate fragment were used to calculate the relative amount of bound acid.
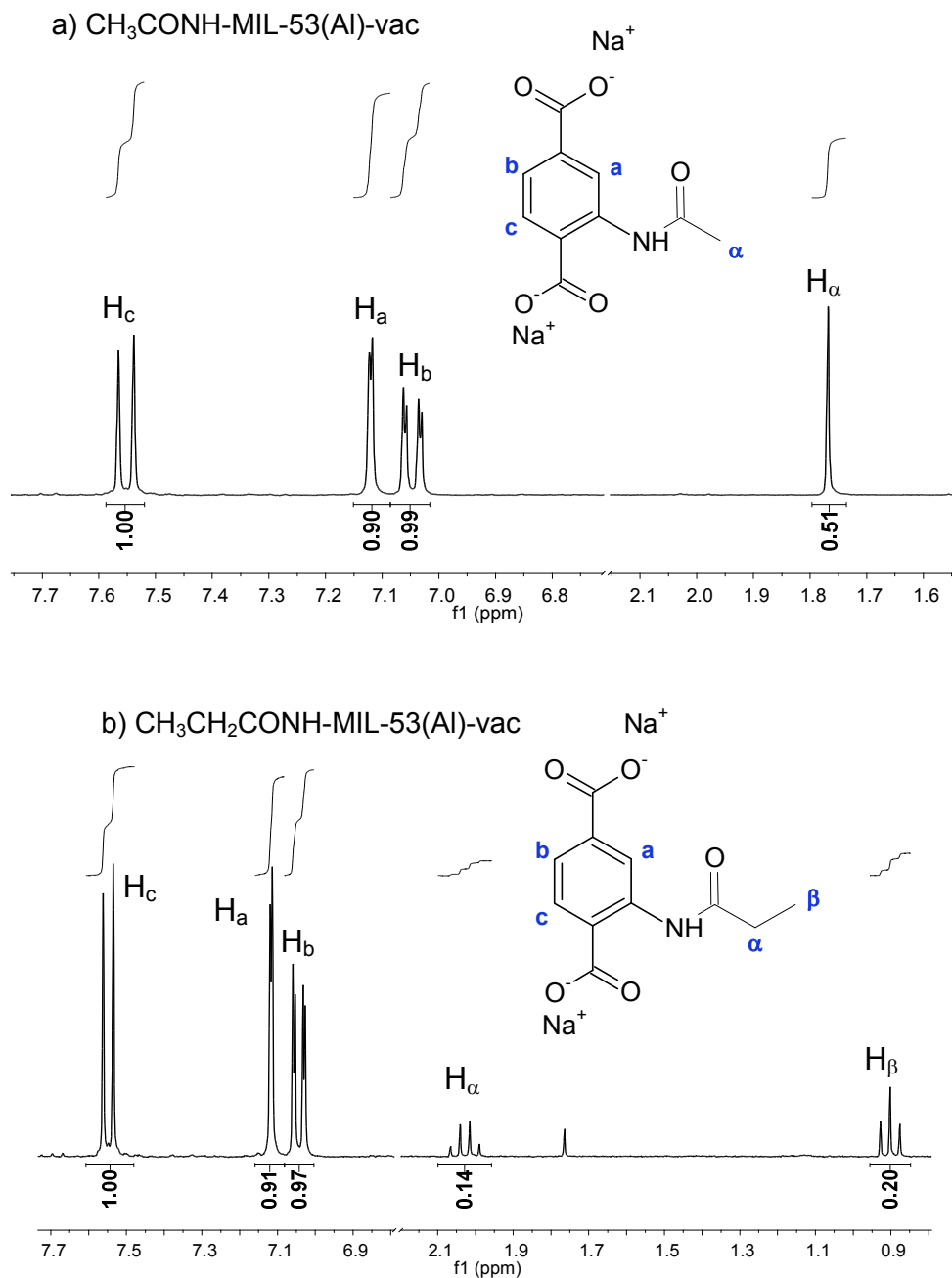
a) CH₃CONH-MIL-53(Al)-vac

b) CH₃CH₂CONH-MIL-53(Al)-vac

Figure 3.16: ^{1}H NMR spectra of CH₃CONH-MIL-53(Al)-vac (a) and CH₃CH₂CONH-MIL-53(Al)-vac (b) obtained after digestion by NaOD/D₂O.

The ^{1}H NMR spectrum of CH₃CONH-MIL-53(Al)-vac (Figure 3.16 a, p 60) displays a singlet at 1.77 ppm for the CH₃ protons of the acetamido group giving a minimum conversion of 17.6%. The ^{1}H NMR spectrum of CH₃CH₂CONH-MIL-53(Al)-vac (b) displays a quartet and a triplet for the CH₂ and CH₃ protons respectively resulting in 7.1% conversion for this compound. Conversion percentages from digestive ^{1}H NMR studies are minimum values, since hydrolysis of the amide bond prior to measurement may occur.

Thermogravimetric (TG) analyses performed on the evacuated forms of HCONH-MIL-53(Al), CH$_3$CONH-MIL-53(Al) and CH$_3$CH$_2$CONH-MIL-53(Al) (Figure 3.17, p 61 (See Appendix, Spectrum 12b-d (A-10) for the TGAs of the as-synthesised products) show three steps in mass loss in the case of HCONH-MIL-53(Al)-vac and CH$_3$CH$_2$CONH-MIL-53(Al)-vac of which step 1 is the loss of adsorbed water. No adsorption of water vapour could be detected in CH$_3$CONH-MIL-53(Al)-vac. The thermogravimetric behaviour of the fourth compound (CH$_3$(CH$_2$)$_2$CONH-MIL-53(Al)) will be discussed in detail in section 3.3.2 (p 63).

For the three compounds in (Figure 3.17, p 61), the mass loss due to the covalent bound aliphatic fragments can be observed between 150°C and 400°C. All three compounds show structural integrity up to 400°C.
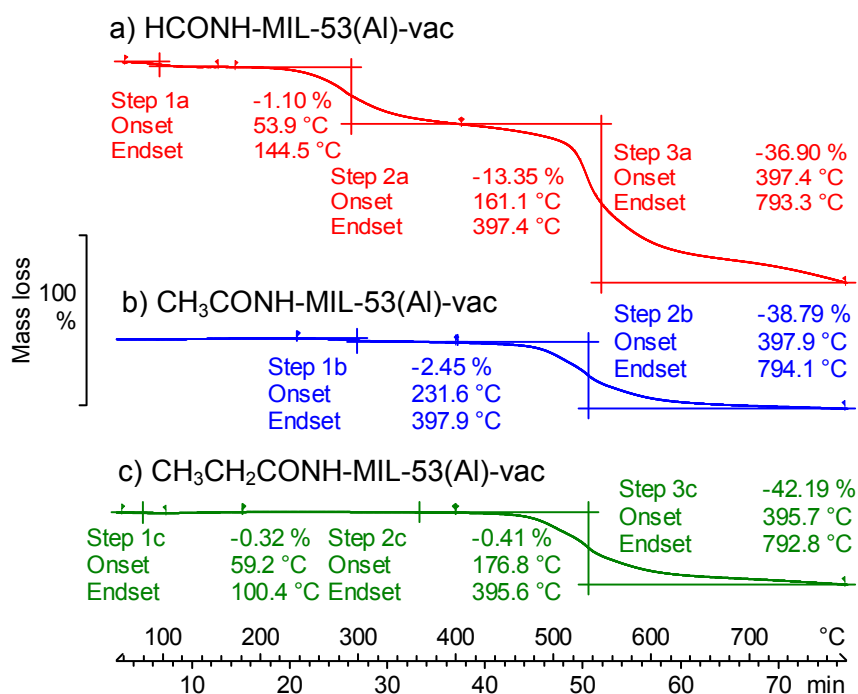

Figure 3.17: TGA thermograms of HCONH-MIL-53(Al)-vac (a, red), CH$_3$CONH-MIL-53(Al)-vac (b, blue) and CH$_3$CH$_2$CONH-MIL-53(Al)-vac (c, green).

The PXRD analyses of HCONH-MIL-53(Al)-vac to CH$_3$(CH$_2$)$_2$CONH-MIL-53(Al)-vac (16 hours intrusion time) are displayed in Figure 3.18 (p 62). When comparing HCONH-MIL-53(Al)-vac (a) to the original amino-MIL-53(Al)-lt (e), additional peaks were found at 2θ = 10.5° (i), 15° (ii) and 21.5° (iii) which could indicate the presence of formic acid molecules packed in the framework since the bound formamido molecules will form part of the existing peaks of amino-MIL-53(Al). Due to the thoroughly evacuated HCONH-MIL-53(Al)-vac, the small amount of formic acid which was left, could have formed extremely strong hydrogen

bonds with the framework making them very difficult to be removed without destroying the framework. The additional peaks (a) could also result from structural deformation due to the presence of formic acid in the framework channels. The PXRD spectrum of HCONH-MIL-53(Al)-vac correlates well with the same product obtained by Stock *et al.*,[6] indicating a high conversion, supported by its FTIR spectrum by showing no NH_2 stretching frequencies (Figure 3.15 a, p 59). The PXRD spectra of CH_3CONH-MIL-53(Al)-vac (b) and CH_3CH_2CONH-MIL-53(Al)-vac (c) display similar patterns when compared to amino-MIL-53(Al)-lt (e), meaning that the evacuation of the free acid was successful. The PXRD spectrum of $CH_3(CH_2)_2CONH$-MIL-53(Al)-vac also displays three extra peaks at $2\theta = 10.5°$ (iv), $16.5°$ (v) and $20.5°$(vi) which directs to a very small amount of free acid left probably due to free acid molecules, which could not be evacuated because of the bound butyramido molecules blocking the path inside the framework.
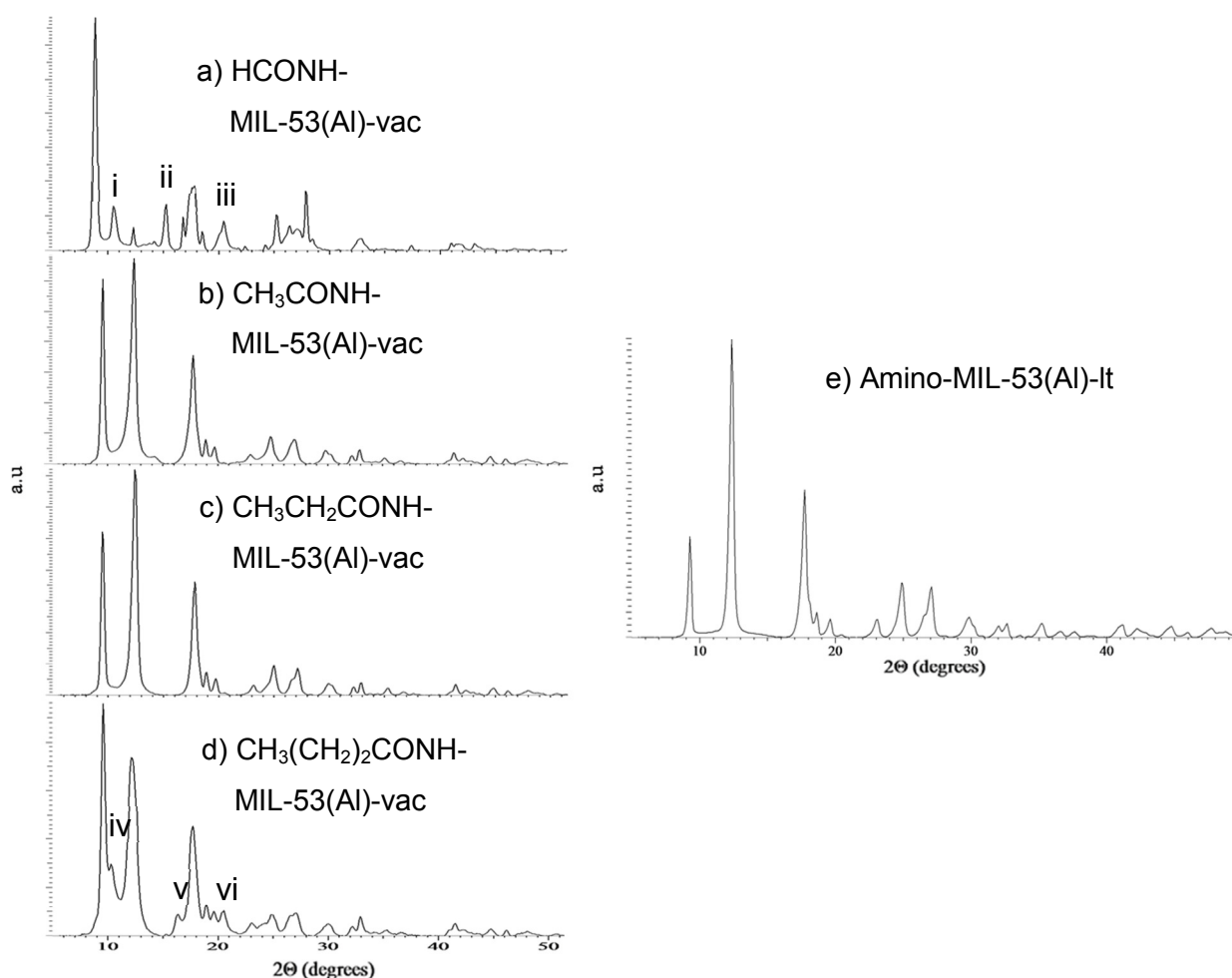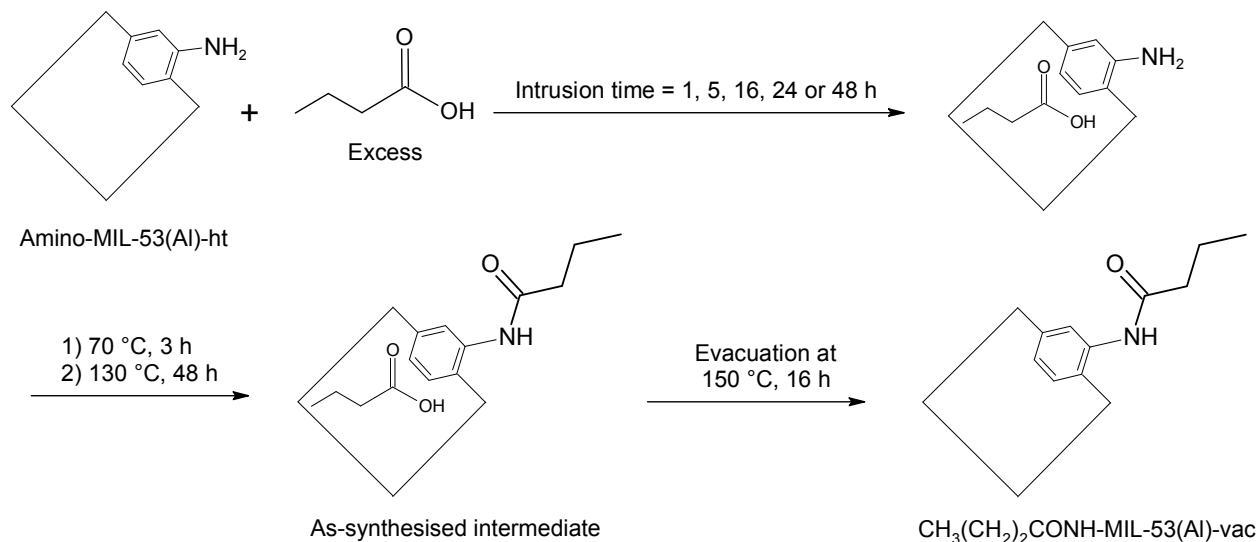

Figure 3.18: PXRD analysis of HCONH-MIL-53(Al)-vac (a), CH_3CONH-MIL-53(Al)-vac (b), CH_3CH_2CONH-MIL-53(Al)-vac (c), $CH_3(CH_2)_2CONH$-MIL-53(Al)-vac (d) compared to the PXRD of amino-MIL-53(Al)-lt (e).

3.3.2. CH₃(CH₂)₂COOH in amino-MIL-53(Al) – Time-Resolved Study

Scheme 3.8: Reaction scheme for the chemical binding of butyric acid to amino-MIL-53(Al) through amidation while varying the intrusion time before amidation.

The synthesis of CH₃(CH₂)₂CONH-MIL-53(Al) (using the same method as seen in Scheme 3.7 (p 58) in section 3.3.1.2) was used to study the internal migration behaviour of molecules in the channels of amino-MIL-53(Al). The reaction was repeated (using the same scale of reagents every time) for five times by varying the intrusion time (1, 5, 16, 24 or 48 hours) when introducing butyric acid to amino-MIL-53(Al) after activation. From these five reactions, the as-synthesised products (CH₃(CH₂)₂CONH-MIL-53(Al)-as), as well as the evacuated products (CH₃(CH₂)₂CONH-MIL-53(Al)-vac) were obtained. To obtain the evacuated or activated products, the as-synthesised products were heated at 150°C under high vacuum overnight. These two types of products were then compared in order to determine the amount of free, unreacted butyric acid in the channels of the framework, as well as the amount of butyric acid covalently bound to the framework. The as-synthesised products contain both free and bound butyric acid, whereas the evacuated products contain only the bound butyric acid. The relative amounts of free and bound butyric acid of the five different timed-intrusions (1, 5, 16, 24 and 48 hours) where determined by comparison of ^{1}H NMR and TGA results.

The FTIR spectrum of CH₃(CH₂)₂CONH-MIL-53(Al)-vac (16 hours intrusion time) was already discussed in Figure 3.15 d (p 59). The FTIR spectra of both the as-synthesised and the evacuated forms of CH₃(CH₂)₂CONH-MIL-53(Al) (from the other intrusion times) resulted in similar spectra (see Appendix, Spectrum 4, A-2).

In Figure 3.19 (p 64), the ^{1}H NMR spectra of the $CH_3(CH_2)_2CONH$-MIL-53(Al) products, as-synthesised (a) and evacuated (b), after an intrusion time of 16 hours, are shown as representative of the five pairs of products (see Appendix, Spectrum 8 & 9, A-6 to A-7) for the other eight products). The two sets of CH_2 protons of the aliphatic carbon chains are situated at 2.00 ppm (triplet) and 1.47-1.35 ppm (multiplet) respectively while the end CH_3 protons are found at 0.75 ppm (triplet). From (a) it is clear that the peaks of the protons of the free and bound butyric acid completely overlap, showing no shift in position due to the binding to amino-MIL-53(Al). From the relative peak integrations, the amount of butyric acid (bound and free from (a), and bound from (b)) can be obtained. These amounts will be expressed relative to the number of 2-aminoterephthalate linkers in the framework structure, and can be found (for all five intrusion times) in Table 3.5 (p 65).
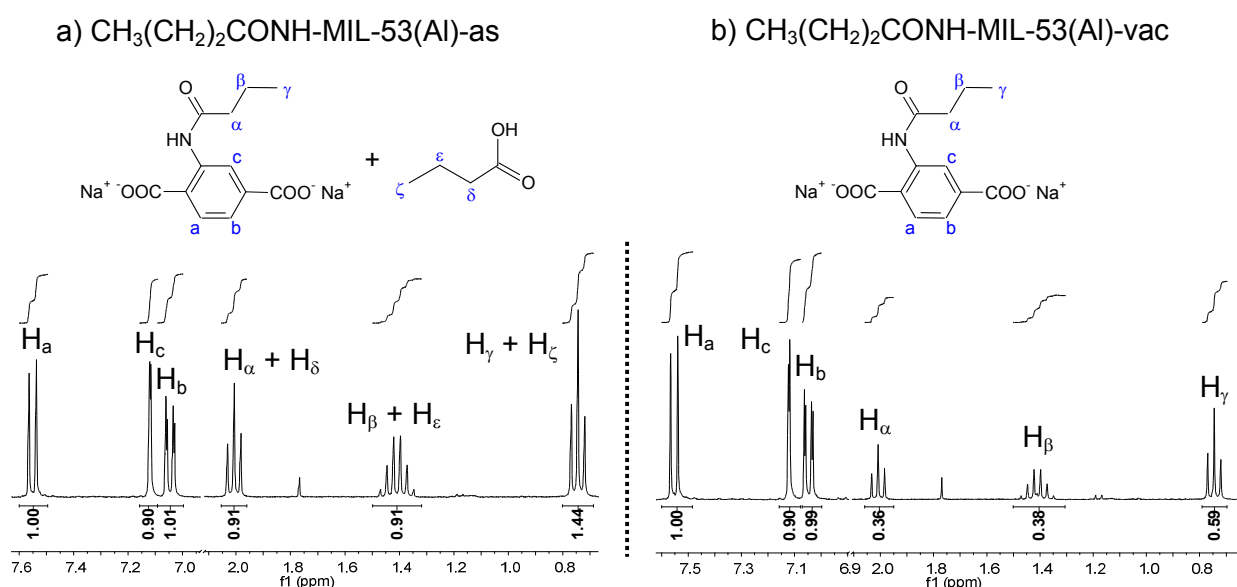

a) $CH_3(CH_2)_2CONH$-MIL-53(Al)-as

b) $CH_3(CH_2)_2CONH$-MIL-53(Al)-vac

Figure 3.19: ^{1}H NMR spectra obtained after digestion of $CH_3(CH_2)_2CONH$-MIL-53(Al)-as (16 hours intrusion) (a) and $CH_3(CH_2)_2CONH$-MIL-53(Al)-vac (16 hours intrusion) (b) in NaOD/D$_2$O showing the peak integration values before (a) and after (b) evacuation (150°C, 16 h, 2 x 10^{-2} mbar) of the free butyric acid. For clarity the structure of the unreacted 2-aminoterephthalate fragments is not shown.

64

Table 3.5: Relative amounts of butyric acid (both free and covalently bound in amino-MIL-53(Al)) after five different intrusion times, as determined by digestive ^{1}H NMR measurements in NaOD/D$_2$O, before and after evacuation (150°C, 16 h, 2 x 10^{-2} mbar) of the free butyric acid.

Intrusion Time for Butyric Acid (h)	Before evacuation: average integration values		Free and bound butyric acid (%)	After evacuation: average integration values		Bound butyric acid (NH$_2$ groups amidated) (%)
	Aromatic protons	Aliphatic protons		Aromatic protons	Aliphatic protons	
1	0.96	0.25	25.8	0.96	0.14	14.4
5	0.97	0.43	44.2	0.97	0.16	16.0
16	0.97	0.47	48.0	0.96	0.19	19.7
24	0.98	0.38	39.2	0.96	0.15	15.2
48	0.96	0.37	38.8	0.97	0.14	14.0

From Table 3.5 (p 65) as well as Graph 3.3 (p 65), it can be seen that a maximum load of butyric acid in amino-MIL-53(Al) was obtained after a 16 hours intrusion time (48.0% before evacuation and 19.7% after evacuation of unreacted butyric acid). Longer intrusion times (24 h and 48 h) lead to decreased loads of butyric acid.
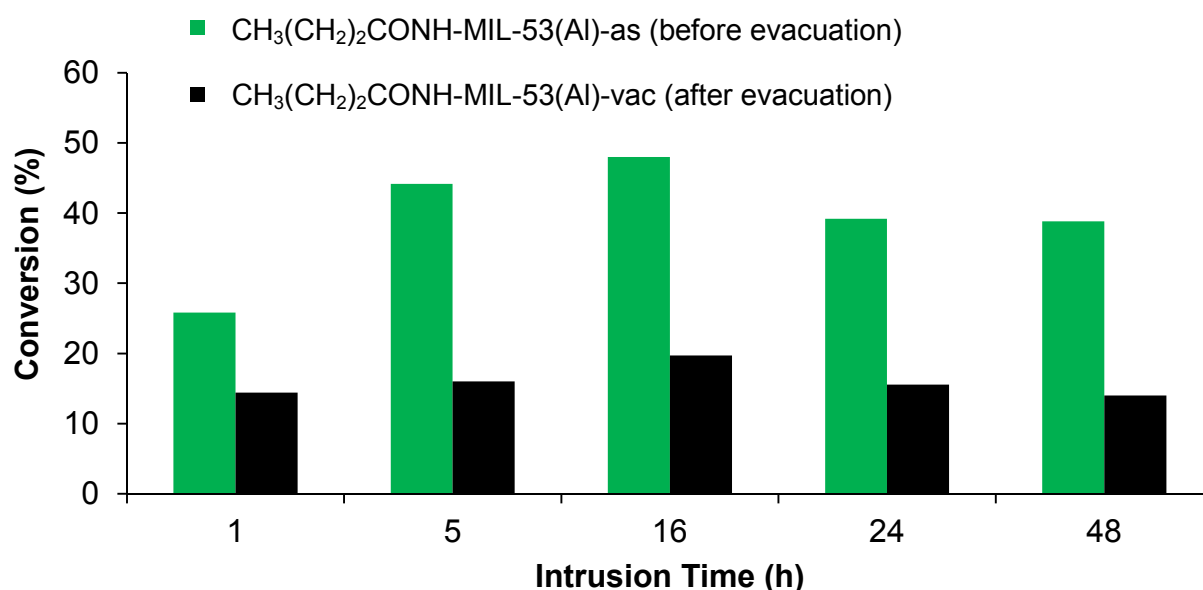
Graph 3.3: The relative percentages of butyric acid intruded into amino-MIL-53(Al), using five different intrusion times, obtained by digestive ^{1}H NMR analysis in NaOD/D$_2$O. The green bars represent the amount of butyric acid (unreacted and bound) directly after synthesis and the black bars the amount of bound butyric acid after evacuation of the unreacted butyric acid.

This phenomenon was investigated by performing TGA on the same five products before and after evacuation. As a representative pair, the TGA thermograms of $CH_3(CH_2)_2CONH$-MIL-53(Al)-as (a) and $CH_3(CH_2)_2CONH$-MIL-53(Al)-vac (b), both after 16 hours of intrusion as shown in Figure 3.20 (p 66), gave a first mass loss step of 10.45% (step 1a) and 4.57% (step 1b) respectively. Step 1a for the as-synthesised compound, shows the loss of both unreacted and chemically bound butyric acid. Step 1b for the evacuated compound originates only from the loss of covalently bound butyric acid. It is important to see that step 1b starts at 44°C higher than step 1a, indicating the absence of free butyric acid in the compound after evacuation. In all cases the presence of butyric acid (unreacted or covalently bound) had no significant influence on the onset temperature of structural breakdown, starting at 400°C. TGA thermograms of the other four sets of butyric acid-intruded products can be found in Appendix, Spectrum 13-16 (A-11 to A-12).

A comparison of the TGA results of this timed-intrusion study is found in Table 3.6 (p 67), with a representation of the mass losses before and after evacuation in Graph 3.4 (p 68).
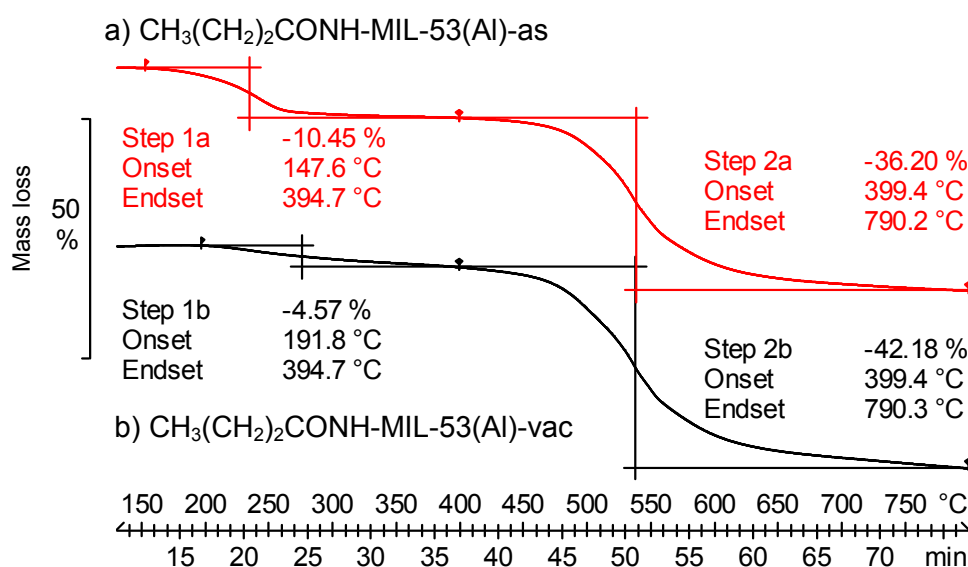

Figure 3.20: TGA thermograms (in an Argon atmosphere) of amino-MIL-53(Al) after a 16 hours intrusion and reaction with butyric acid: before evacuation (a, red) and after evacuation (b, black) of the unreacted butyric acid.
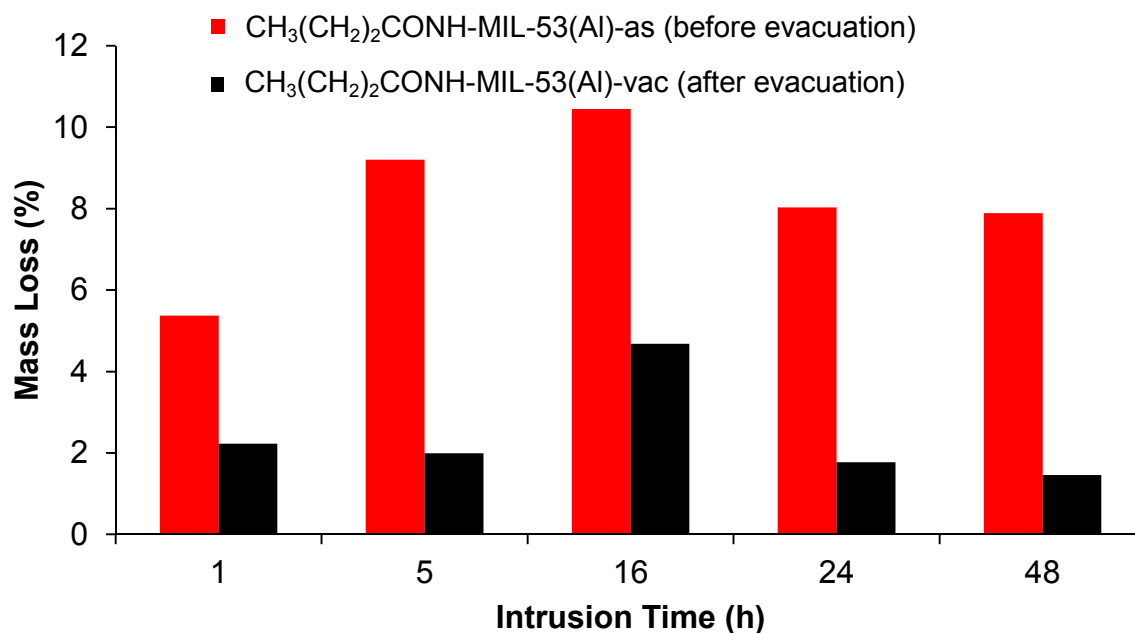
Table 3.6: Relative amounts of butyric acid (both free and covalently bound in amino-MIL-53(Al)) after five different intrusion times as determined by TGA (under Argon), before and after evacuation (150°C, 16 h, 2 x 10^{-2} mbar) of the free butyric acid.

Intrusion Time for Butyric Acid (h)	Before evacuation of unreacted butyric acid		After evacuation of unreacted butyric acid	
	Mass loss (wt%)	Onset temperature (°C)	Mass loss (wt%)	Onset temperature (°C)
1	5.4	156	2.3	197
5	9.1	160	1.9	206
16	10.5	148	4.6	192
24	8.0	163	2.0	221
48	7.9	167	1.7	210

Table 3.6 (p 67) shows that for $CH_3(CH_2)_2CONH$-MIL-53(Al)-as (1 hour intrusion), the minimum intrusion of butyric acid was found as 5.4%. After 16 hours of intrusion, the amount of butyric acid intruded into amino-MIL-53(Al) doubles to 10.5%. With the amount of butyric acid covalently bound to the framework (remaining after evacuation), the same effect is seen (2.3% for 1 hour and 4.6% for 16 hours).

When comparing the butyric acid content of $CH_3(CH_2)_2CONH$-MIL-53(Al), obtained from TGA (Graph 3.4, p 68) with that obtained from ^{1}H NMR analyses (Graph 3.3, p 65), they are in good correlation. Both show a maximum butyric acid content after a 16 hours intrusion. In Graph 3.4 (p 68), the differences between the as-synthesised and evacuated products are an indication of the amount of free acid still present in the framework after the amidation reaction.

The PXRD analyses for the other four $CH_3(CH_2)_2CONH$-MIL-53(Al)-vac products are given in Appendix, Spectrum 25 (A-16).

Graph 3.4:　The relative mass loss percentages are given due to butyric acid present in amino-MIL-53(Al), after five different intrusion times, as determined by TGA (under Argon).　The red bars represent the mass loss of both unreacted and covalently bound butyric acid directly after synthesis (CH$_3$(CH$_2$)$_2$CONH-MIL-53(Al)-as) and the black bars the mass loss after evacuation of the covalently bound butyric acid (CH$_3$(CH$_2$)$_2$CONH-MIL-53(Al)-vac).

3.3.3.　Loading of Ferrocene in MIL-53(Al) Derivatives

3.3.3.1.　MIL-53(Al)

Fc@MIL-53(Al)-vap was produced by Chemical Vapour Deposition (CVD) (Scheme 3.9, p 69).[7]　To allow better physisorption of the ferrocene molecules into the channels of MIL-53(Al), MIL-53(Al)-lt and ferrocene were mixed in a schlenk tube which was then evacuated down to 1.3 x 10^{-2} mbar and sealed.　The tube was heated evenly in an oven to allow the ferrocene to vaporise (110°C) and intrude into the channels of the MOF whilst under vacuum.　After completion of the process, the orange-brown product was washed with n-hexane and centrifuged to remove residual ferrocene on the external surface of the framework.　This washing procedure was repeated about five times until no more discolouring of the n-hexane was seen, ensuring that only intruded ferrocene is present in the MIL-53(Al) structure.
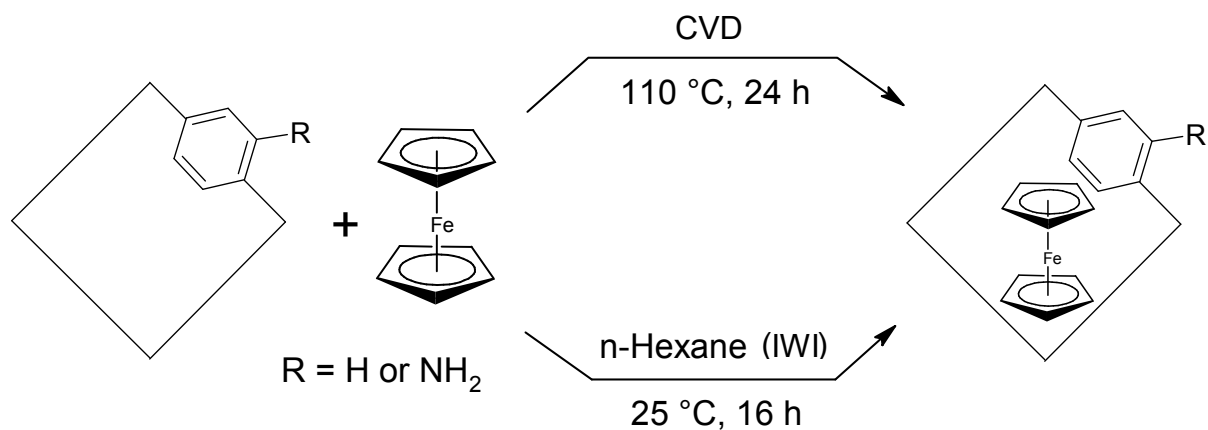
Scheme 3.9: Reaction scheme for the physisorption (intrusion) of ferrocene into MIL-53(Al)-lt (R = H) as well as amino-MIL-53(Al) (R = NH_2) with the use of Chemical Vapour Deposition (CVD) and Incipient Wetness Impregnation (IWI).

Ferrocene was also intruded into MIL-53(Al)-ht by Incipient Wetness Impregnation (IWI), using a saturated solution of ferrocene in dry n-hexane to cover the activated MOF still under vacuum (Scheme 3.9, p 69). After relieving the vacuum, the ferrocene solution was allowed to intrude into the MOF's channels for 16 hours by action of the vacuum still present in the framework, as well as the atmospheric pressure above the solution. The product, Fc@MIL-53(Al)-sol was washed and obtained as a pale-orange powder after drying it at room temperature.

The FTIR spectra of Fc@MIL-53(Al)-vap (a) and Fc@MIL-53(Al)-sol (b), seen in Figure 3.21 (p 70), show an extra transmittance peak for ferrocene at 1100 cm^{-1} (i) when compared to the FTIR spectrum of MIL-53(Al)-lt as the reference.
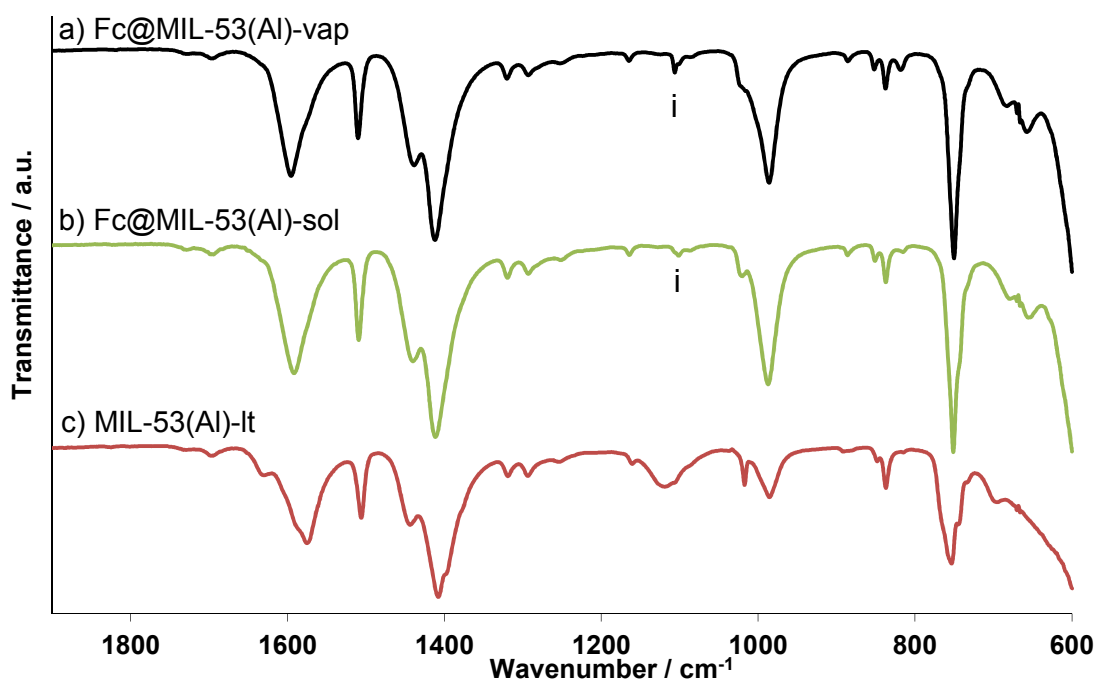
Figure 3.21: FTIR spectra of Fc@MIL-53(Al)-vap (a, black), Fc@MIL-53(Al)-sol (b, green) and MIL-53(Al)-lt (c, red).

When comparing the TG thermograms of Fc@MIL-53(Al)-vap (a) and Fc@MIL-53(Al)-sol (b) (referenced to MIL-53(Al)-lt (c)) in Figure 3.22 (p 70), the amount of mass loss due to ferrocene from the CVD method (step 1a, 6.17%) is less than that of the IWI method (step 1b , 7.59%). IWI is thus a more effective method for loading ferrocene into the framework channels than CVD.
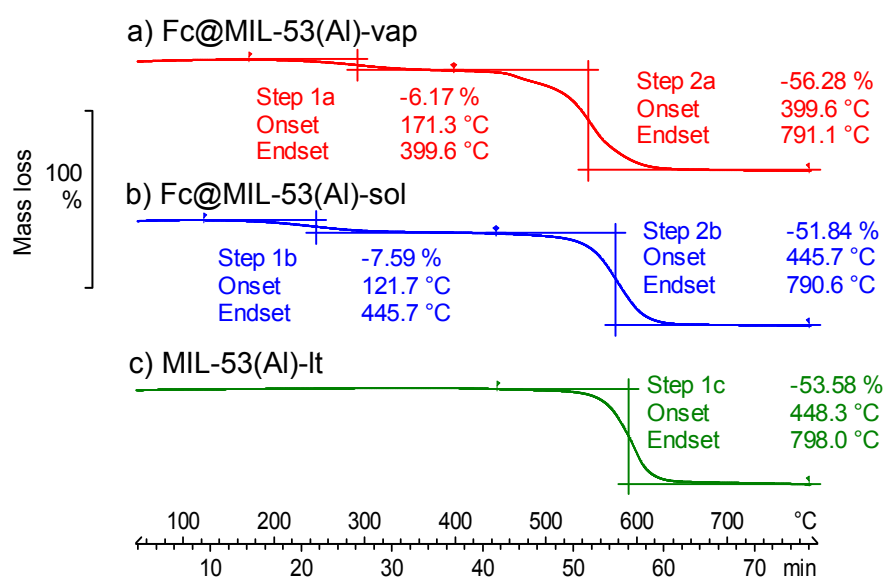

Figure 3.22: TGA thermograms of Fc@MIL-53(Al)-vap (a, red), Fc@MIL-53(Al)-sol (b, blue) and MIL-53(Al)-lt (c, green), obtained under Argon atmosphere.

When the PXRD spectra of Fc@MIL-53(Al)-vap (a) and Fc@MIL-53(Al)-sol (b) are compared to the spectrum of MIL-53(Al)-lt (c) in Figure 3.23 (p 71), new peaks at $2\theta = 14°$ (i) and $21.5°$ (ii) are indicative of the presence of free ferrocene in the porous, crystalline structure of MIL-53(Al) and is in agreement with the PXRD results of Fischer *et al.*[7] Additional reflections between $2\theta = 8°$ and $13°$ as well as between $2\theta = 16°$ and $21°$ (shaded bands) seen in (a) and (b) (and compared to (c)) could be ascribed to the ferrocene molecules packed into the framework channels.
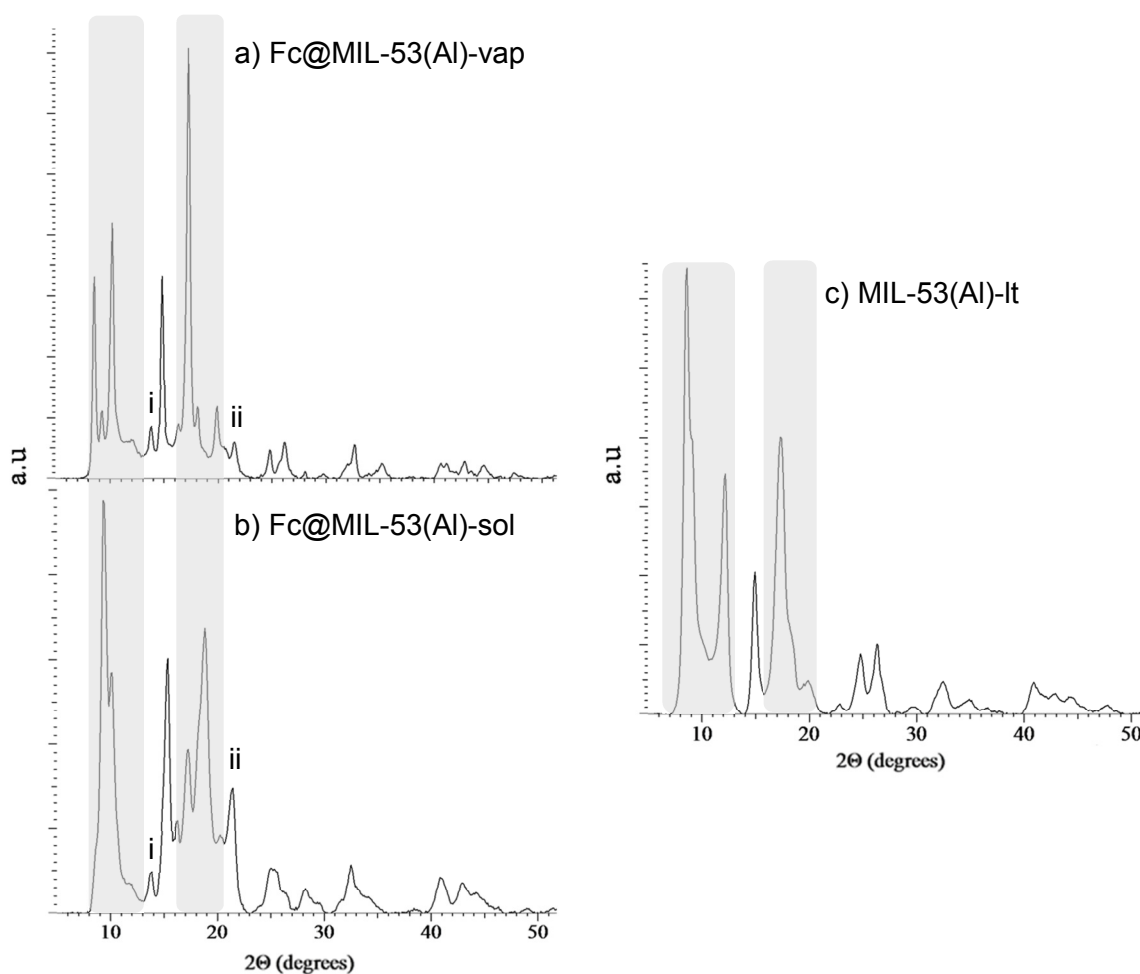

Figure 3.23   PXRD spectra of Fc@MIL-53(Al)-vap (a), Fc@MIL-53(Al)-sol (b) and MIL-53(Al)-lt (c) .

3.3.3.2.   Amino-MIL-53(Al)

To intrude ferrocene into amino-MIL-53(Al), the same procedure was applied as for Fc@MIL-53(Al)-vap and Fc@MIL-53(Al)-sol using CVD and IWI respectively to obtain Fc@amino-MIL-53(Al)-vap and Fc@amino-MIL-53(Al)-sol (Scheme 3.9, p 69). This was done to determine whether the amine groups inside the channels of amino-MIL-53(Al) may affect the intrusion of the ferrocene molecules.

The FTIR spectra of Fc@amino-MIL-53(Al)-vap (a) and Fc@amino-MIL-53(Al)-sol (b) are shown in Figure 3.24 (p 72) together with that of amino-MIL-53(Al)-lt (c) as reference. Too little ferrocene was adsorped into amino-MIL-53(Al), using the CVD method (Figure 3.24, p 72) to be detected by FTIR, as spectrum (a) is identical to spectrum (c) for amino-MIL-53(Al)-lt. The spectrum of Fc@amino-MIL-53(Al)-sol (b), showed one peak at 1104 (i) cm^{-1} originating from the ferrocene intruded into amino-MIL-53(Al) using incipient wetness impregnation (IWI). This result is a clear indication that during this study, IWI was a more effective method than CVD for intruding ferrocene molecules into the channels of MIL-53 derivatives.
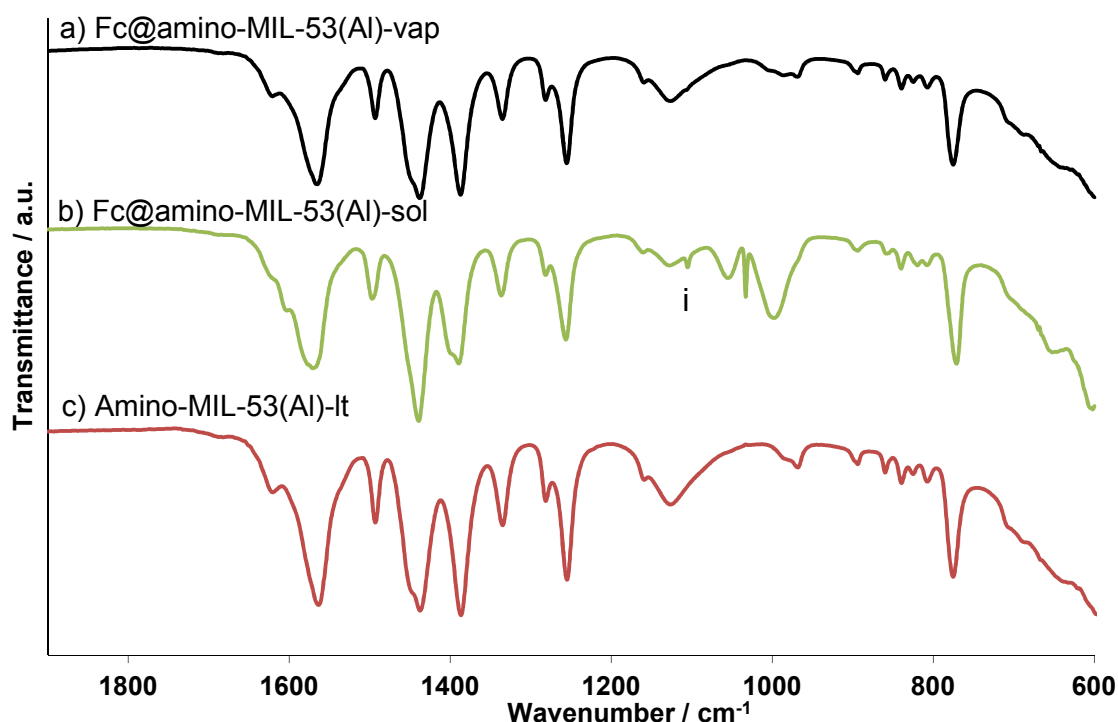

Figure 3.24: FTIR spectra of Fc@amino-MIL-53(Al)-vap (a-black), Fc@amino-MIL-53(Al)-sol (b-green) and amino-MIL-53(Al)-lt (c-red).

TGA thermograms of Fc@amino-MIL-53(Al)-vap (a) and Fc@amino-MIL-53(Al)-sol (b) (referenced to amino-MIL-53(Al)-lt (c)) seen in Figure 3.25 (p 73), show that the CVD method gave a product that contains much less ferrocene (1.66%, step 2a) than the product of the IWI method (11.02%, step 2b). This result is in agreement with the FTIR result above. With the IWI method, an almost tenfold increase in the amount of intruded ferrocene was achieved when compared to the CVD method. The ferrocene content in Fc@amino-MIL-53(Al)-sol (11.02%) is also more than that obtained by the IWI method for MIL-53(Al) (7.59%) (Figure 3.22, p 70 (b)), showing that the IWI method has a higher capability to introduce ferrocene molecules to the framework structure of MIL-53(Al) and amino-MIL-53(Al). It is also possible that the presence

of the amine groups in the framework of amino-MIL-53(Al) results in a higher uptake of ferrocene. From Figure 3.25 (p 73), it can also be seen that Fc@amino-MIL-53(Al)-sol (b), with its high ferrocene content (11.02%, step 2b), contains less water (0.13%, step 1b) than Fc@amino-MIL-53(Al)-vap (0.73%, step 1a) with its low ferrocene content (1.66%, step 2a). This could be the result of better evacuation of the amino-MIL-53(Al) framework prior to IWI than in the case of CVD.
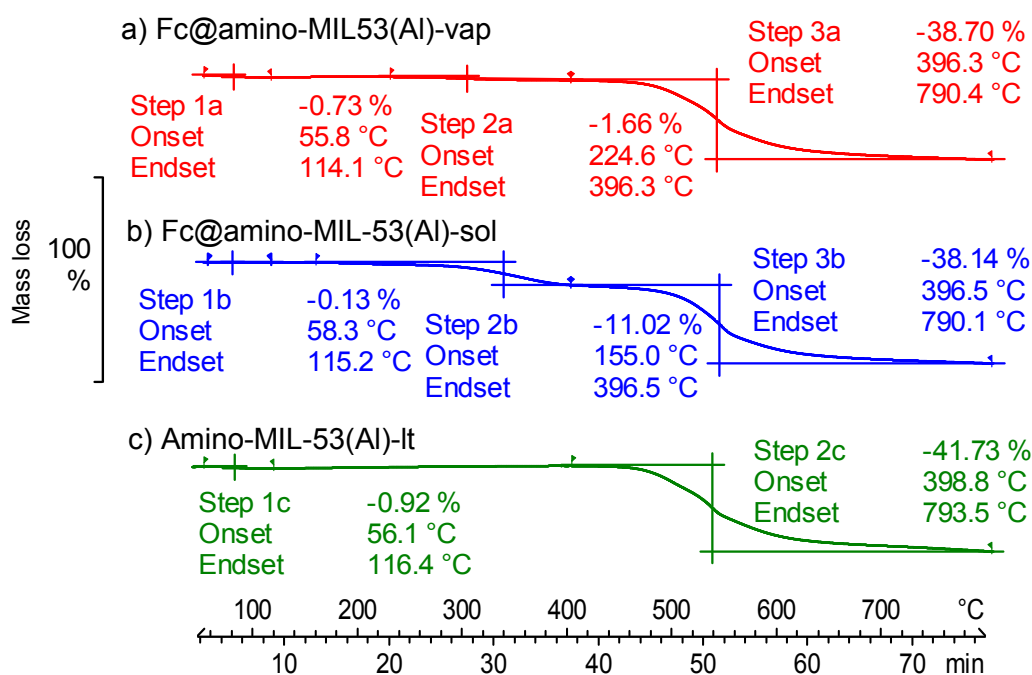

Figure 3.25:   TGA thermograms of Fc@amino-MIL-53(Al)-vap (a, red), Fc@amino-MIL-53(Al)-sol (b, blue) and amino-MIL-53(Al)-lt (c, green), obtained in Argon atmosphere.

The PXRD spectra of Fc@amino-MIL-53(Al)-vap (a) and Fc@amino-MIL-53(Al)-sol (b), shown in Figure 3.26 (p 74), both display two extra peaks at $2\theta = 10.5°$ (i) and $15.5°$ (ii) when referenced to amino-MIL-53(Al)-lt (c). These two reflections, caused by the intruded ferrocene, are more prominent in the spectrum of amino-MIL-53(Al)-sol (b) due to the higher concentration of ferrocene as confirmed earlier by FTIR and TGA studies.
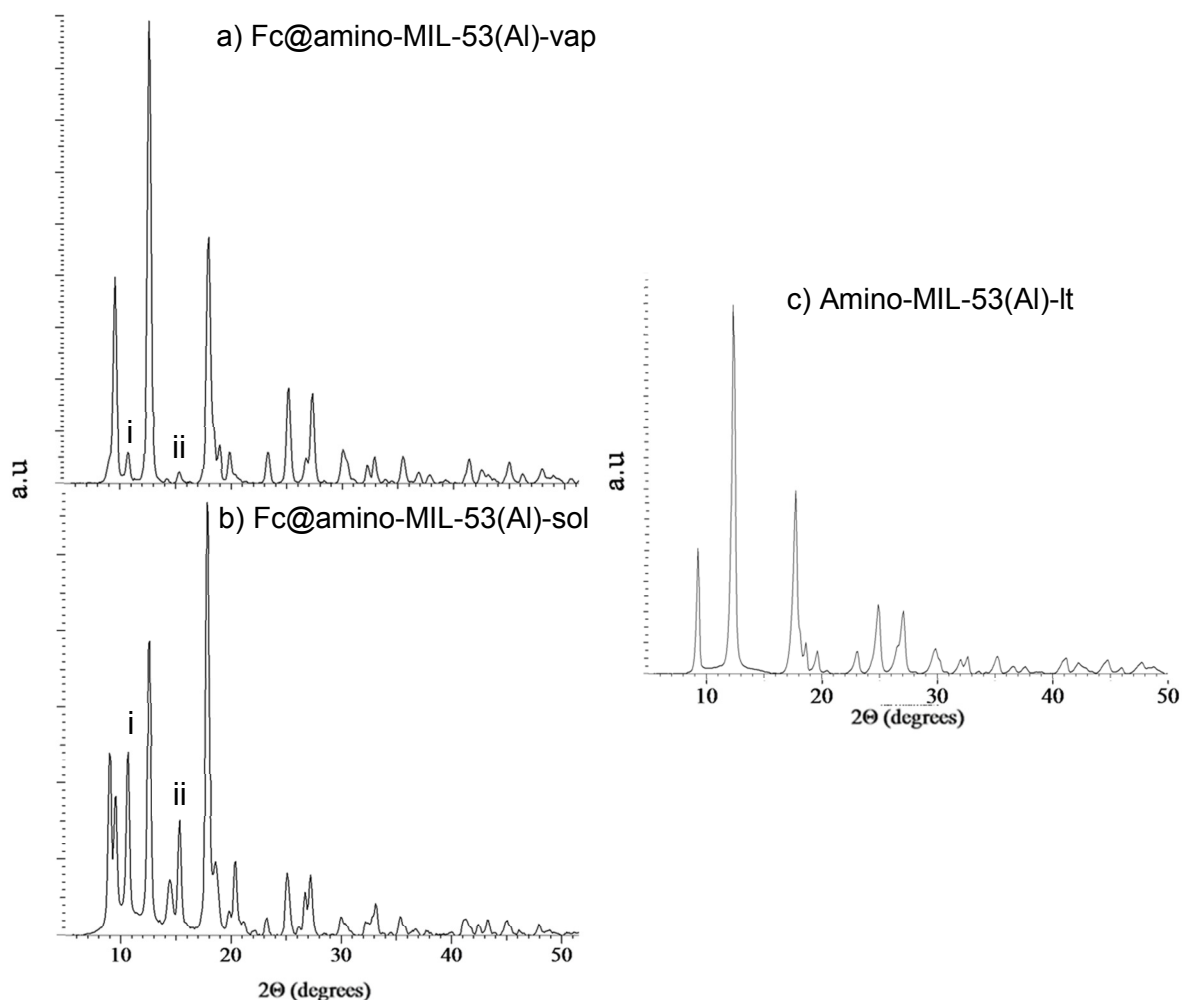
73

Figure 3.26: PXRD spectra of Fc@amino-MIL-53(Al)-vap (a), Fc@amino-MIL-53(Al)-sol (b) and amino-MIL-53(Al)-lt (c).

3.3.4. FcCOOH in Amino-MIL-53(Al) – Time-Resolved Study

After proving that incipient wetness impregnation (IWI) is a successful method for loading ferrocene in MIL-53(Al), this method was used to intrude ferrocene carboxylic acid (FcCOOH) into amino-MIL-53(Al) in a time-resolved intrusion study. After each of the five intrusions, the FcCOOH was allowed to react with the amine groups of the organic linkers to produce FcCONH-MIL-53(Al) (Scheme 3.10, p 75). Prior to intrusion, amino-MIL-53(Al) was activated at 150°C overnight under vacuum. After cooling down to room temperature, ferrocenecarboxylic acid, dissolved in anhydrous toluene, was dispensed to cover the MOF still under vacuum. The vacuum was relieved and the solution allowed to intrude into the evacuated framework at room temperature for 1, 5, 16, 24 or 48 hours, using the pressure difference inside and outside the MOF channels to force the liquid inside the porous structure. After intrusion, the temperature was increased and kept at 100°C for 16 hours to promote amidation of the amine

groups by FcCOOH. High boiling toluene was used as solvent to prevent rupture of the framework during the amidation reaction. Another advantage of using toluene is that it can form an azeotrope with the water formed as a by-product. The experiment included a distillation column to ensure the removal of water by-product and thus promote product formation. After the products were washed, isolated and dried, the as-synthesised products (FcCONH-MIL-53(Al)-as) were analysed by ^{1}H NMR spectroscopy and TGA and then evacuated at 100°C overnight to obtain the final products (FcCONH-MIL-53(Al)-vac) as dark-orange powders.
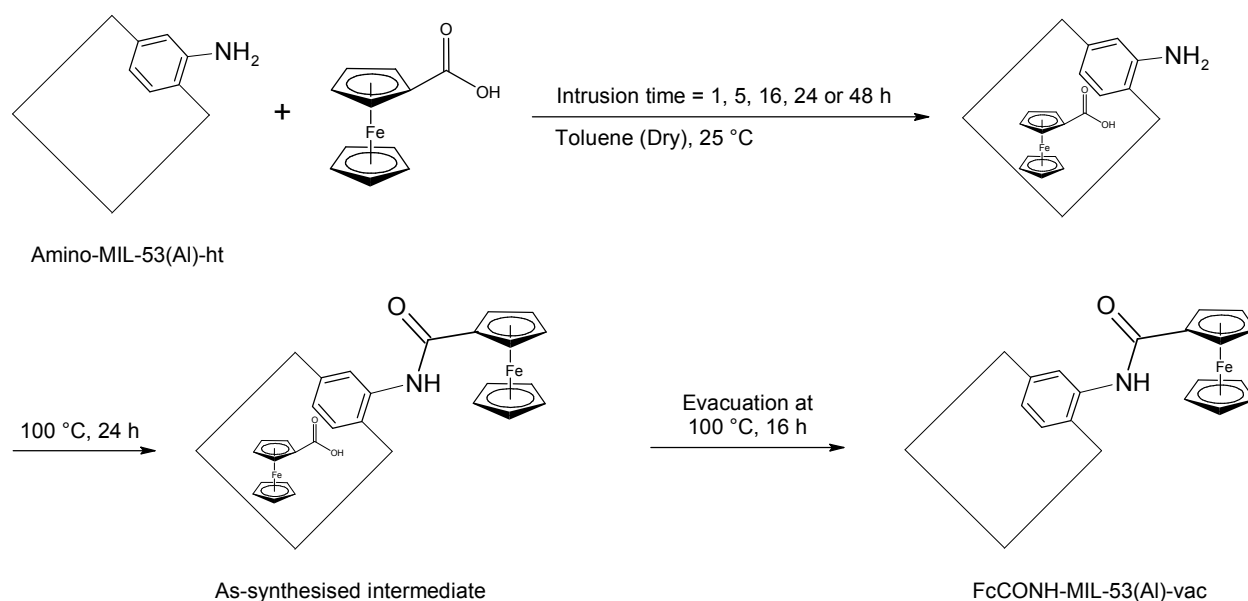
Scheme 3.10:   Reaction scheme for the intrusion and subsequent chemical binding of ferrocenecarboxylic acid to amino-MIL-53(Al) through amidation. Five different intrusion times were applied before amidation.

In Figure 3.27 (p 76), the FTIR spectrum of FcCONH-MIL-53(Al)-vac (b) (obtained after a 16 hours intrusion) shows a small carbonyl stretching frequency at 1663 cm^{-1} (i) (from the amide bond) as well as two peaks at 1100 and 982 cm^{-1}(ii), due to the presence of monosubstituted ferrocene. The FTIR spectra of the other four FcCONH-MIL-53(Al)-vac products display the same peaks and can be seen in Appendix, Spectrum 5, A-3).
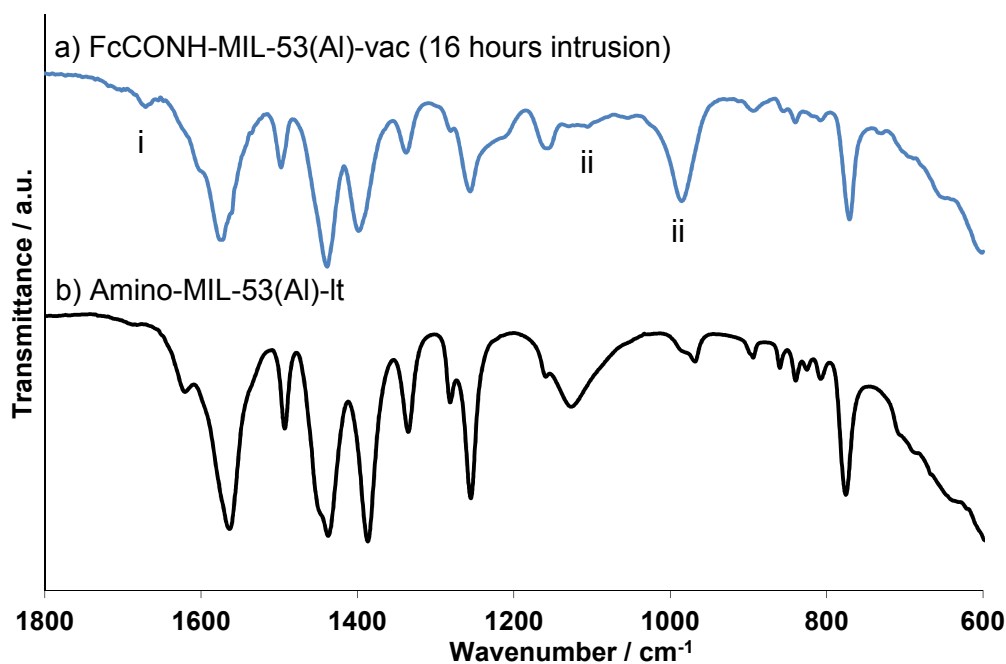
Figure 3.27:   FTIR spectrum of FcCONH-MIL-53(Al)-vac (16 hours intrusion) (a) showing the amide's stretching frequency at 1663 cm^{-1}, as well as the peaks relating to the ferrocenyl groups at 1100/982 cm^{-1} and compared to the amino-MIL-53(Al)-lt reference (b).

The PXRD spectra of FcCONH-MIL-53(Al) (a) (Figure 3.28, p 77) gave two extra peaks (i and ii) at the same positions as in the previous section when ferrocene was adsorpbed into amino-MIL-53(Al) at $2\theta = 10.5°$ and $15.5°$. This indicates as well, that a very small amount of free carboxylic acid was still present after evacuation at 150°C overnight.   The bound FcCONH moieties did have a suppressive effect on the resonance peaks in the region between $2\theta = 20°$ and $35°$ (iii). The PXRD scans for FcCONH-MIL-53(Al)-vac (1, 5, 24 and 48 hours intrusion) are given in the Appendix, Spectrum 26, A-17.
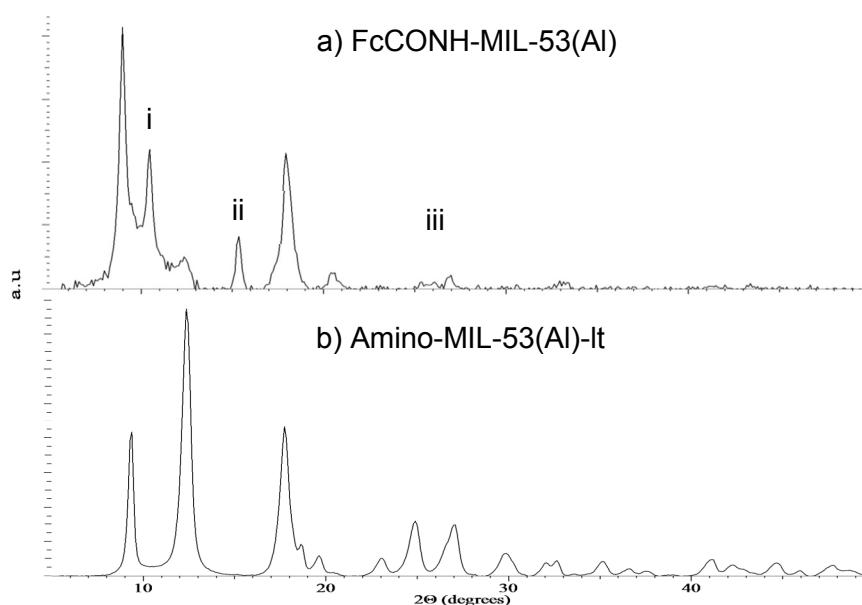
Figure 3.28: PXRD spectrum of FcCONH-MIL-53(Al) (a) (obtained after a 16 hours intrusion time) and amino-MIL-53(Al)-lt (b).

To investigate the migration behaviour of ferrocenecarboxylic acid inside the channels of amino-MIL-53(Al), ^{1}H NMR spectroscopy and TG analyses were performed on all five products in their as-synthesised (FcCONH-MIL-53(Al)-as) and evacuated (FcCONH-MIL-53(Al)-vac) forms. In order to perform liquid phase ^{1}H NMR, the products were digested in NaOD/D$_2$O to form dissolved sodium terephthalate fragments as seen in Figure 3.29 (p 78). Provided that the spectrum is obtained within 30 minutes after digestion, to minimise hydrolysis of the amide bond, the bound ferrocenecarboxylic acid will also be detected. Unreacted FcCOOH is insoluble in the basic aqueous NMR solvent and will thus not be detected during ^{1}H NMR analyses. This fact was used advantageously; knowing that only bound FcCONH moieties will be "visible" during ^{1}H NMR analyses.

As a representative example for the five sets of FcCONH-MIL-53(Al) products, the ^{1}H NMR analyses of FcCONH-MIL-53(Al)-as and FcCONH-MIL-53(Al)-vac (obtained after a 16 hours intrusion time) are shown in Figure 3.29 (p 78). When comparing the integration of the seven protons (marked H$_\gamma$ and H$_\beta$) on the substituted cyclopentadienyl ring of the as-synthesised product (a) to that of the evacuated product (b), it stays constant. This proves that the evacuation procedure (which took place at 100°C for 16 hours under a 2 x 10^{-2} mbar vacuum) had no appreciable effect on the amide bonds. The protons marked H$_\alpha$, could not be integrated due to their position near the solvent peak. No protons from unreacted ferrocene were detected. These observations were also true for the other four sets of products (Appendix, Spectrum 10 & 11, A-8 to A-9). A summary of the ^{1}H NMR results for the evacuated products of FcCONH-MIL-

53(Al)-vac, is given in Table 3.7 (p 78), with a graphical representation of the conversion percentage of the formed amide bonds in Graph 3.5 (p 79)
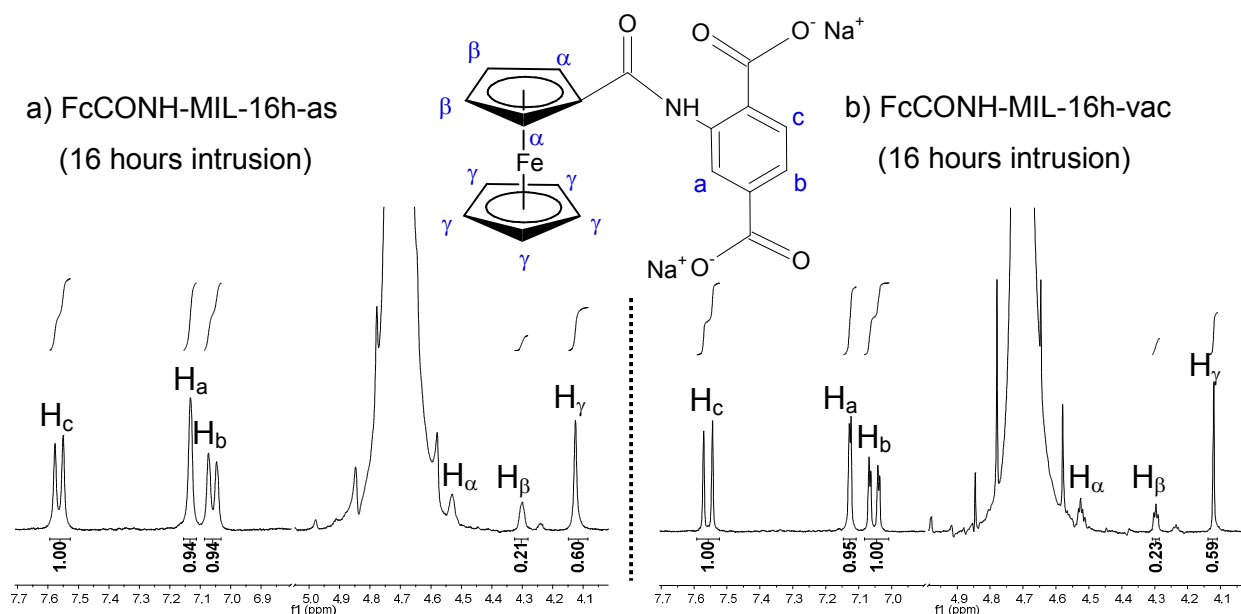

Figure 3.29: ^{1}H NMR spectra, in NaOD/D$_2$O, of FcCONH-MIL-16h-as (a) and FcCONH-MIL-16h-vac (b). The structure of the unreacted 2-aminoterephthalate fragment is not shown.

Table 3.7: Relative amounts of FcCOOH (covalently bound in amino-MIL-53(Al)) after five different intrusion times as, determined by digestive ^{1}H NMR measurements in NaOD/D$_2$O, after evacuation of the unreacted FcCOOH.

Intrusion Time for FcCOOH (h)	After evacuation average integration values		Binding% (NH$_2$ groups amidated)
	Aromatic protons	Aliphatic protons	
1	1.00	0.07	8.1
5	1.01	0.10	9.6
16	0.98	0.12	11.9
24	0.98	0.08	8.2
48	0.99	0.08	7.9

From Table 3.7 (p 78), a conversion of 8% is observed after an intrusion time of one hour, with a maximum of 12% after a 16 hours intrusion time and then reaches 8% after an intrusion time of 48 hours). The as-synthesised and evacuated products of FcCONH-MIL-53(Al) both show

nearly equal amounts of ferrocenyl content in Graph 3.5 (p 79), because the NMR only detects the FcCONH moieties covalently bound to the framework.
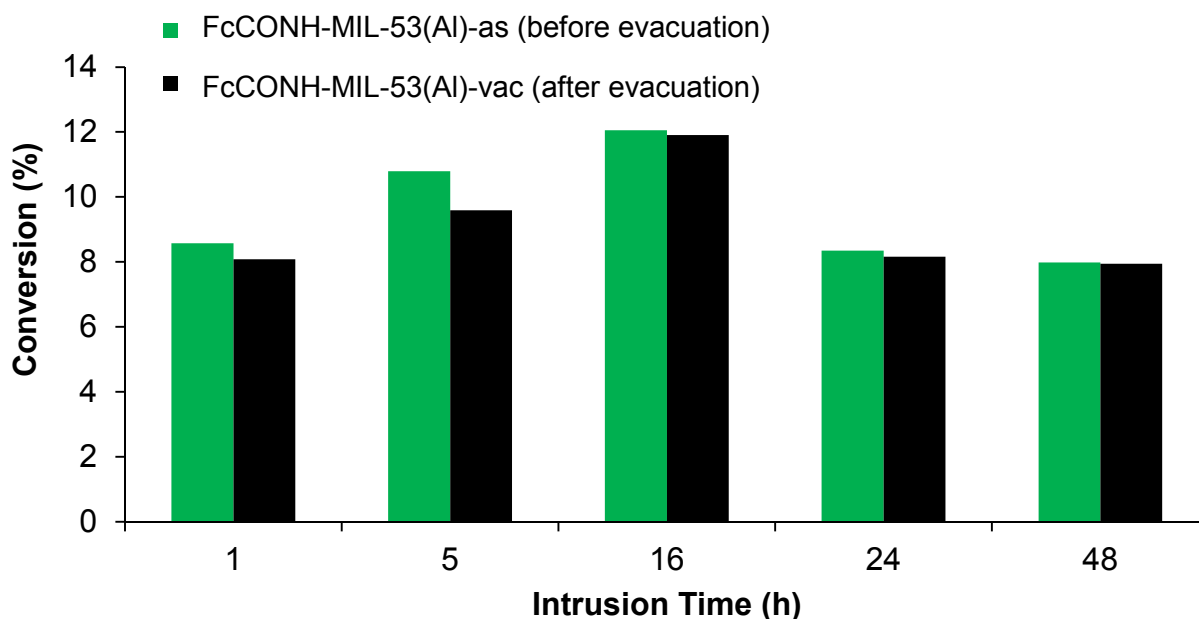
Graph 3.5:   Percentages of amine groups in amino-MIL-53(Al) amidated with ferrocenecarboxylic acid to produce FcCONH-MIL53(Al)-as (green bars) and FcCONH-MIL53(Al)-vac (black bars), as determined by digestive ^{1}H NMR in NaOD/D_2O.

TG thermograms of FcCONH-MIL-53(Al)-as (a) and FcCONH-MIL-53(Al)-vac (b) (obtained after a 16 hours intrusion) (Figure 3.30, p 80) both showed a two-step mass loss process. For FcCONH-MIL-53(Al)-as (a), the first step, starting at 86°C (step 1a), represents the mass loss (14.2%) due to both the bound FcCONH and unreacted FcCOOH moieties in the channels of amino-MIL-53(Al). With FcCONH-MIL-53(Al)-vac (b), the first mass-loss step (step 1b) starts ~50°C higher than with FcCONH-MIL-53(Al)-as, indicating only the bound FcCONH moieties present in the structure. This temperature difference is ~100°C in the case of the other four intrusion times as shown in Table 3.8 (p 80). All the ferrocene-containing structures break down similarly after 400°C, as seen from steps 2a and 2b (Figure 3.30, p 80), indicating that the presence of the bound and unbound FcCOOH have no significant influence on the thermal stability of the amino-MIL-53(Al) structure. The TGA thermograms for the other four sets of FcCONH-MIL-53(Al) products showed similar mass-loss behaviour and can be seen in Appendix, Spectrum 17-20 (A-12 to A-13). A summary of the TGA results of all the FcCONH-MIL-53(Al) products is found in Table 3.8 (p 80).
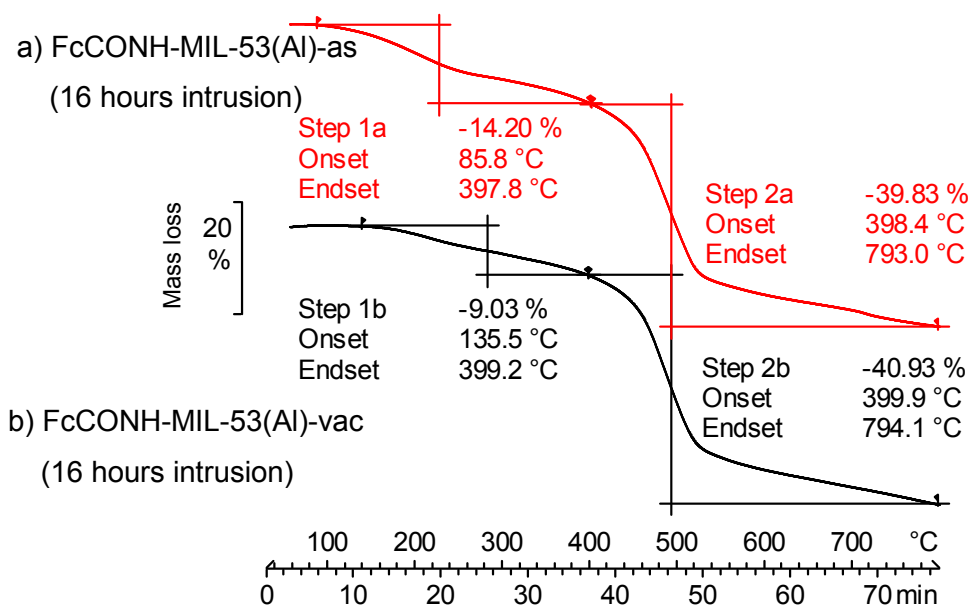
Figure 3.30:   TGA thermograms (under Argon atmosphere) of FcCONH-MIL-53(Al)-as (a, red) and FcCONH-MIL-53(Al)-vac (b, black) (obtained after a 16 hours intrusion time).

Table 3.8:   Relative amounts of FcCOOH (both free and covalently bound in amino-MIL-53(Al)) after five different intrusion times as determined by TGA (under Argon), before and after evacuation (100°C, 16 h, 2 x 10^{-2} mbar) of the free FcCOOH.

| Intrusion Time for FcCOOH (h)	Before evacuation of unreacted FcCOOH		After evacuation of unreacted FcCOOH	
	Mass loss (wt%)	Onset temperature (°C)	Mass loss (wt%)	Onset temperature (°C)
1	12.8	83	6.5	183
5	13.2	92	6.0	184
16	14.2	86	9.0	136
24	12.5	87	6.2	187
48	11.9	95	5.3	189

From Table 3.8 (p 80) and Graph 3.6 (p 81), it is observed that the amount of FcCOOH (unreacted and covalently bound) present in amino-MIL-53(Al) reaches a maximum after 16 hours of intrusion with a 14.2% load for the as-synthesised product and 9.0% ferrocenyl moieties in the evacuated product.   The percentages found for the evacuated products represent the FcCONH-fragments covalently bound to the amino-MIL-53(Al) structure.
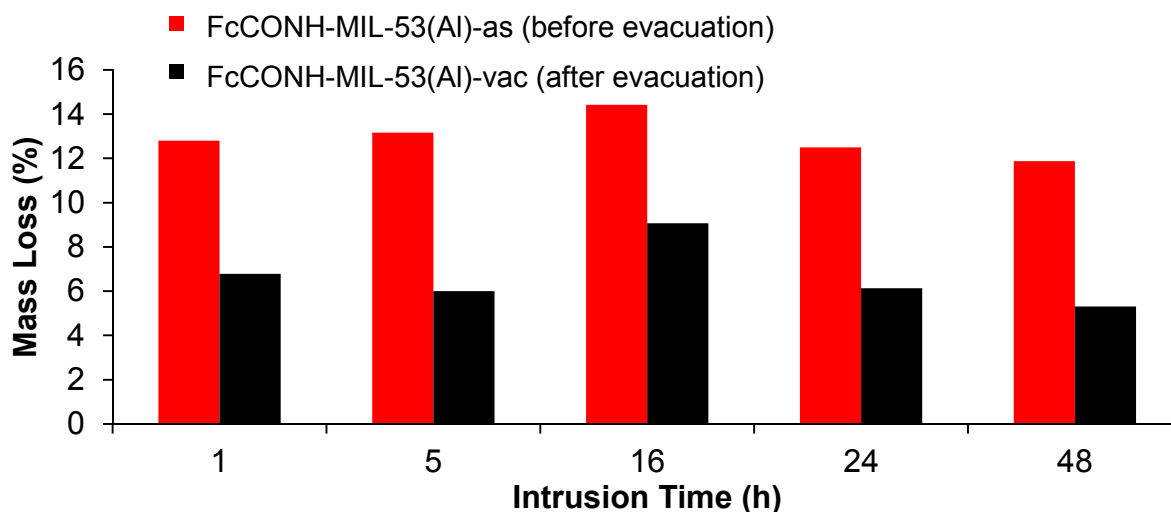
Graph 3.6: Percentages of mass loss due to the presence of unreacted and bound ferrocenecarboxylic acid as determined by TG analyses (under Argon atmosphere) of FcCONH-MIL-53(Al)-as (red bars) and FcCONH-MIL-53(Al)-vac (black bars).

The ^{1}H NMR results from Table 3.7 (p 78) were converted to a weight percentage in order to compare it to the TGA mass losses for FcCONH-MIL-53(Al)-vac (Table 3.8, p 80). The results are found in Table 3.9 (p 82) and illustrated in Graph 3.7 (p 81).
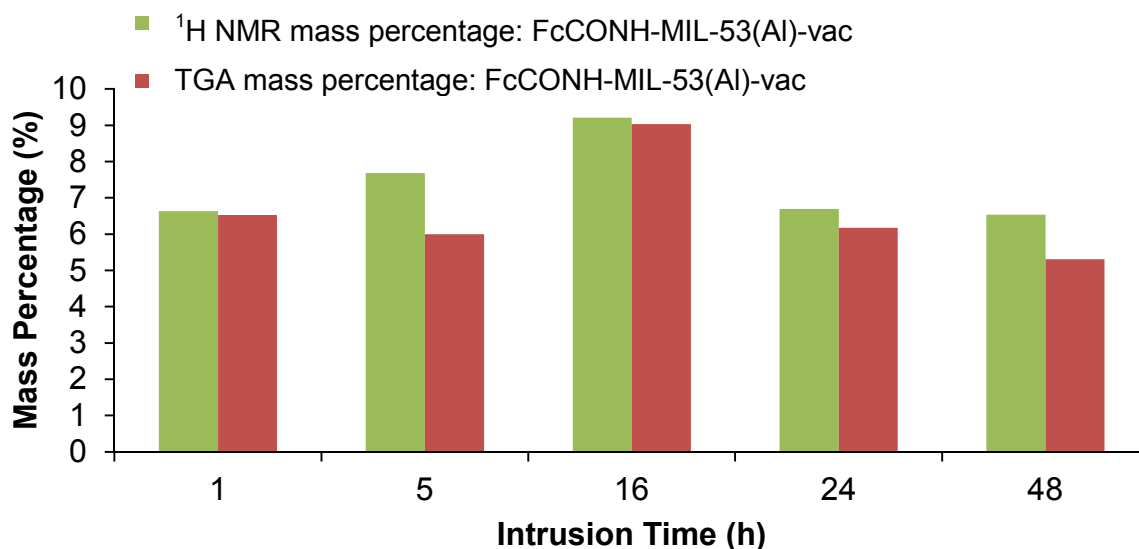
Graph 3.7: Mass percentages calculated from ^{1}H NMR analyses (green bars) and TGA mass loss percentages (red bars) of FcCONH-MIL-53(Al)-vac, synthesised after intrusion of amino-MIL-53(Al) with FcCOOH using the five different intrusion times indicated.

Table 3.9: Mass percentages calculated from ^{1}H NMR analyses compared to the TGA mass loss percentages of FcCONH-MIL-53(Al)-vac.

Intrusion Time for FcCOOH (h)	Calculated ^{1}H NMR FcCONH-fragment (wt%)	TGA mass loss of bound FcCOOH (wt%)
1	7.13	6.53
5	8.36	6.00
16	10.20	9.03
24	7.20	6.17
48	7.02	5.31

The mass percentages shown in Table 3.9 (p 82), obtained from the ^{1}H NMR analyses, representing covalently bound FcCONH moieties in the amino-MIL-53(Al) structure, are, within experimental error, closely matched by the mass loss percentages obtained from the TG analyses for FcCONH-MIL-53(Al)-vac. The slightly lower percentages obtained by the TG analyses could be attributed to carbonisation of a small fraction of the FcCONH-fragments in the pores of amino-MIL-53(Al) during the TG analyses. The good correlation between the mass percentages calculated from ^{1}H NMR spectroscopy and the mass loss percentages obtained by the TG analyses, confirms that little or no hydrolysis occurred during the digestion of the FcCONH-MIL-53(Al)-vac products with NaOD/D$_2$O prior to the ^{1}H NMR analyses.

3.4. Electrochemistry

Cyclic voltammetry (CV) studies were performed in the solid state on three different ferrocene containing products: Fc@MIL-53(Al)-sol, Fc@amino-MIL-53(Al)-sol and FcCONH-MIL-53(Al)-vac (obtained after a 16 hours intrusion time). In the first two products, ferrocene was physisorbed and in the latter, chemically bound (all produced by the IWI method). For these studies, a solid state electrochemical setup as displayed in Figure 3.31 (p 83) was used with the analyte (the ferrocene-containing MOF powder) deposited onto the surface of the glassy carbon working electrode. Prior to deposition, the MOF powder was suspended in an aqueous KCl solution, dropped onto the electrode surface and allowed to dry. Potassium chloride was used as a conductive shell keeping the analyte attached to the surface, while using DCM as an organic

solvent for the supporting electrolyte, $[NBu_4][PF_6]^{\dagger}$. To prevent interference from atmospheric water and oxygen, the solution was purged and kept under an Argon atmosphere. Measurements were done with decamethylferrocene as internal reference and the results reported *vs.* Fc/Fc$^+$.
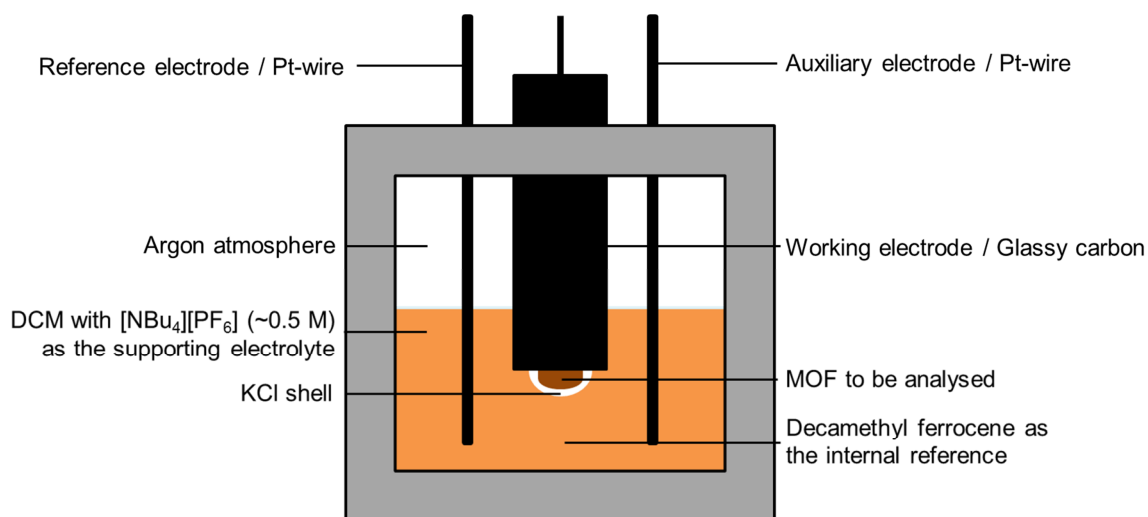

Figure 3.31: The triple-electrode, electrochemical setup used for solid state cyclic voltammetric (CV) studies performed under Argon atmosphere on Fc@MIL-53(Al)-sol, Fc@amino-MIL-53(Al)-sol and FcCONH-MIL-53(Al)-vac (obtained after a 16 hours intrusion).

After establishing that plain, unfunctionalised MIL-53(Al)-lt and amino-MIL-53(Al)-lt are both electrochemically inactive in the measurement window, cyclic voltammetry was performed on Fc@MIL-53(Al)-sol, Fc@amino-MIL-53(Al)-sol and FcCONH-MIL-53(Al)-vac with the result displayed in Figure 3.32 (p 84) and Table 3.10 (p 85).

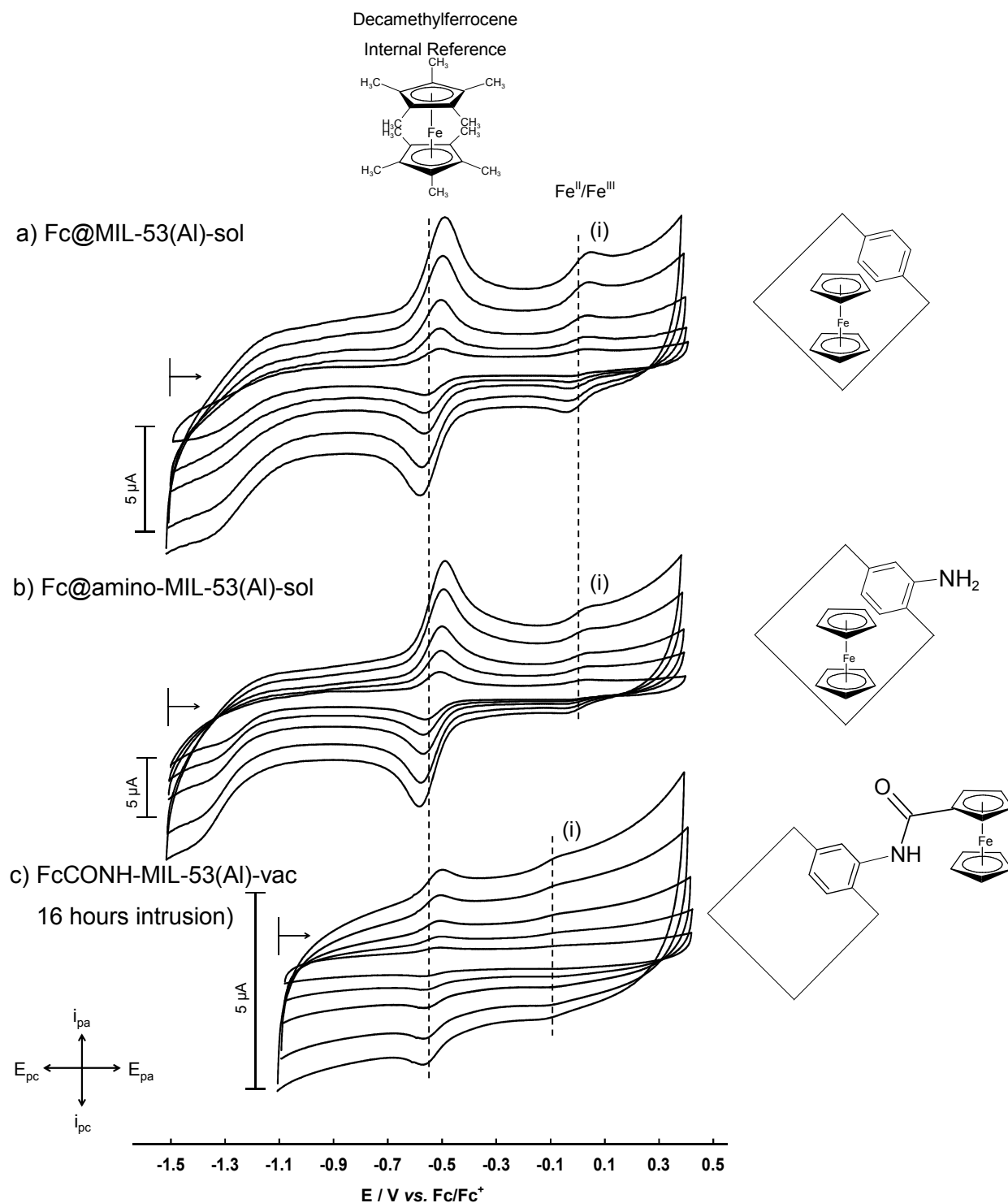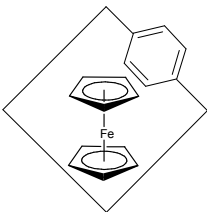† Tetrabutylammonium hexafluorophosphate (~0.5 M)
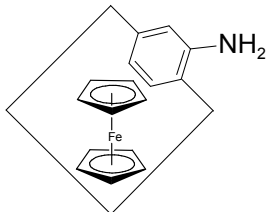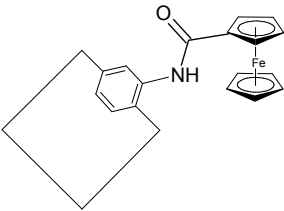
Figure 3.32   Cyclic voltammograms obtained under an Argon atmosphere for Fc@MIL-53(Al)-sol (a), Fc@amino-MIL-53(Al)-sol (b) and FcCONH-MIL-53(Al)-vac (obtained after a 16 hours intrusion) (c) using scan speeds 20, 50, 100, 200 and 300 mV s^{-1} in DCM with [NBu$_4$][PF$_6$] (~0.5 M) as supporting electrolyte and decamethylferrocene as internal reference. The Fe^{II}/Fe^{III} redox couples of the title compounds are marked as (i).

84

Table 3.10: Cyclic voltammetry data for Fc@MIL-53(Al)-sol (a), Fc@amino-MIL-53(Al)-sol (b) and FcCONH-MIL-53(Al)-vac (after a 16 hours intrusion) (c), obtained during solid state measurements in DCM with [NBu$_4$][PF$_6$] (~0.5 M) as supporting electrolyte under an Argon atmosphere. All potentials for the Fe^{II}/Fe^{III} redox couples of the title compounds are reported *vs*. Fc/Fc$^+$

Compound	Scan rate (mV s^{-1})	E_{pa} (mV)	E_{pc} (mV)	$E^{0'}$ (mV)	ΔE_p (mV)	i_{pa} (µA)	i_{pc}/i_{pa}
Fc@MIL-53(Al)-sol	20	27	-29	-1	56	0.27	0.63
	50	39	-35	2	74	0.4	0.59
	100	39	-37	1	76	0.54	0.75
	200	43	-46	-2	89	0.74	0.67
	300	49	-39	5	88	0.97	0.69
Average	-	-	-	**1**	**77**	-	**0.67**
Fc@amino-MIL-53(Al)-sol	20	-6	-22	-14	16	0.28	0.79
	50	8	-30	-11	38	0.53	0.56
	100	16	-38	-11	54	0.66	0.64
	200	22	-56	-17	78	0.63	0.54
	300	38	-65	-14	102	0.89	0.71
Average	-	-	-	**-13**	**57**	-	**0.65**
FcCONH-MIL-53(Al)-vac	20	-50	-56	-53	6	0.03	0.63
	50	-51	-60	-55	9	0.06	0.62
	100	-56	-81	-68	25	0.24	0.52
	200	-73	-103	-88	30	0.11	0.74
	300	-75	-111	-93	36	0.16	0.67
Average	-	-	-	**-71**	**21**	-	**0.64**

In all three CV's, the redox couple, Fe^{II}/Fe^{III} (marked (i) in Figure 3.32 (p 84)) is observed. The average ΔE_p values for Fc@MIL-53(Al)-sol, Fc@amino-MIL-53(Al)-sol and FcCONH-MIL-53(Al)-vac (obtained after a 16 hours intrusion time) are 77, 57 and 21 mV respectively. This indicates that Fc@MIL-53(Al)-sol undergoes a quasi-reversible electrochemical process whereas Fc@amino-MIL-53(Al)-sol and FcCONH-MIL-53(Al)-vac (obtained after a 16 hours intrusion time) are electrochemically reversible, with FcCONH-MIL-53(Al)-vac showing the best reversibility. Binding ferrocene covalently to the amino-MIL-53(Al) structure (as in FcCONH-MIL-53(Al)) thus results in increased electrochemical reversibility when compared to ferrocene existing as free molecules inside the pores of amino-MIL-53(Al). The values of Fc@amino-MIL-53(Al)-sol and FcCONH-MIL-53(Al)-vac are higher than the theoretical value ($\Delta E_p = 0$ mV) for an electrochemical reversible process in the solid state, but are still within the experimental limits for electrochemical reversibility. This is a remarkable improvement on the results found by Marken *et al.* which analysed the same product (FcCONH-MIL-53(Al)) with a different experimental setup (Chapter 2, p 27) and finding $\Delta E_p = 120$ mV at similar scan speeds.[8]

The current ratio, analysed for this study ($0.64 \leq i_{pc}/i_{pa} \leq 0.67$), is not close enough to unity to support the electrochemical reversibility found for Fc@amino-MIL-53(Al)-sol and FcCONH-MIL-53(Al)-vac, but does support the quasi-reversible electrochemical process found for Fc@MIL-53(Al). This could be an indication of a small amount of ions irreversibly migrating to the bulk solution.

Of the three compounds, FcCONH-MIL-53(Al) is the easiest to oxidise with an average $E^{0'} = -71$ mV. The two structures containing free ferrocene in the channels, Fc@MIL-53(Al)-sol and Fc@amino-MIL-53(Al)-sol, showed average redox potentials at $E^{0'} = 1$ mv and -13 mV respectively. This means that by binding ferrocene inside the MOF framework, its redox potential is lowered by more than 50 mV when compared to free, unbound ferrocene in the structure of amino-MIL-53(Al).

3.5. References

1   T. Loiseau, C. Serre, C. Huguenard, G. Fink, F. Taulelle, M. Henry, T. Bataille and G. Férey *Chem. Eur. J.*, 2004, **10**, 1373-1382.

2   E. Stavitski, M. Goesten, J. Juan-Alcañiz, A. Martinez-Joaristi, P. Serra-Crespo, A.V. Petukhov, J. Gascon, and F. Kapteijn, *Angew. Chem. Int. Ed.*, 2011, **50**, 9624-9628.

3   C. Serre, F. Millange, C. Thouvenot, M. Noguès, G. Marsolier, D. Louër and G. Férey, *J. Am. Chem. Soc.*, 2002, **124**, 13519-13526.

4   S. Couck, T. Rémy, G. V. Baron, J. Gascon, F. Kapteijn and J. F. M. Denayer, *Phys. Chem. Chem. Phys.*, 2010, **12**, 9413-9418.

5   E. Stavitski, M. Goesten, J. Juan-Alcañiz, A. Martinez-Joaristi, P. Serra-Crespo, A. V. Petukhov, J. Gascon, and F. Kapteijn, *Angew. Chem. Int. Ed.*, 2011, **50**, 9624–9628.

6   T. Ahnfeldt, D. Gunzelmann, T. Loiseau, D. Hirsemann, J. Senker, G. Férey and N. Stock, *Inorg. Chem.*, 2009, **48**, 3057-3064.

7   M. Meilikhov, K. Yusenko and R.A. Fischer, *Dalton Trans.*, 2009, 600–602.

8   J. E. Halls, A. Hernán-Gómez, A. D. Burrows and F. Marken, *Dalton Trans.*, 2012, **41**, 1475-1480.

4 Experimental

4.1 Introduction

In this chapter, the chemicals, equipment, synthesis procedures and electrochemical analysis techniques are described.

4.2 Instrumentation and Software

Fourier transformed infrared spectroscopy were either performed on a Bruker Tensor 27 IR spectrometer with OPUS v1.1 software or a Thermo Scientific Nicolet iS50 ATR Infrared Spectrometer with OMNIC v9.2.86 software.

Nuclear magnetic resonance spectroscopy was performed on a Bruker Advance DPX 300 NMR spectrometer. All MOF-based NMR samples were digested in $NaOD/D_2O$ and analysed immediately. Organic compounds were dissolved in $CDCl_3$. The ^1H spectra were reported relative to $Si(CH_3)_4$ (TMS) at 0 ppm, and analysed with MestReNova v5.3.0-4469 software.

Surface area and porosity measurements were performed on a Micromeritics ASAP 2020 Surface Area and Porosity Analyzer with ASAP 2020 v2.0 software. Data refinement was done with Microactive v1.01 software.

Thermogravimetric analyses were performed under an Argon atmosphere on a Mettler Toledo TGA/SDTA851 with software: STAR SW v8.10.

Powder X-ray diffraction patterns were collected on a Bruker D2 Phaser powder X-ray diffractometer at room temperature, employing a flat plate sample holder and Cu radiation (λ = 1.54 Å). Diffraction patterns were collected in the 2θ range, 5° to 90°, with a step size of 0.1° and a counting time of two seconds per step.

4.3 Solid State Electrochemistry

A glassy carbon electrode with a 3 mm diameter, was employed by polishing the surface first with 1 micron and then a ¼ micron diamond paste on a Bueler microcloth and then washing the electrode with methanol, acetone, water and DCM before use. The analyte was fixated (~0.01 mg) as a solid onto the electrode surface by evaporative deposition of a potassium chloride "shell" and drying the electrode at 40°C for 8 minutes. The three-electrode cell setup included a platinum wire as reference electrode and a platinum auxiliary electrode to complete the circuit. A ~0.5 M solution of $[NBu_4][PF_6]$ in anhydrous DCM were used, with decamethyl ferrocene (~0.07 M) as the internal reference to be referenced back to Fc/Fc^+ (0 V). Prior to each experiment, the solution was purged with Argon.
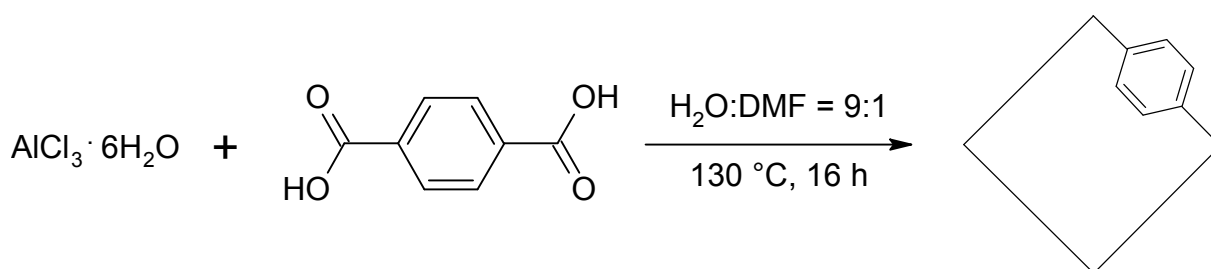
4.4 Aluminium Terephthalate (MIL-53(Al))

4.4.1 Method 1: In Water
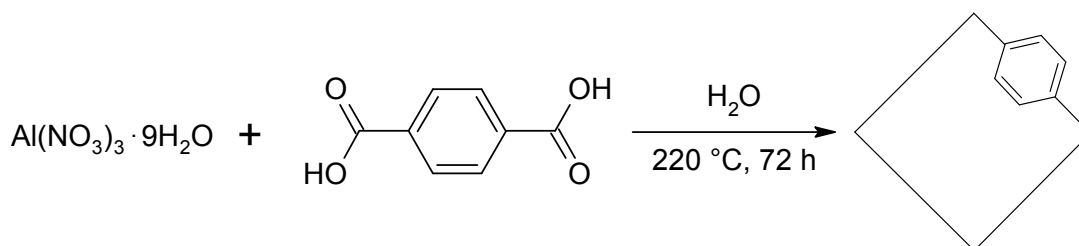
Terephthalic acid (3.456 g, 20.80 mmol) was added to a stirring solution of aluminium nitrate nonahydrate (15.601 g, 41.59 mmol) in water (60 cm^3). The reaction mixture was transferred to a Teflon cup, put in a stainless steel bomb reactor and heated for 72 hours at 220°C. The crude product was isolated by centrifugation (8500 rpm, 15°C, 15 min). The product was washed with water (~ 20 cm^3) and centrifuged three times. The white powder was dried in air overnight to obtain crude MIL-53(Al)-as (4.794 g). A portion of the crude product (1.644 g) was activated at 330°C for 72 hours to obtain MIL-53(Al)-ht which changes to MIL-53(Al)-lt (0.914 g, 57% based on terephthalic acid) upon cooling to room temperature. IR v /cm^{-1} (MIL-53(Al)-lt): 3620 (Al-OH), 1577/1506 (C=O, anti-symmetric), 1446/1409 (C=O, symmertric) (Figure 3.2b, p 39); ^{1}H NMR (300 MHz, NaOD/D$_2$O)/ppm: 7.69 (s; 4H; C$_6$$\underline{H}_4$) (Spectrum 6a, A-4); PXRD: Spectrum 23 (A-15).
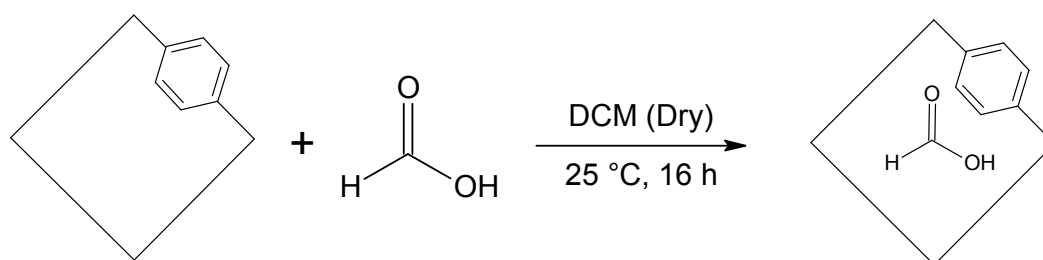
4.4.2 Method 2: In Water:DMF = 9:1

Aluminium chloride hexahydrate (0.805 g, 3.33 mmol), dissolved in distilled water (54 cm^3), was added to a hot (~60°C), stirring solution of terephthalic acid (0.560 g, 3.37 mmol), dissolved in DMF (6 cm^3), instantly forming a white suspension which was stirred for one minute before being transferred to a Teflon cup, put in an autoclave and allowed to react at 130°C for 16 hours. The crude product was isolated by centrifugation (8500 rpm, 15°C, 15 min). The product was washed twice with methanol (25 cm^3) and centrifuged. The white powder was dried in air overnight to obtain crude MIL-53(Al)-as (0.938 g), which was activated in a three-step procedure. MIL-53(Al)-as was dispersed in DMF (30 cm^3) and autoclaved at 150°C for 16 hours. The precipitate was isolated by centrifugation and washed three times with methanol (25 cm^3) and centrifuged (x3). After this, the solid residue was refluxed in methanol (50 cm^3) for 16 hours, isolated by centrifugation, washed three times with methanol (25 cm^3) and centrifuged. The product was activated at 350°C for three days in N$_2$ flow to obtain MIL-53(Al)-ht which changes upon cooling to MIL-53(Al)-lt (0.500 g, 2.21 mmol, 66.4% based on AlCl$_3$·6H$_2$O). IR *v* /cm^{-1} (MIL-53(Al)-lt): 3709 (Al-OH), 1597 (C=O, symmetric), 1416 (C=O, anti-symmetric) (Figure 3.3d, p 40); ^{1}H NMR (300 MHz, NaOD/D$_2$O)/ppm: 7.74 (s; 4H; C$_6$<u>H$_4$</u>) (spectrum 6b, A-4); PXRD: Figure 3.5a (p 44).

4.5   Post Synthetic Modification of MIL-53(Al)
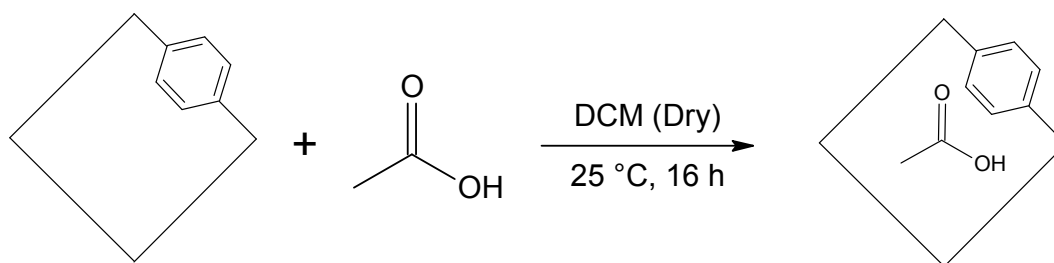
4.5.1 HCOOH@MIL-53(Al)

MIL-53(Al)-lt (0.252 g, 1.21 mmol) was re-activated in a schlenk tube with a septum overnight at 150°C in a vacuum of 4.0 x 10^{-2} mbar. After cooling to room temperature, one eq.
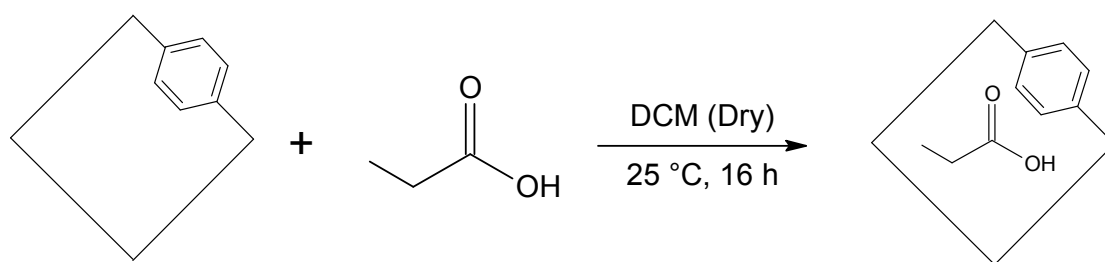
of formic acid (0.0458 cm^3, 1.21 mmol), dissolved in anhydrous DCM (20 cm^3) was dispensed with a syringe to cover the MIL-53 still under vacuum. The vacuum was relieved and the liquid allowed to intrude into the pores for 16 hours at room temperature. The product mixture was centrifuged (8500 rpm, 10 min, 15°C) and the mother liquor decanted. The product was washed with DCM and centrifuged (8500 rpm, 10 min, 15°C). The washing procedure was repeated twice to yield [HCOOH]$_{0.80}$@MIL-53(Al)* (0.238 g). IR v /cm^{-1}: 3599 (Al-OH), 3417 (C-OH, acid), 1690 (C=O, acid), 1572 (C=O, symmetric), 1405 (C=O, anti-symmetric) (Spectrum 2a, A-1); ^{1}H NMR (300 MHz, NaOD/D$_2$O)/ppm: 8.30 (s, 0.2H, C$\underline{H}$O) 7.72 (s, 4H, C$_6\underline{H}_4$) (Figure 3.11a, p 54); PXRD: Figure 3.14a (p 57).
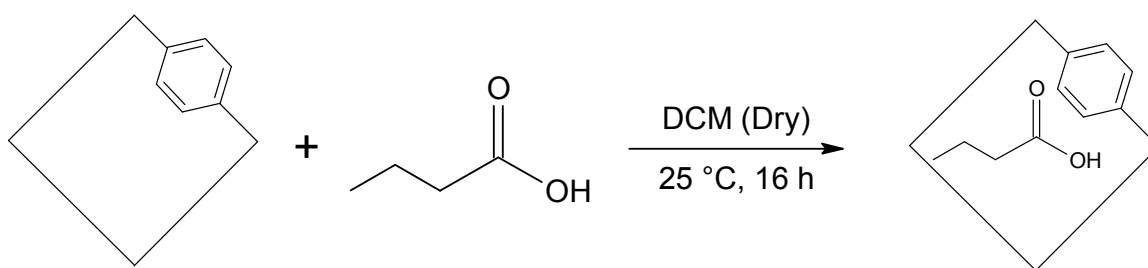
4.5.2 CH$_3$COOH@MIL-53(Al)

MIL-53(Al)-lt (0.255 g, 1.23 mmol) was re-activated in a schlenk tube with a septum overnight at 150°C in a vacuum of 4.0 x 10^{-2} mbar. After cooling to room temperature, one eq. of acetic acid (0.0699 cm^3, 1.22 mmol), dissolved in anhydrous DCM (20 cm^3) was dispensed with a syringe to cover the MIL-53 still under vacuum. The vacuum was relieved and the liquid allowed to intrude into the pores for 16 hours at room temperature. The product mixture was centrifuged (8500 rpm, 10 min, 15°C) and the mother liquor decanted. The product was washed with DCM and centrifuged (8500 rpm, 10 min, 15°C). The washing procedure was repeated twice to yield [CH$_3$COOH]$_{0.63}$@MIL-53(Al)* (0.254 g). IR v /cm^{-1}: 3600 (Al-OH), 3424 (C-OH, acid), 1689 (C=O, acid), 1571 (C=O, symmetric), 1405 (C=O, anti-symmetric) (Spectrum 2b, A-1); ^{1}H NMR (300 MHz, NaOD/D$_2$O)/ppm: 7.73 (s, 4H, C$_6\underline{H}_4$), 1.77 (s, 0.57H, C$\underline{H}_3$) (Figure 3.11b, p 54); PXRD: Figure 3.14b (p 57).

---

* The amount of acid loaded in the MIL-53 structure is expressed as a number of molecules per unit cell.

4.5.3 CH₃CH₂COOH@MIL-53(Al)

MIL-53(Al)-lt (0.255 g, 1.23 mmol) was re-activated overnight at 150°C in a vacuum of 4.0 x 10^{-2} mbar. After cooling to room temperature, one eq. of propionic acid (0.0917 cm^3, 1.23 mmol), dissolved in anhydrous DCM (20 cm^3) was dispensed with a syringe to cover the MIL-53 still under vacuum. The vacuum was relieved and the liquid allowed to intrude into the pores for 16 hours at room temperature.   The product mixture was centrifuged (8500 rpm, 10 min, 15°C) and the mother liquor decanted. The product was washed with DCM and centrifuged (8500 rpm, 10 min, 15°C).   The washing procedure was repeated twice to yield [CH₃CH₂COOH]$_{0.55}$@MIL-53(Al)* (0.246 g).. IR v /cm^{-1}: 3590 (Al-OH), 3423 (C-OH, acid), 1689 (C=O, acid), 1573 (C=O, symmetric), 1407 (C=O, anti-symmetric) (Spectrum 2c, A-1); ^{1}H NMR (300 MHz, NaOD/D₂O)/ppm: 7.73 (s, 4H, C₆$\underline{H}_4$), 2.07-1.99, (q, 0.28H, C$\underline{H}_2$), 0.91, (t, 0.41H, C$\underline{H}_3$) (Figure 3.11c, p 54); PXRD: Figure 3.14c (p 57).

4.5.4 CH₃(CH₂)₂COOH@MIL-53(Al)

MIL-53(Al)-lt (0.253 g, 1.22 mmol) was re-activated overnight at 150°C in a vacuum of 3.9 x 10^{-2} mbar. After cooling to room temperature, one eq. of butyric acid (0.1116 cm^3, 1.22 mmol), dissolved in anhydrous DCM (20 cm^3) was dispensed with a syringe to cover the MIL-53 still under vacuum. The vacuum was relieved and the liquid allowed to intrude into the pores for 16 hours at room temperature.   The product mixture was centrifuged (8500 rpm, 10 min, 15°C) and the mother liquor decanted. The product was washed with DCM and centrifuged (8500 rpm, 10 min, 15°C).   The washing procedure was repeated twice to yield [CH₃(CH₂)₂COOH]$_{0.39}$@MIL-53(Al)* (0.254 g).. IR v /cm^{-1}: 3590 (Al-OH), 3431 (C-OH, acid), 1675 (C=O, acid), 1573 (C=O, symmetric), 1408 (C=O, anti-symmetric) (Figure 3.13, p 56); ^{1}H

93

NMR (300 MHz, NaOD/D$_2$O)/ppm: 7.73 (s, 4H, C$_6$$\underline{H}$$_4$), 2.01 (t, 0.19H, C$\underline{H}$$_2$), 1.45-1.35 (m, 0.18H, C$\underline{H}$$_2$), 0.74 (t, 0.32H, C$\underline{H}$$_3$) (Figure 3.11d, p 54); PXRD: Figure3.14d (p 57).

4.5.5 Fc@MIL-53(Al)-vap (Chemical Vapour Deposition (CVD))
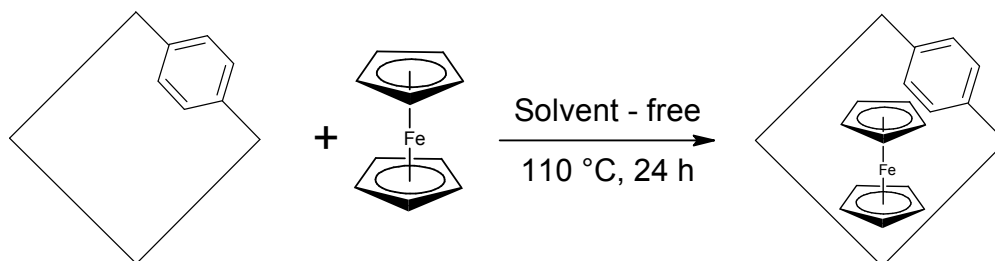
MIL-53(Al)-lt (0.249 g, 1.20 mmol) was re-activated in a sealed schlenk tube overnight at 150°C in a vacuum of 3.2 x 10^{-2} mbar. After cooling down to room temperature, ferrocene (0.495 g, 2.66 mmol) was added to the MOF and the vessel evacuated 3.2 x 10^{-2} mbar. The vessel was sealed and heated to 110°C for 24 hours. After cooling, the product was washed with n-hexane (~ 20 cm^3) and centrifuged (8500 rpm, 10 min, 15°C). The washing procedure was repeated another four times and allowed to dry at room temperature to yield Fc@MIL-53(Al)-vap (0.218 g). IR v /cm^{-1}: 3713-3650 (H-O-H and Al-OH), 1595/1510 (C=O, asymmetric), 1413 (C=O, symmetric), 1107 (C-C, Cp-ring) (Figure 3.21a, p 70); PXRD: Figure 3.23a (p 71).

## 4.5.6 Fc@MIL-53(Al)-sol (Incipient Wetness Impregnation (IWI))
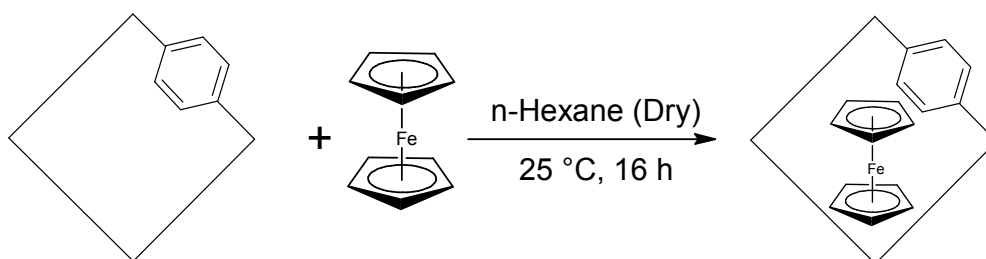
MIL-53(Al)-lt (0.250 g, 1.20 mmol) was re-activated in a sealed schlenk tube overnight at 150°C in a vacuum of 5.6 x 10^{-2} mbar. After cooling down to room temperature, a saturated solution of ferrocene (0.101 M, 1.52 mmol), dissolved in *n*-hexane (anhydrous), was dispensed with a syringe to cover the MIL-53 whilst still under vacuum. The vacuum was relieved and the solution allowed to intrude for 16 hours. The product was centrifuged (8500 rpm, 10 min, 15°C) and the mother liquor decanted. The product was again washed with n-hexane (~20 cm^3) and centrifuged (8500 rpm, 10 min, 15°C). The washing procedure was repeated another four times and allowed to dry at room temperature to yield Fc@MIL-53(Al)-sol (0.154 g).

IR v /cm^{-1}: 3688-3654 (H-O-H and Al-OH), 1594/1510 (C=O, asymmetric), 1412 (C=O, symmetric), 1104 (C-C, Cp-ring) (Figure 3.21b, p 70); PXRD: Figure 3.23b (p 71).
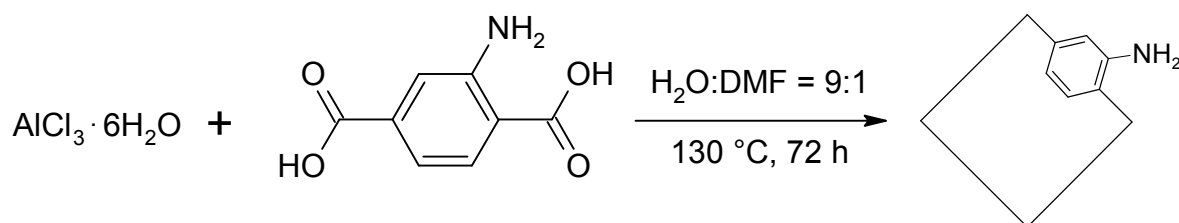
4.6 Synthesis of Amino-MIL-53(Al)

4.6.1 Method 1: DMF (72 Hours)
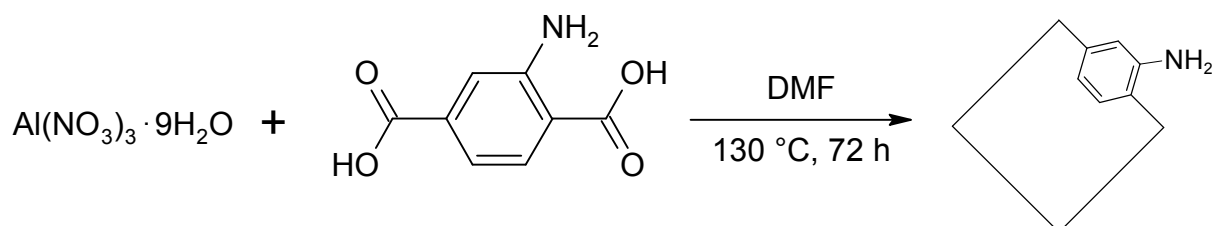
Al(NO$_3$)$_3$·9H$_2$O (1.567 g, 4.18 mmol) dissolved in DMF (30 cm^3) was added to a stirring solution of 2-aminoterephthalic acid (1.133 g, 6.25 mmol) in DMF (30 cm^3). After five minutes of stirring, the solution was transferred to a Teflon cup, put in a stainless steel autoclave and allowed to react at 130°C for 72 hours. The crude product was isolated by centrifugation (8500 rpm, 15°C, 15 min), washed twice with methanol (40 cm^3) and centrifuged. The yellow powder was dried in air overnight to obtain amino-MIL-53(Al)-as (1.174 g). The crude product was refluxed in methanol (30 cm^3) for 16 hours, isolated by centrifugation, washed three times with methanol (40 cm^3) and centrifuged. The product (0.972 g) was activated at 330°C for 72 hours in N$_2$ flow to obtain amino-MIL-53(Al)-ht, which changes upon cooling to amino-MIL-53(Al)-lt (0.833 g, 82.6% based on Al(NO$_3$)$_3$·9H$_2$O). IR v /cm^{-1} (amino-MIL-53(Al)-lt): 3598 (Al-OH), 3493/3382 (N-H, amine), 1564/1461 (C=O, asymmetric), 1436 (C=O, symmetric) (Figure 3.6b, p 46); ^{1}H NMR (300 MHz, NaOD/D$_2$O)/ppm: 7.58, 7.55 (d; 1H; C$_6$$\underline{H}_3$), 7.13 (d; 1H; C$_6$$\underline{H}_3$), 7.07-7.04 (dd, 1H; C$_6$$\underline{H}_3$) (Spectrum 6d, A-4); PXRD: Spectrum 24 (A-15).

4.6.2 Method 2: In Water:DMF = 9:1

Aluminium chloride hexahydrate (2.600 g, 10.77 mmol) dissolved in H_2O (72 cm^3) was slowly added to a warm (~70°C) solution of 2-aminoterephthalic acid (1.998 g, 11.03 mmol) dissolved in DMF (8 cm^3). The mixture was transferred to a Teflon cup, put in a stainless steel autoclave and allowed to react at 130°C for 72 hours. The crude product was isolated by centrifugation (8500 rpm, 15°C, 15 min), washed twice with methanol (60 cm^3) and centrifuged. The yellow amorphous powder was dried in air overnight to obtain crude amino-MIL-53(Al)-as (2.501 g). The obtained amino-MIL-53(Al)-as was dispersed in DMF (30 cm^3) and autoclaved at 150°C for 16 hours. The precipitate was isolated by centrifugation and washed three times with methanol (25 cm^3) and centrifuged (x3). After this, the solid residue was refluxed in methanol (50 cm^3) for 16 hours, isolated by centrifugation and washed three times with methanol (25 cm^3) and centrifuged. A portion of the product (0.359 g) activated at 300°C for 72 hours to obtain amino-MIL-53(Al)-ht which changes to amino-MIL-53(Al)-lt (0.322 g, 87.3% based upon $AlCl_3 \cdot 6H_2O$) upon cooling to room temperature. IR v /cm^{-1} (amino-MIL-53(Al)-lt): 3637 (Al-OH), 3501/3391 (N-H, amine), 1566/1493 (C=O, asymmetric), 1439 (C=O, symmetric) (Figure 3.7d, p 47); ^{1}H NMR (300 MHz, NaOD/D_2O)/ppm: 7.52-7.49 (d; 1H; C$_6$$\underline{H}_3$), 7.07 (d; 1H; C$_6$$\underline{H}_3$), 7.02-6.99 (dd, 1H; C$_6$$\underline{H}_3$) (Figure 3.8, p 48); PXRD: Figure 3.10 (p 51).

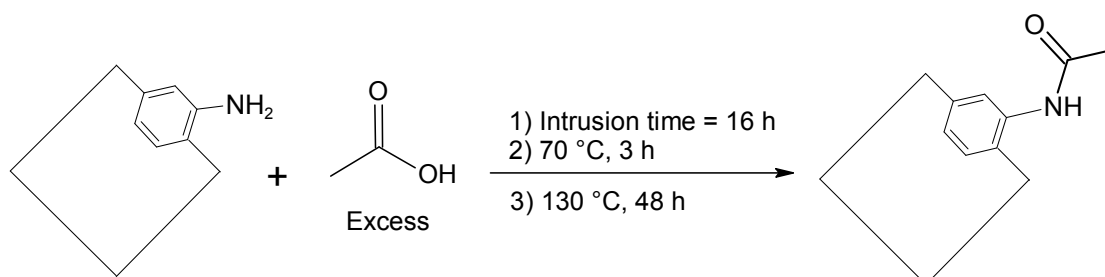# 4.7 Postsynthetic Modification of Amino-MIL-53(Al)

4.7.1 HCONH-MIL-53(Al)
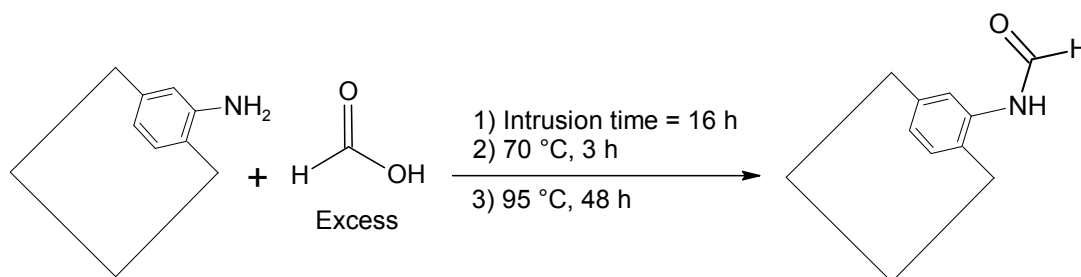
Amino-MIL-53(Al)-lt (0.204 g, 0.91 mmol) was re-activated at 150°C and a vacuum of 3.1 x 10^{-2} mbar overnight. After cooling to room temperature, formic acid (5 cm^3, 0.13 mol) was dispensed with a syringe to cover the amino-MIL-53 still under vacuum. The vacuum was relieved and the liquid allowed to intrude into the pores for 16 hours at room temperature. The mixture was heated up to 70°C in air for three hours after which it was washed three times with water (25 cm^3) and centrifuged (8500 rpm, 15°C, 15 min). After drying the product overnight at 40°C, it was heated at 95°C for two days to obtain HCONH-MIL-53(Al)-as (0.137 g). The unbound acid was removed by evacuation at 80°C overnight to obtain [HCONH]$_x$-MIL-53(Al)-

vac† (0.124 g).   IR v /cm^{-1}: 3307 (N-H, amide), 1685 (C=O, amide), 1594/1510 (C=O, asymmetric), 1414 (C=O, symmetric), 1296 (C-N, amide) (Figure 3.15a, p 59); ^{1}H NMR (300 MHz, NaOD/D$_2$O)/ppm: Spectrum could not be determined due to compound decomposition; PXRD: Figure 3.18a (p 62).
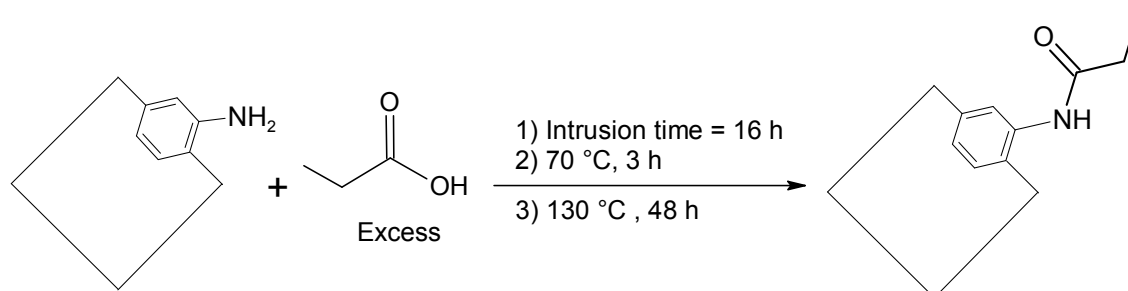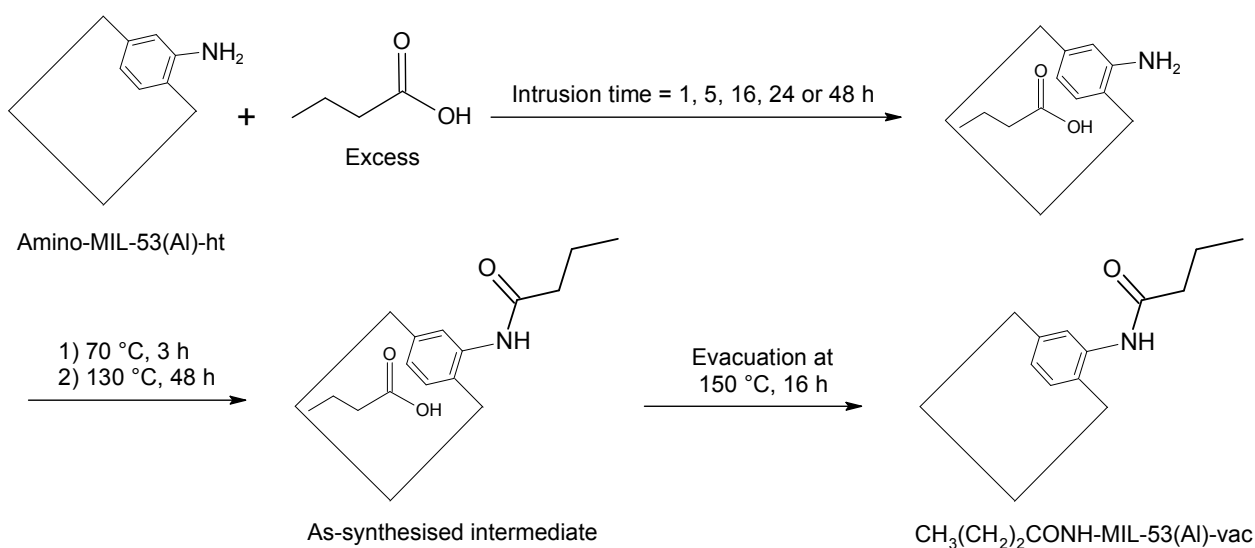
4.7.2 CH$_3$CONH-MIL-53(Al)

Amino-MIL-53(Al)-lt (0.204 g, 0.91 mmol) was re-activated at 150°C and a vacuum of 1.1 x 10^{-2} mbar overnight.   After cooling to room temperature, acetic acid (5 cm^3, 0.087 mol) was dispensed with a syringe to cover the amino-MIL-53 still under vacuum. The vacuum was relieved and the liquid allowed to intrude into the pores for 16 hours at room temperature. The mixture was heated up to 70°C in air for three hours after which it was washed three times with water (25 cm^3) and centrifuged (8500 rpm, 15°C, 15 min). After drying the product overnight at 40°C, it was again heated up to 130°C for two days to yield crude CH$_3$COONH-MIL-53(Al)-as (0.195 g).   The unbound acid was removed by evacuation at 100°C overnight to obtain [CH$_3$COONH]$_{17.6}$-MIL-53(Al)-vac‡ (0.158 g).   IR v /cm^{-1}: 3649 (Al-OH), 3507/3393 (N-H, amine), 1694 (C=O, amide), 1572/1494 (C=O, asymmetric), 1439 (C=O, symmetric) (Figure 3.15b, p 59); ^{1}H NMR (300 MHz, NaOD/D$_2$O)/ppm: 7.57-7.54 (d; 1H; C$_6$H$_3$), 7.20 (d; 1H; C$_6$H$_3$), 7.06-7.03 (dd, 1H; C$_6$H$_3$), 1.77 (s; 0.51H; CH$_3$) (Figure 3.16a, p 60); PXRD: Figure 3.18b (p 62).

---

† The amount of formic acid bound to amino-MIL-53(Al) could not be determined by ^{1}H NMR spectroscopy due to product decomposition prior to measurement.

‡ The amount of acid chemisorbed in amino-MIL-53(Al) is expressed as a direct conversion percentage.

4.7.3 CH₃CH₂CONH-MIL-53(Al)

Amino-MIL-53(Al)-lt (0.200 g, 0.90 mmol) was re-activated at 150°C and a vacuum of 2.8×10^{-2} mbar overnight. After cooling to room temperature, propionic acid (5 cm^3, 0.067 mol) was dispensed with a syringe to cover the amino-MIL-53 still under vacuum. The vacuum was relieved and the liquid allowed to intrude into the pores for 16 hours at room temperature. The mixture was heated up to 70°C in air for three hours after which it was washed three times with water (25 cm^3) and centrifuged (8500 rpm, 15°C, 15 min). After drying the product overnight at 40°C, it was again heated up to 130°C for two days to yield crude CH₃CH₂COONH-MIL-53(Al)-as (0.187 g). The unbound acid was removed by evacuation at 120°C overnight to yield [CH₃CH₂COONH]$_{7.1}$-MIL-53(Al)-vac‡ (0.176 g). IR v /cm^{-1}: 3607 (Al-OH), 3490/3382 (N-H, amine), 1658 (C=O, amide), 1564/1491 (C=O, asymmetric), 1435 (C=O, symmetric) (Figure 3.15c, p 59); ^{1}H NMR (300 MHz, NaOD/D₂O)/ppm: 7.56-7.53 (d; 1H; C₆$\underline{H}$₃), 7.11 (d; 1H; C₆$\underline{H}$₃), 7.06-7.03 (dd, 1H; C₆$\underline{H}$₃), 2.07-1.99 (q; 0.14H; C$\underline{H}$₂), 0.90 (t; 0.20H; C$\underline{H}$₃) (Figure 3.16b, p 60); PXRD: Figure 3.18c (p 62).

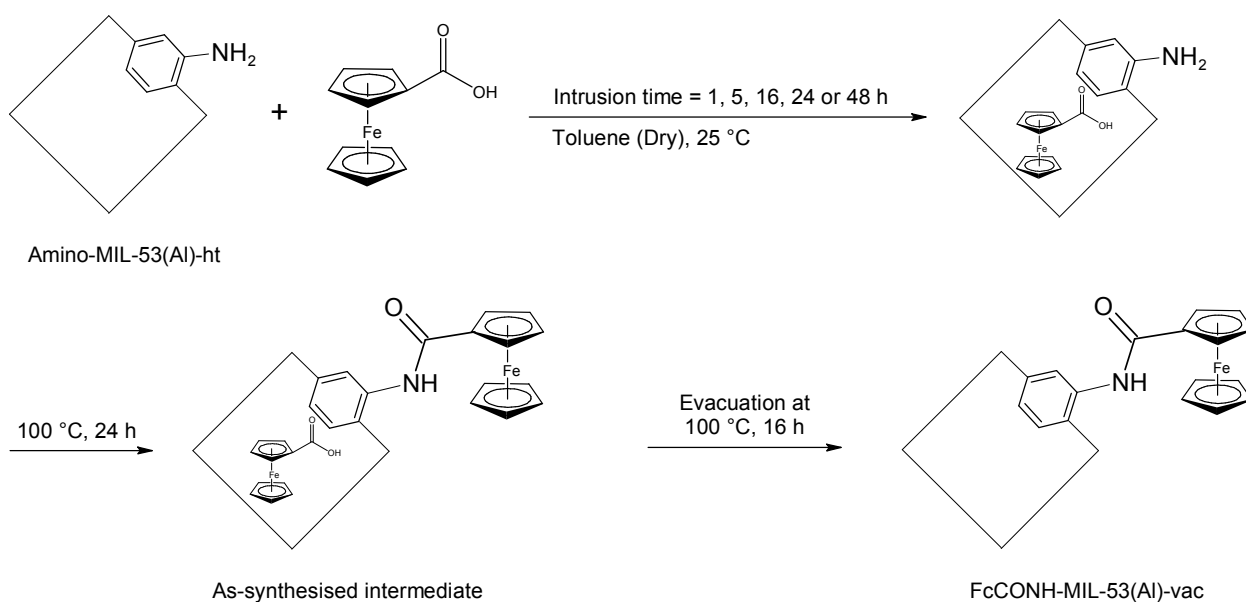## 4.7.4 CH₃(CH₂)₂CONH-MIL-53(Al) (Time-Controlled Intrusions)

98

Amino-MIL-53(Al)-lt (0.202 g, 0.91 mmol) was re-activated at 150°C and a vacuum of 2.8 x 10^{-2} mbar overnight. After cooling to room temperature, butyric acid§ (5 cm^3, 0.054 mol) was dispensed with a syringe to cover the amino-MIL-53 still under vacuum. The vacuum was relieved and the liquid allowed to intrude into the pores for 16 hours at room temperature. The mixture was heated up to 70°C in air for three hours, after which it was washed three times with water (25 cm^3) and centrifuged (8500 rpm, 15°C, 15 min). After drying the product overnight at 40°C, it was again heated up to 130°C for two days to yield crude $CH_3(CH_2)_2CONH$-MIL-53(Al)-as. The unbound acid was removed by evacuation at 150°C overnight to yield $[CH_3(CH_2)_2CONH]_{19.7}$-MIL-53(Al)-vac‡(obtained after 16 hours of intrusion). IR v /cm^{-1} ($CH_3(CH_2)_2CONH$-MIL-53(Al)-vac): 3654 (Al-OH), 3510/3393 (N-H, amine), 1698, (C=O, amide), 1575/1496 (C=O, asymmetric), 1439 (C=O, symmetric) (Figure 3.15d, p 59); ^{1}H NMR (300 MHz, NaOD/D$_2$O)/ppm: 7.57-7.54 (d; 1H; C$_6$H$_3$), 7.12 (d; 1H; C$_6$H$_3$), 7.06-7.03 (dd, 1H; C$_6$H$_3$), 2.00 (t; 0.36H; CH$_2$), 1.47-1.35 (m; 0.38H; CH$_2$), 0.75 (t; 0.59H; CH$_3$) (Figure 3.19b, p 64); PXRD: Figure 3.18d (p 62).

Table 4.1: Experimental parameters for the synthesis of $CH_3(CH_2)_2CONH$-MIL-53(Al)-vac: intrusion time, NMR integration and binding percentage.

Intrusion Time for Butyric Acid (h)	NMR integration						Spectrum reference in Appendix	Binding% (NH$_2$ groups amidated)
	Ar-H$_a$	Ar-H$_b$	Ar-H$_c$	-CH$_2$-	-CH$_2$-	-CH$_3$		
1	1.00	0.89	0.99	0.27	0.26	0.44	8b (A-6)	14.43
5	1.00	0.91	1.01	0.30	0.29	0.50	8d (A-6)	16.00
16	1.00	0.90	0.99	0.36	0.38	0.59	-	19.72
24	1.00	0.88	0.99	0.29	0.28	0.45	9b (A-7)	15.23
48	1.00	0.89	1.02	0.26	0.26	0.43	9d (A-7)	13.99

---

§ Refer to Table 4.1 (p 99) for the synthesis results of all the $CH_3(CH_2)_2CONH$-MIL-53(Al) conjugates.

4.7.5 FcCONH-MIL-53(Al) (Time-Controlled Intrusions)

Amino-MIL-53(Al)-ht

Intrusion time = 1, 5, 16, 24 or 48 h
Toluene (Dry), 25 °C

100 °C, 24 h

As-synthesised intermediate

Evacuation at
100 °C, 16 h

FcCONH-MIL-53(Al)-vac

Amino-MIL-53(Al)-lt (29 mg, 0.13 mmol)[**] was re-activated at 150°C and a vacuum of 3.0×10^{-2} mbar overnight. After cooling to room temperature, FcCOOH (30 mg, 0.13 mmol) dissolved in anhydrous toluene (20 cm^3) was dispensed with a syringe over the amino-MIL-53 still under vacuum. The vacuum was relieved and the liquid allowed to intrude into the pores for 16 hours at room temperature, then allowed to react (16 h, 100°C). The product mixtures was centrifuged (8500 rpm, 10 min, 15°C), washed three times with n-hexane (~20 cm^3), centrifuged and left at room temperature to dry. The unbound acid was removed by evacuation at 100°C overnight to yield [FcCONH]$_{0.50}$-MIL-53(Al)-vac[‡](obtained after a 16 hours intrusion time). IR v /cm^{-1} (FcCONH-MIL-53(Al)-vac: 3650 (Al-OH), 3492/3380 (N-H, amine), 1663 (C=O, amide), 1570/1496 (C=O, asymmetric), 1437 (C=O, symmetric), 1100/982 (C-C, Cp-ring) (Figure 3.27a, p 76); ^{1}H NMR (300 MHz, NaOD/D$_2$O)/ppm: 7.57-7.54 (d; 1H; C$_6\underline{H}_3$), 7.12 (d; 1H; C$_6\underline{H}_3$), 7.07-7.04 (dd, 1H; C$_6\underline{H}_3$), 4.23 (t; 0.23H; C$_5\underline{H}_2$), 4.12 (s; 0.62H; C$_5\underline{H}_5$) (Figure 3.29b, p 78); PXRD: Figure 3.28a (p 77).

[**] Refer to Table 4. 2 (p 100) for the synthesis results of all the FcCONH-MIL-53(Al) conjugates.

Table 4. 2:   Experimental parameters for the synthesis of FcCONH-MIL-53(Al)-vac: intrusion time, NMR integration and binding percentage.

Intrusion time for FcCOOH (h)	NMR integration					Spectrum reference in Appendix	Binding% (NH₂ groups amidated)
	Ar-H$_a$	Ar-H$_b$	Ar-H$_c$	C$_5$H$_2$	C$_5$H$_5$		
1	1.00	0.96	1.01	0.20	0.36	10b (A-8)	8.08
5	1.00	1.00	1.04	0.21	0.47	10d (A-8)	9.59
16	1.00	0.95	1.00	0.23	0.59	-	11.91
24	1.00	0.95	0.99	0.14	0.42	11b (A-9)	8.16
48	1.00	0.97	1.01	0.16	0.39	11d (A-9)	7.94

4.7.6 Fc@amino-MIL-53(Al)-vap (CVD)
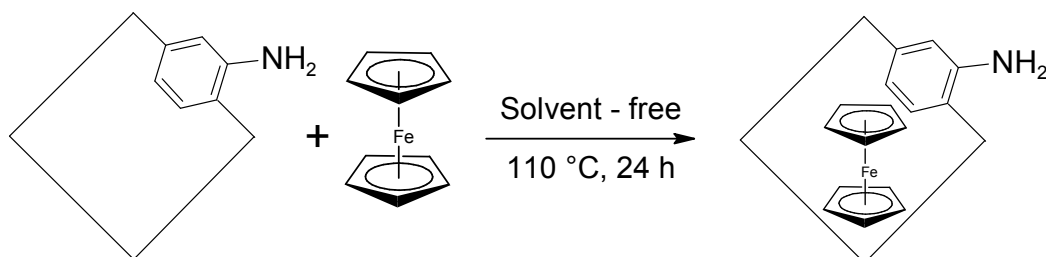
Amino-MIL-53(Al)-lt (0.201 g, 0.90 mmol) was re-activated in a sealed schlenk tube overnight at 150°C in a vacuum of 1.5 x 10^{-2} mbar.   After cooling to room temperature, ferrocene (0.502 g, 2.70 mmol) was added to the MOF and a vacuum of 1.3 x 10^{-2} mbar was drawn over the mixture. The vessel was sealed and heated to 110°C for 24 hours. The product was washed five times with n-hexane (~20 cm^3), centrifuged (8500 rpm, 10 min, 15°C) and dried in air to yield Fc@amino-MIL-53(Al)-vap (0.188 g).   IR v /cm^{-1}: 3643 (Al-OH), 1568/1492 (C=O, asymmetric), 1439 (C=O, symmetric), 992 (C-C, Cp-ring) (Figure 3.24a, p 72); PXRD: Figure 3.26a (p 74).

4.7.7 Fc@amino-MIL-53(Al)-sol (IWI)
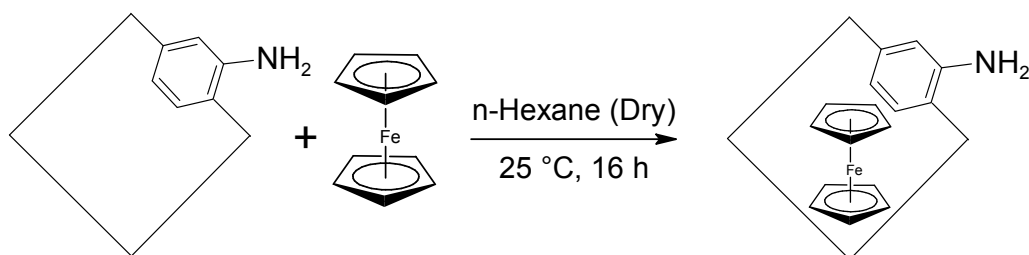
Amino-MIL-53(Al)-lt (0.201 g, 0.90 mmol) was re-activated in a sealed schlenk tube overnight at 150°C in a vacuum of 1.2 x 10^{-2} mbar. After cooling to room temperature, a saturated solution of ferrocene (0.083 M, 1.50 mmol) in n-hexane was dispensed with a syringe over the amino-MIL-53 whilst still under vacuum. The vacuum was relieved and the solution allowed to intrude for 16 hours. The product was isolated by centrifugation (8500 rpm, 10 min, 15°C), washed five times with n-hexane (~20 cm^3), centrifuged and dried in air to yield Fc@amino-MIL-53(Al)-sol (0.189 g). IR v /cm^{-1}: 3697 (Al-OH), 1573/1498 (C=O, asymmetric), 1440 (C=O, symmetric), 1104 (C-C, Cp-ring) (Figure 3.24b, p 72); PXRD: Figure 3.26b (p 74).

5 Conclusions and Future Perspectives

In this study the metal organic frameworks, MIL-53(Al) and amino-MIL-53(Al) were both successfully synthesised in relatively high yields (57 - 87%) by two different solvothermal methods: the one making use of $Al(NO_3)_3 \cdot 9H_2O$ and the other of $AlCl_3 \cdot 6H_2O$ as metal salt precursor. Characterisation of MIL-53(Al) and amino-MIL-53(Al) were done by FTIR, ^{1}H-NMR, TGA, ASAP and PXRD which, where applicable, were all in good agreement with literature. After activation, using a combination of solvent exchange, high temperature and vacuum, these MOFs were used as solid supports for either the physisorption (adsorption without covalent bonding) or chemical binding of organic and organometallic compounds.

Unfunctionalised MIL-53(Al) was used in the first part of this study to investigate the physisorption of a series of aliphatic carboxylic acids with increasing chain length (HCOOH, CH_3COOH, CH_3CH_2COOH and $CH_3(CH_2)_2COOH$) into the microporous channels of the MOF. These acids were intruded into MIL-53(Al) using a newly designed incipient wetness impregnation (IWI) method whereby a high vacuum is maintained over the porous support while covering it with the liquid acid. After relieving the vacuum, the acid was allowed to intrude into the microporous channels under the force of atmospheric pressure. Using this method, high loading e.g. 0.8 molecules of HCOOH per unit cell (the highest) of MIL-53(Al) was achieved. The amount of carboxylic acid molecules per unit cell decreased as the chain length of the carboxylic acid increased till four carbon atoms (0.39 molecules for $CH_3(CH_2)_2COOH$ per unit cell of MIL-53(Al)).

MIL-53(Al) was also intruded by ferrocene (Fc) (a relatively large organometallic molecule) using chemical vapour deposition (CVD) as well as IWI. TGA showed that the latter method was more successful (7.59 wt% of Fc) than CVD (6.17 wt% of Fc) in loading ferrocene into MIL-53(Al).

Amino-MIL-53(Al) was loaded with the same series of aliphatic carboxylic acids by IWI, after which the acids were bound to the MOF framework through amidation of the NH_2 functionalities on the terephthalate linkers. Due to their general insolubility, the products of these amidation reactions were digested in $NaOD/D_2O$ in order to perform ^{1}H NMR analysis. The maximum

conversion and the success of bonding ranged between 7% and 20% as determined by ^{1}H NMR integration values for $CH_3CONH-MIL-53(Al)$-vac, $CH_3CH_2CONH-MIL-53(Al)$-vac and $CH_3(CH_2)_2CONH-MIL-53(Al)$-vac. With $HCONH-MIL-53(Al)$-vac, no ^{1}H NMR measurement was possible, since hydrolysis of the amide bond occurred before measurement.

With the intrusion of butyric acid into amino-MIL-53(Al), a time-resolved study was performed, aimed at quantifying the amount of acid loaded into the framework of the amino-MIL-53(Al) before and after the amidation reaction. Intrusion times of 1, 5, 16, 24 and 48 hours (at room temperature) were employed, with the highest conversion (chemical binding) of 20% (with respect to the total number of NH_2 groups) achieved after an intrusion period of 16 hours, as shown by ^{1}H NMR analysis. This trend was verified with TGA, giving a maximum mass loss of 4.6 wt% for the evacuated product, $CH_3(CH_2)_2CONH-MIL-53(Al)$-vac (obtained after a 16 hours intrusion time).

After intruding amino-MIL-53(Al) with ferrocene using CVD as well as IWI, it was found that IWI was a much more effective (11.02 wt% of Fc in Fc@amino-MIL-53(Al)-sol) method than CVD (1.66 wt% of Fc in Fc@amino-MIL-53(Al)-vap). For the rest of this study, IWI was used to intrude FcCOOH into amino-MIL-53(Al).

The intrusion of amino-MIL-53(Al) with FcCOOH was studied by using different intrusion times prior to the amidation of amino-MIL-53(Al) with FcCOOH. With ^{1}H NMR spectroscopy, a maximum binding of 12% was found after an intrusion time of 16 hours for the evacuated product (FcCONH-MIL-53(Al)-vac). A maximum load after 16 hours of intrusion was also confirmed by TG analyses. Longer intrusion times resulted in lower binding percentages. Excellent correlation between the ^{1}H NMR and TG analyses were found by calculating the mass percentage from the ^{1}H NMR results. This good agreement indicated that no or little hydrolysis occurred during the digestion of the FcCONH-MIL-53(Al)-vac products for ^{1}H NMR analysis.

A novel solid state electrochemical method was employed to probe ferrocene-containing MOFs, Fc@MIL-53(Al)-sol, Fc@amino-MIL-53(Al)-sol and FcCONH-MIL-53(Al)-vac (obtained after a 16 hours intrusion time) for electrochemical activity. With cyclic voltammetry, the Fc^{II}/Fc^{III} couple could be detected in all three compounds. Although an electrochemical reversibility was found for Fc@amino-MIL-53(Al)-sol and FcCONH-MIL-53(Al)-vac, with $\Delta E_p = 57$ and 21 mV respectively, migration of material into the bulk solution could be possible since $0.6 \leq i_{pc}/i_{pa} \leq 0.7$. A quasi-reversible electrochemical process found for Fc@MIL-53(Al)-sol ($\Delta E_p = 77$) is

accompanied by its limited chemical reversibility (i_{pc}/i_{pa} = 0.67). It was also found that FcCOOH, covalently bound to the amino-MIL-53(Al) structure, is easier to oxidise ($E^{0'}$ = -71 mV for FcCONH-MIL-53(Al)-vac) than free ferrocene adsorbed into MIL-53(Al) ($E^{0'}$ = 1 mV for Fc@MIL-53(Al)-sol) and amino-MIL-53(Al) ($E^{0'}$ = -13 mV for Fc@amino-MIL-53(Al)-sol).

The future perspectives for this study mainly lie in the further advancement of post-synthetic modification using IWI. From this study, it was proven that IWI is a very good method for the incorporation of both organic and organometallic moieties in MIL-53(Al) and amino-MIL-53(Al). The IWI method in this study makes use of a pressure gradient, which differs from conventional IWI methods where only capillary action is used to allow intrusion of catalysts into solid supports. This IWI method, which can have a great impact on applications where higher loads of a catalyst is wanted, is not restricted to the MIL-53 range and can be implemented on MOFs such as MIL-101, IRMOF-3 or even mesoporous silica like MCM-41. A higher loading of active ingredients in the porous material can improve its performance in fields such as heterogeneous catalysis and drug delivery.

The binding reaction after intrusion should be optimised in terms of functional groups, synthesis conditions as well as the metal centre of the MOF depending on the intended application of need. In case of a biomedical application, an amine functional group would be preferred, since it could result in a biodegradable peptide bond. The metal centre should also be bio-compatible e.g. Zn and Fe. If a catalytic product is wanted, the functional groups and metal centre of the MOF can be specifically selected to suit the catalytic reaction of choice.

The successful attachment of ferrocenecarboxylic acid to amino-MIL-53(Al) has paved the way for a series of functionalised metallocenes like ruthenocene and osmocene to be covalently bound to amino-MIL-53(Al) for applications in heterogeneous catalysis. Since ferrocene is used as a slow release catalyst in solid, rocket propellants, FcCONH-MIL-53(Al) can be tested for catalytic activity in this regard since leaching of ferrocene from the framework is impossible when it is chemically bound to the structure.[1,2] Methods to reduce the intruded metallocene without damage to the MOF structure should be investigated, since it could lead to catalytically active metal clusters supported in the framework.

As shown during digestive ^{1}H NMR, MIL-53(Al) and amino-MIL-53(Al) derivatives are sensitive to high pH levels. A study can be conducted to investigate the decomposition process

of the MOFs at different alkalinities. It is important to find the optimum decomposition rate, especially when keeping drug and catalyst release in mind.

In conclusion, the amino-MIL-53(Al) metal organic framework was found to be a solid support material with good thermal stability and versatile chemical functionality. Greater insight was obtained on the migration behaviour of organic and organometallic molecules in the microporous channels of MIL-53(Al) and amino-MIL-53(Al).
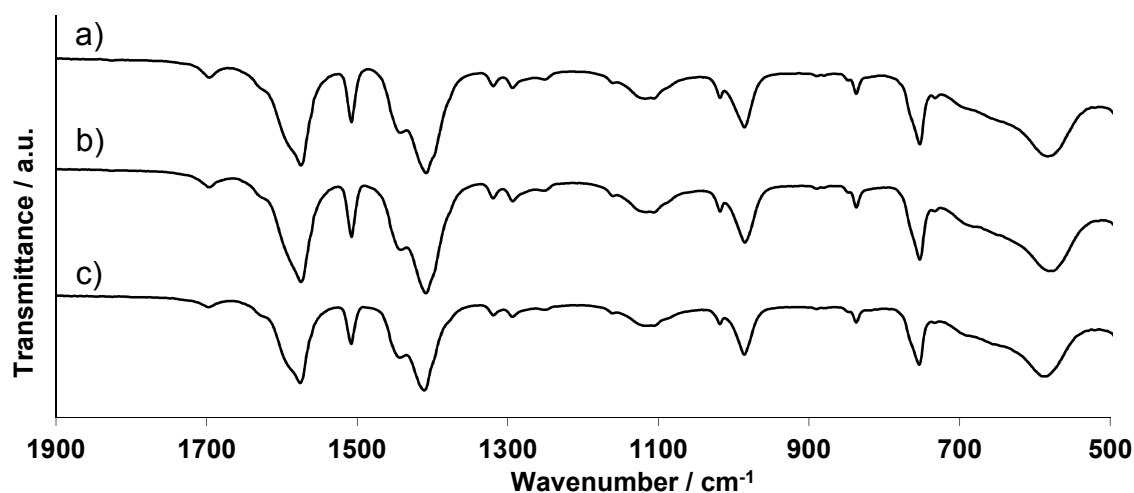
References

1   G. M. Gore, K. R. Tipare, R. G. Bhatewara, U. S. Prasad, M. Gupta and S. R. Mane, *Def. Sci. J.*, 1999, **49**, 151-158.

2   D. Saravanakumar, N. Sengottuvelan, V. Narayanan, M. Kandaswam and T. L. Varghese, *J. Appl. Polyl. Sci.*, 2010, **119**, 2517-2524.

Appendix

Fourier Transform Infrared Spectroscopy (FTIR)
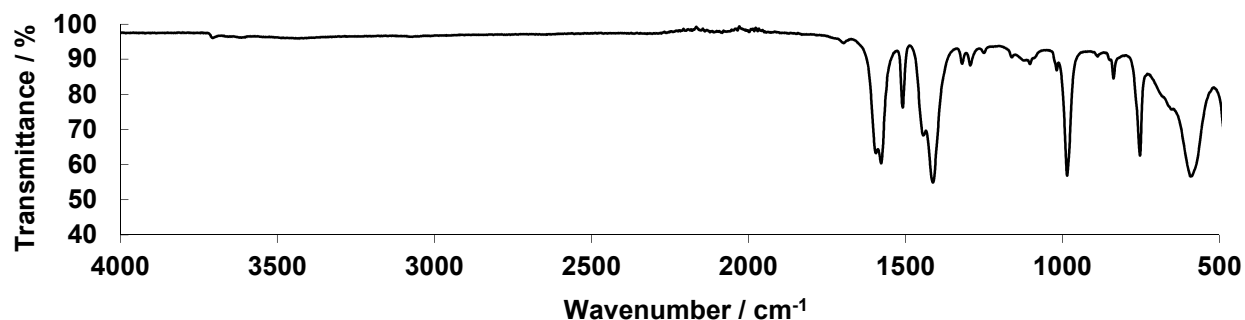
**Spectrum 1: FTIR of commercial MIL-53(Al)-lt.**

Spectrum 2: FTIR spectra of HCOOH@MIL-53(Al) (a), CH₃COOH@MIL-53(Al) (b) and CH₃CH₂COOH@MIL-53(Al) (c).
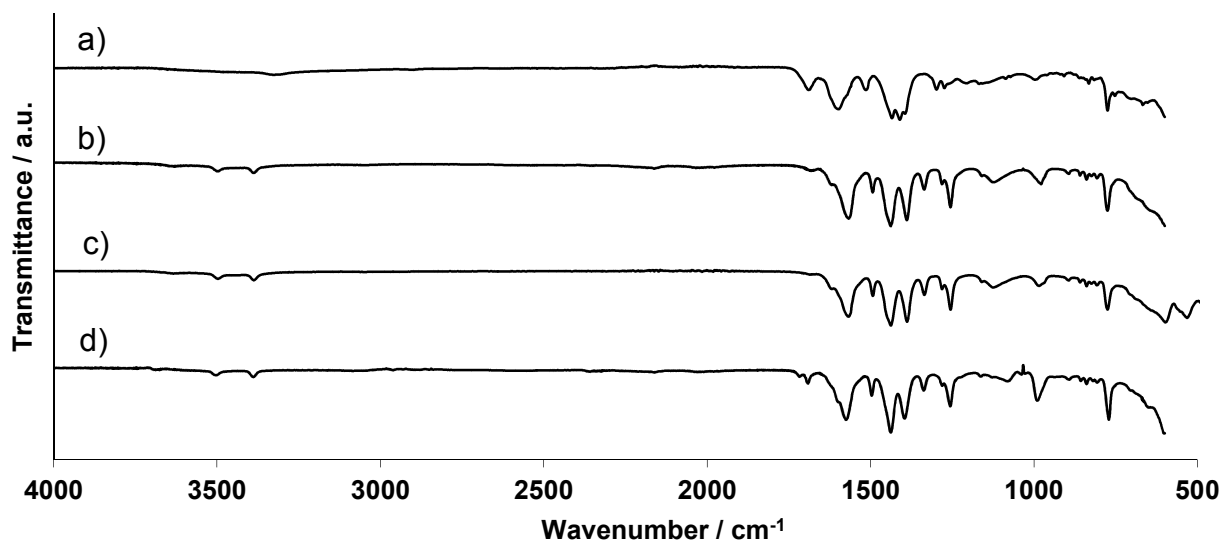
Spectrum 3: FTIRs of a) HCONH-MIL-53(Al)-as, b) CH₃CONH-MIL-53(Al)-as, c) CH₃CH₂CONH-MIL-53(Al)-as and d) CH₃CH₂CH₂CONH-MIL-53(Al)-16h-as.
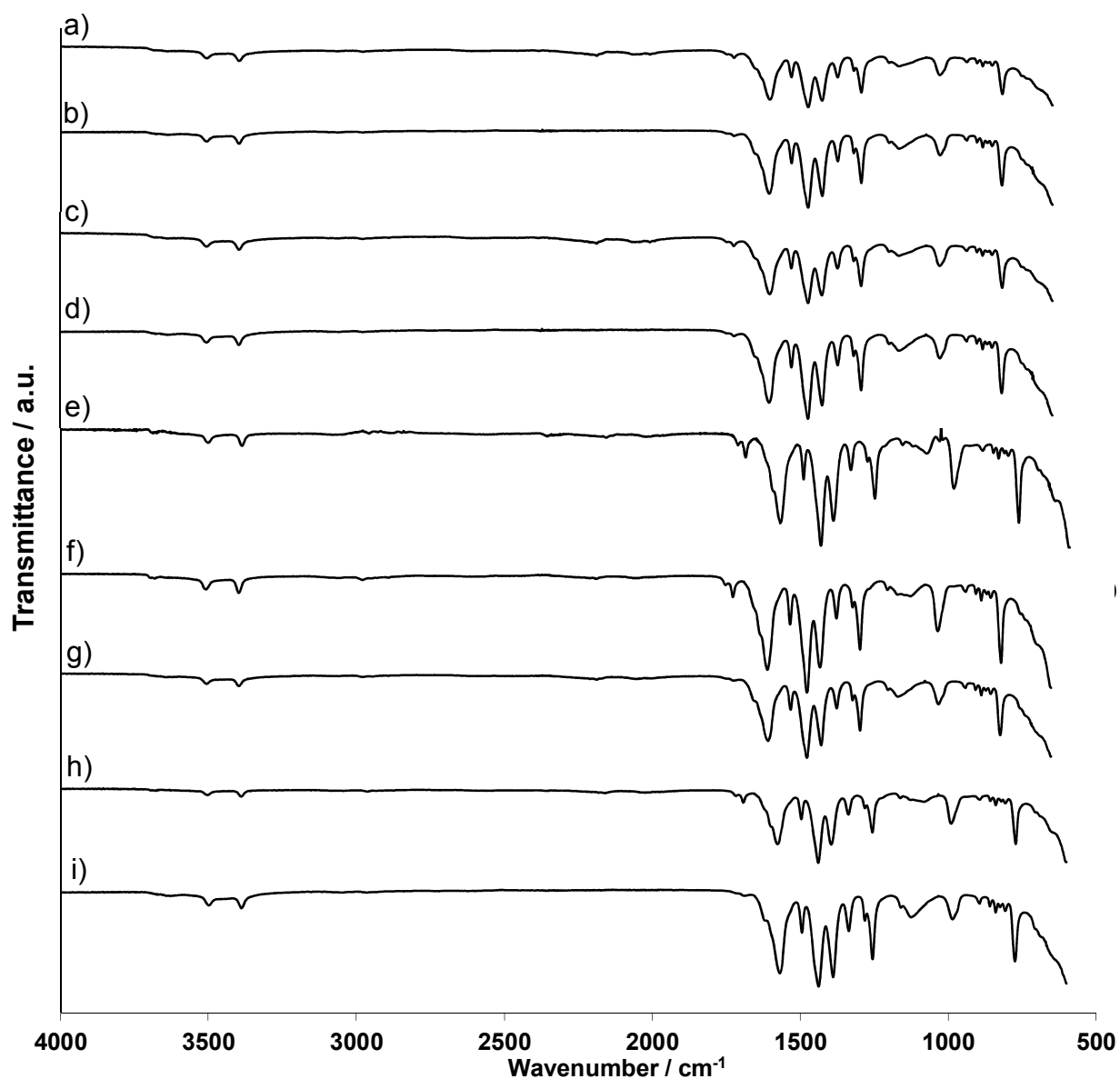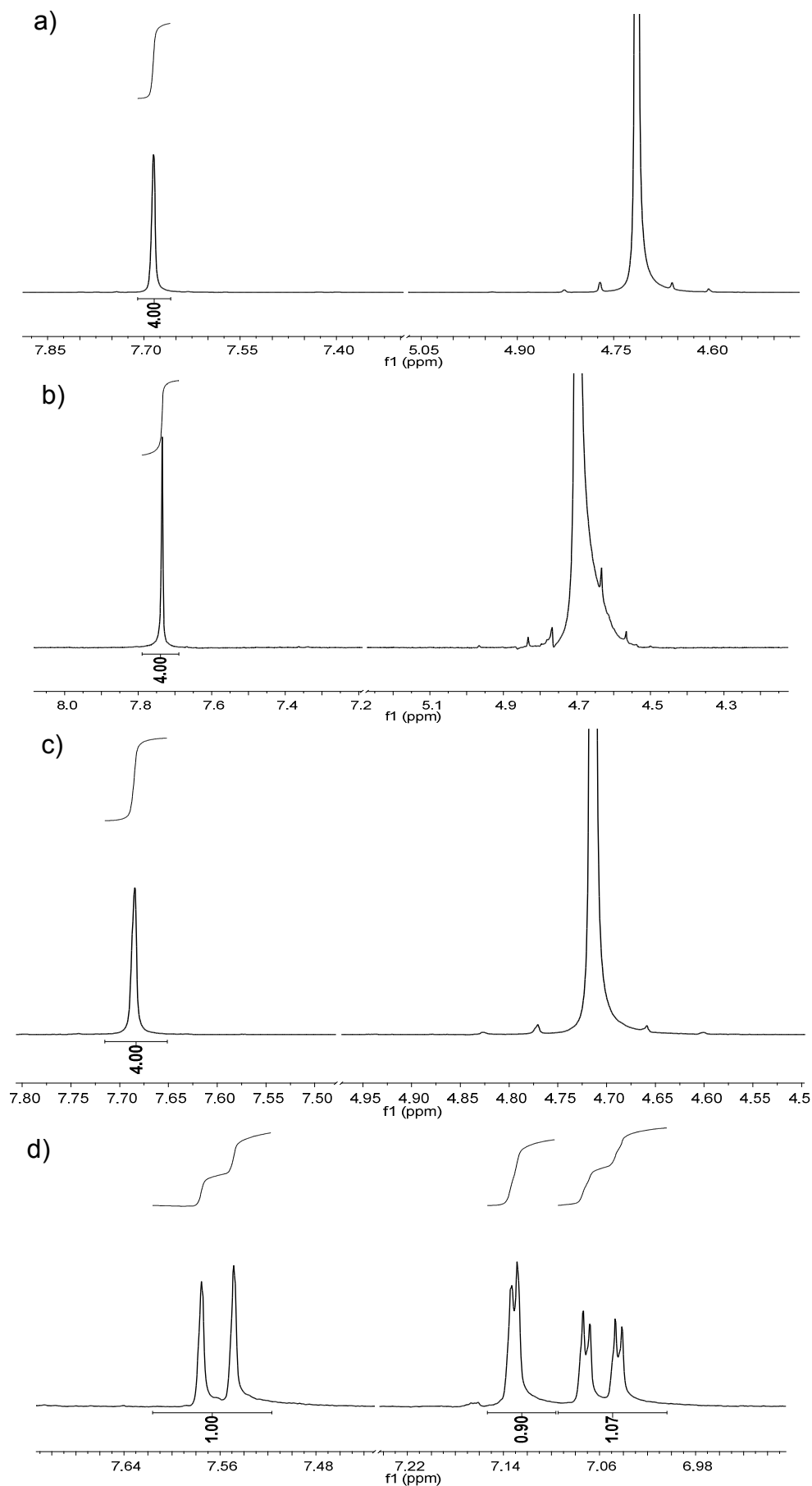
Spectrum 4: FTIRs of a) CH$_3$(CH$_2$)$_2$CONH-MIL-53(Al)-1h-as, **b)** CH$_3$(CH$_2$)$_2$CONH-MIL-53(Al)-1h-vac, **c)** CH$_3$(CH$_2$)$_2$CONH-MIL-53(Al)-5h-as, **d)** CH$_3$(CH$_2$)$_2$CONH-MIL-53(Al)-5h-vac, **e)** CH$_3$(CH$_2$)$_2$CONH-MIL-53(Al)-16h-as, **f)** CH$_3$(CH$_2$)$_2$CONH-MIL-53(Al)-24h-as, **g)** CH$_3$(CH$_2$)$_2$CONH-MIL-53(Al)-24h-vac, **h)** CH$_3$(CH$_2$)$_2$CONH-MIL-53(Al)-48h-as, **i)** CH$_3$(CH$_2$)$_2$CONH-MIL-53(Al)-48h-vac.
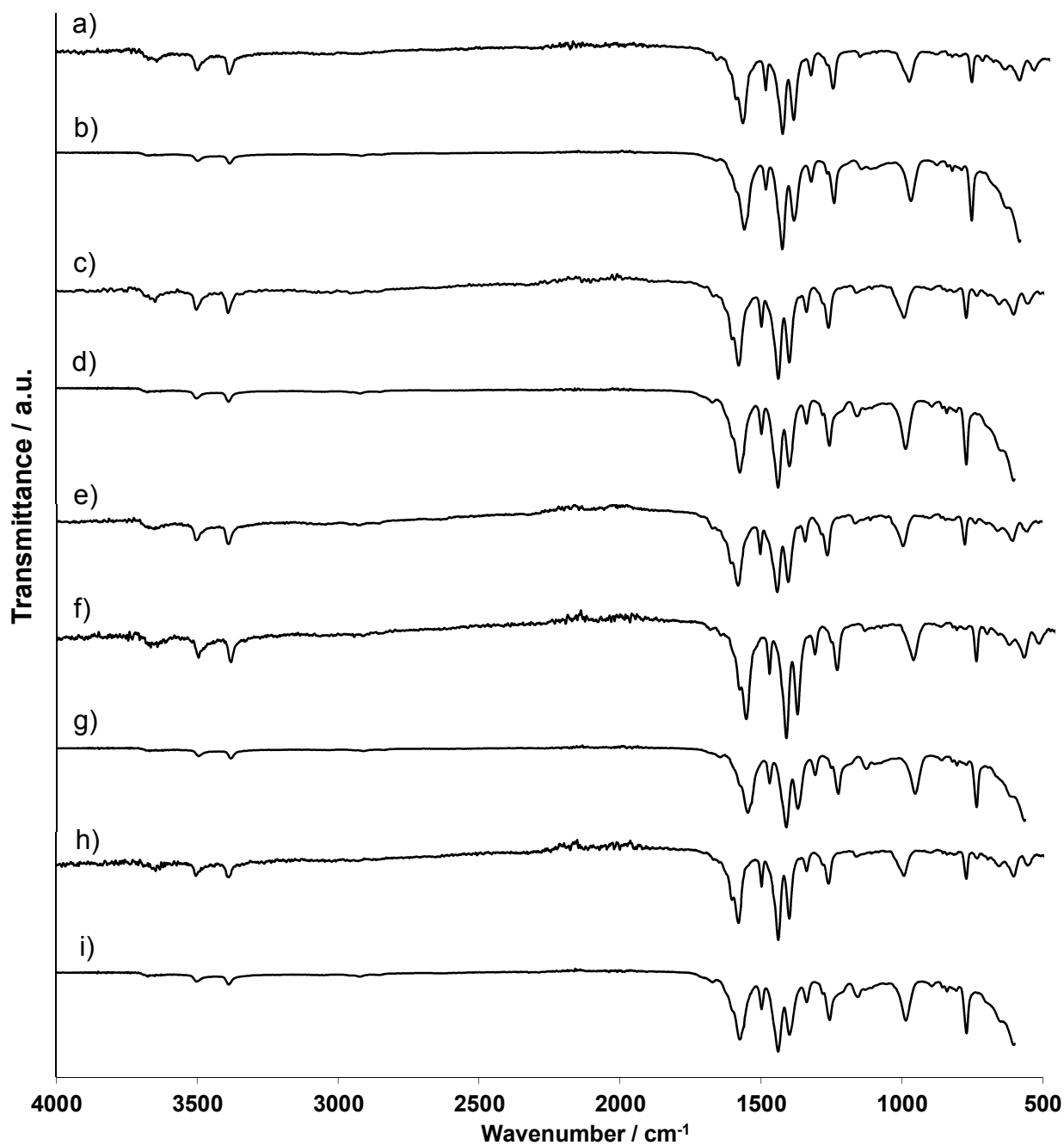
Spectrum 5: a) FcCONH-MIL-53(Al)-1h-as, b) FcCONH-MIL-53(Al)-1h-vac, c) FcCONH-MIL-53(Al)-5h-as, d) FcCONH-MIL-53(Al)-5h-vac, e) FcCONH-MIL-53(Al)-16h-as, f) FcCONH-MIL-53(Al)-24h-as, g) FcCONH-MIL-53(Al)-24h-vac, h) FcCONH-MIL-53(Al)-48h-as, i) FcCONH-MIL-53(Al)-48h-vac.
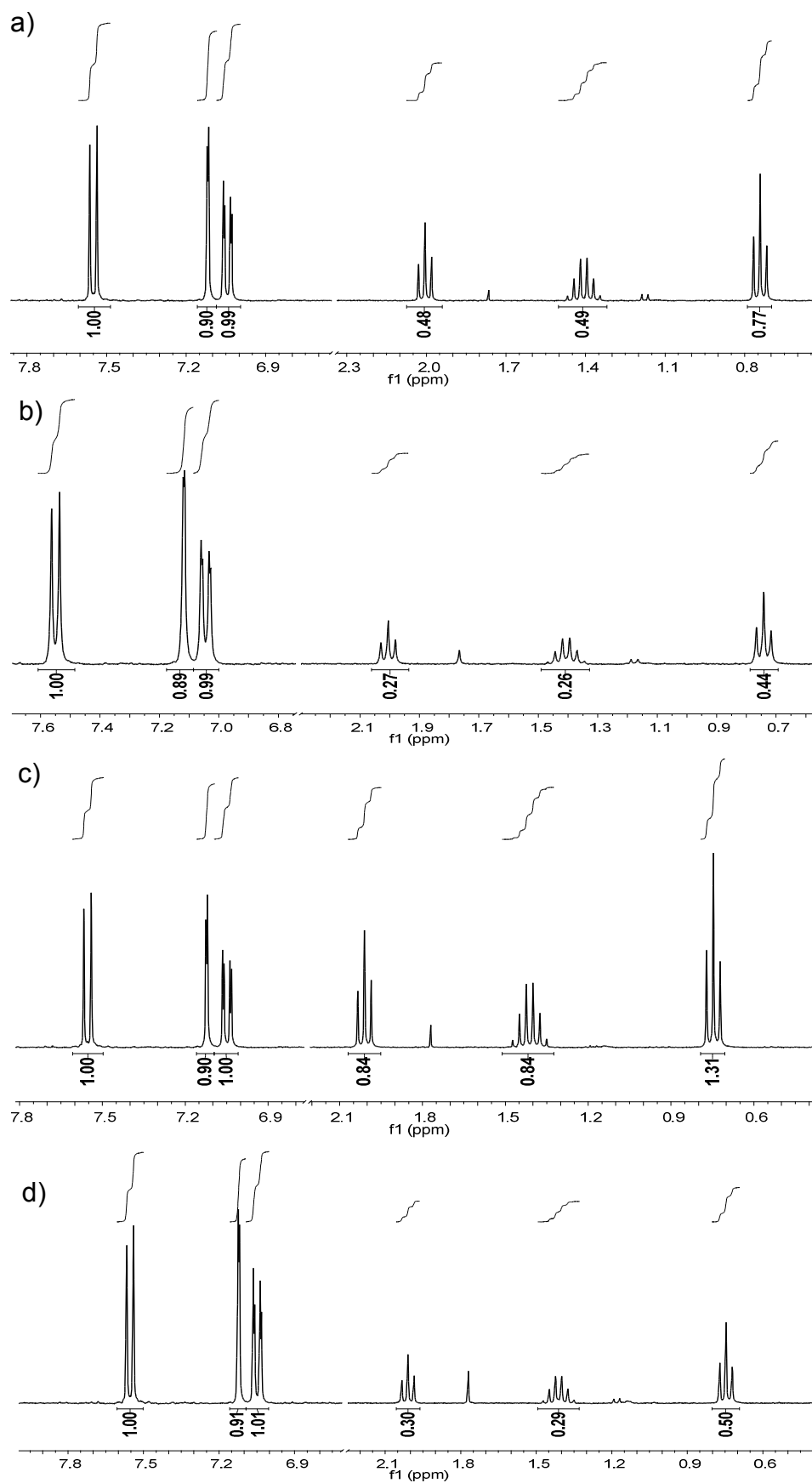
# Nuclear Magnetic Resonance Spectroscopy (NMR)

Spectrum 6: ^{1}H NMR of a) MIL-53(Al)-lt produced with method 1, b) MIL-53(Al)-lt produced with method 2, c) commercial MIL-53(Al)-lt and d) amino-MIL-53(Al)-lt produced with method 1.
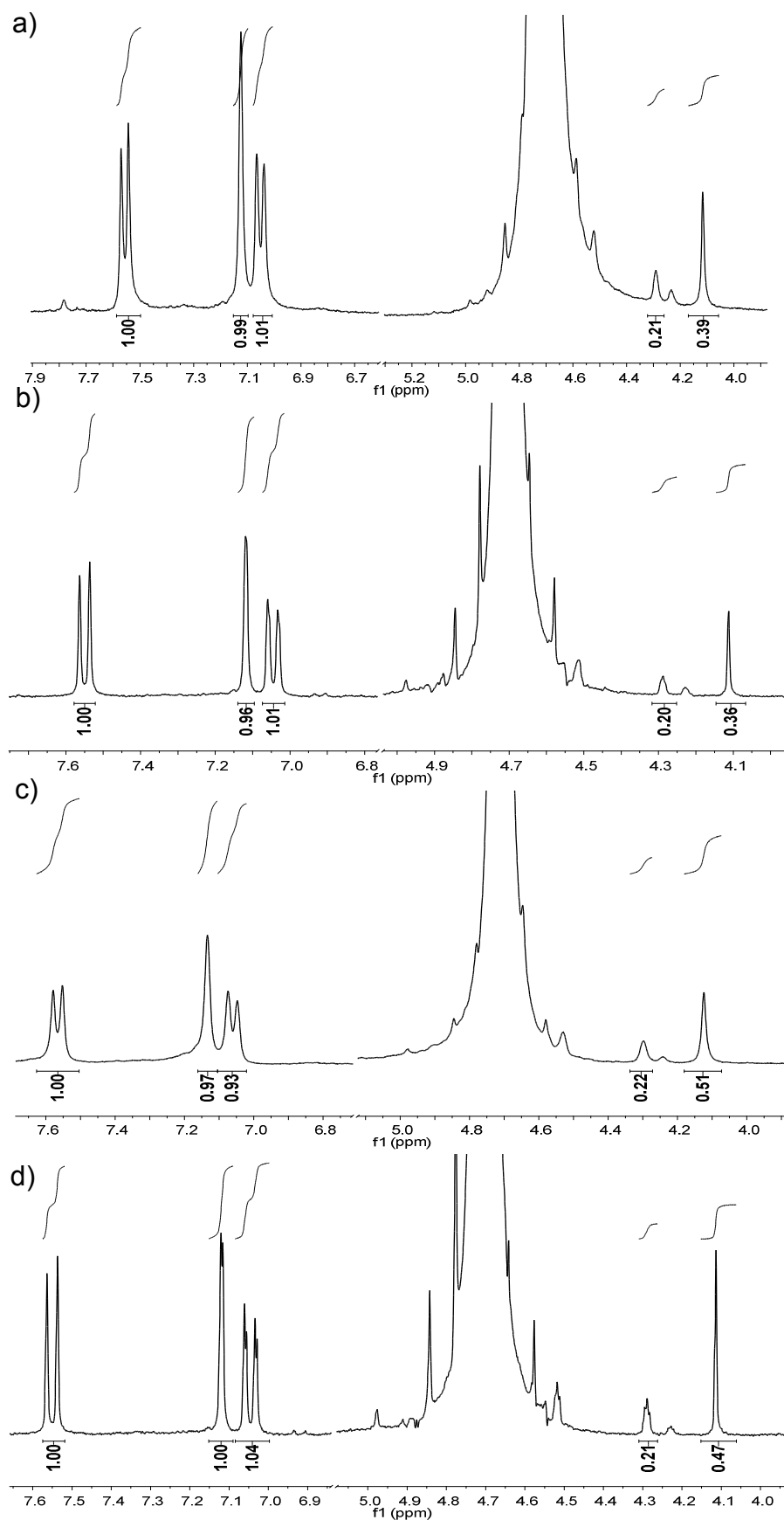
a)

b)
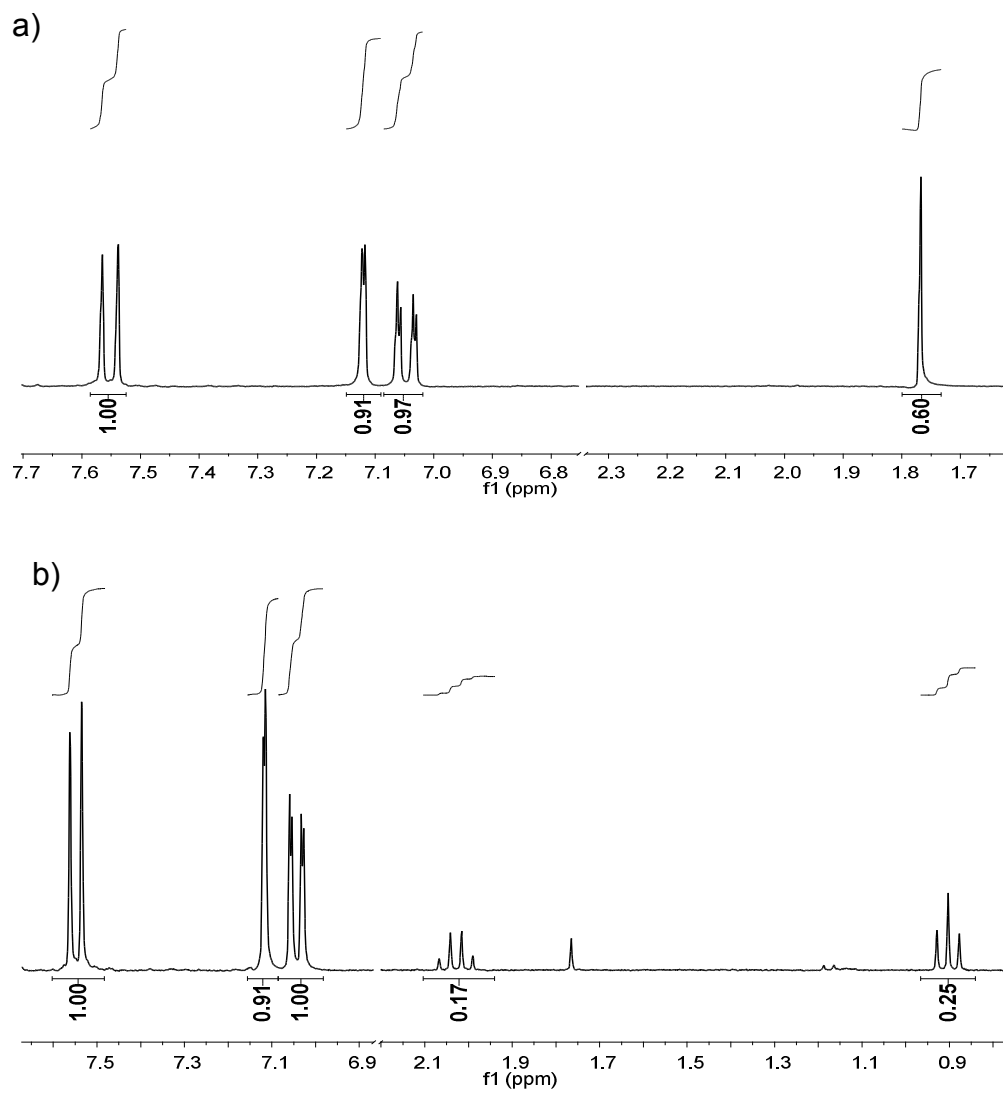
Spectrum 7: ^{1}H NMR of a) CH$_3$CONH-MIL-53(Al)-as and b) CH$_3$CH$_2$CONH-MIL-53(Al)-as.

Spectrum 8: ^{1}H NMR of a) CH$_3$(CH$_2$)$_2$CONH-MIL-53(Al)-1h-as, b) CH$_3$(CH$_2$)$_2$CONH-MIL-53(Al)-1h-vac, c) CH$_3$(CH$_2$)$_2$CONH-MIL-53(Al)-5h-as and d) CH$_3$(CH$_2$)$_2$CONH-MIL-53(Al)-5h-vac.

a)

b)

c)

d)
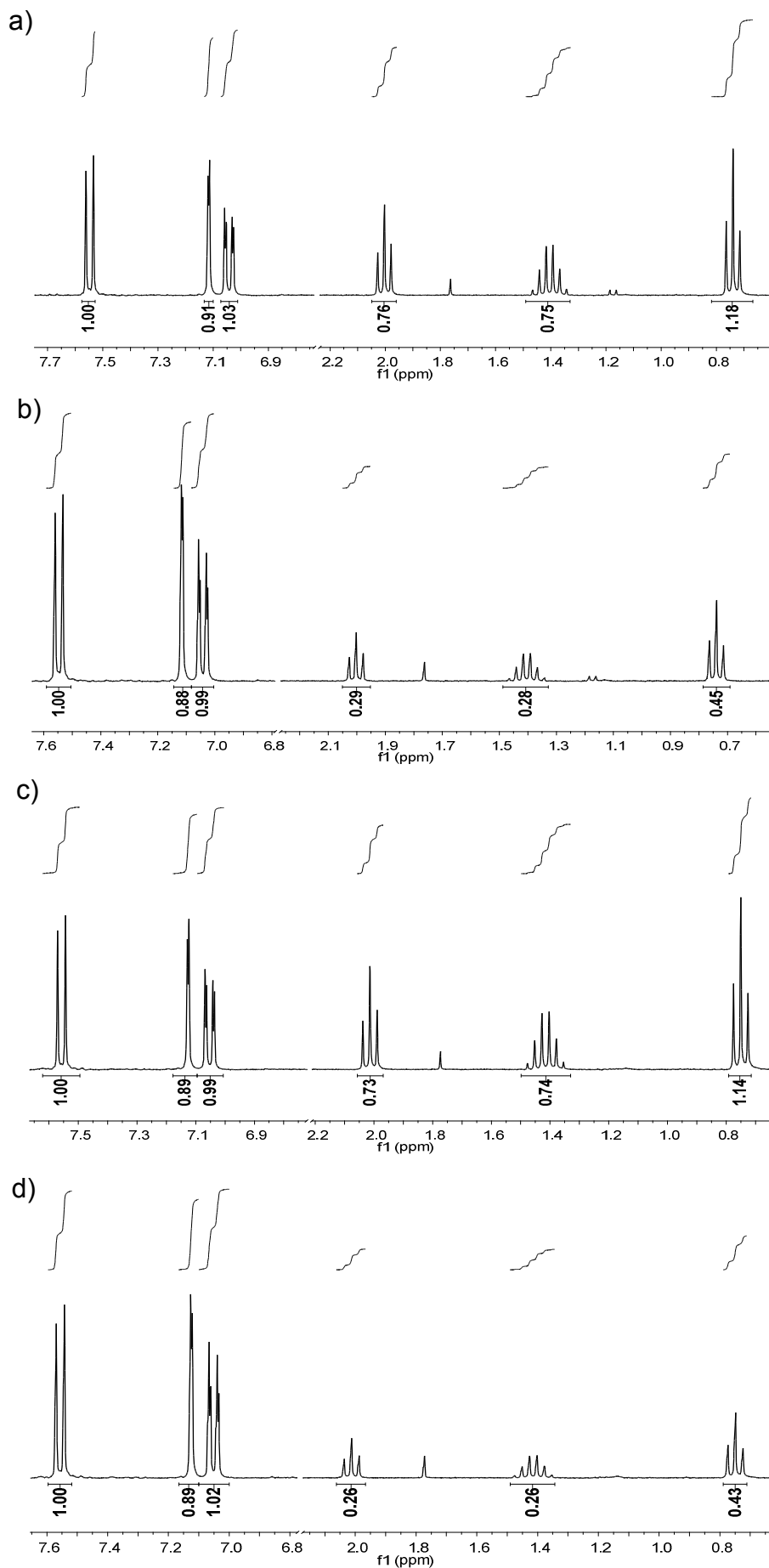
Spectrum 9: ^{1}H NMR of a) CH$_3$(CH$_2$)$_2$CONH-MIL-53(Al)-24h-as, b) CH$_3$(CH$_2$)$_2$CONH-MIL-53(Al)-24h-vac, c) CH$_3$(CH$_2$)$_2$CONH-MIL-53(Al)-48h-as and d) CH$_3$(CH$_2$)$_2$CONH-MIL-53(Al)-48h-vac.

a)

b)

c)

d)

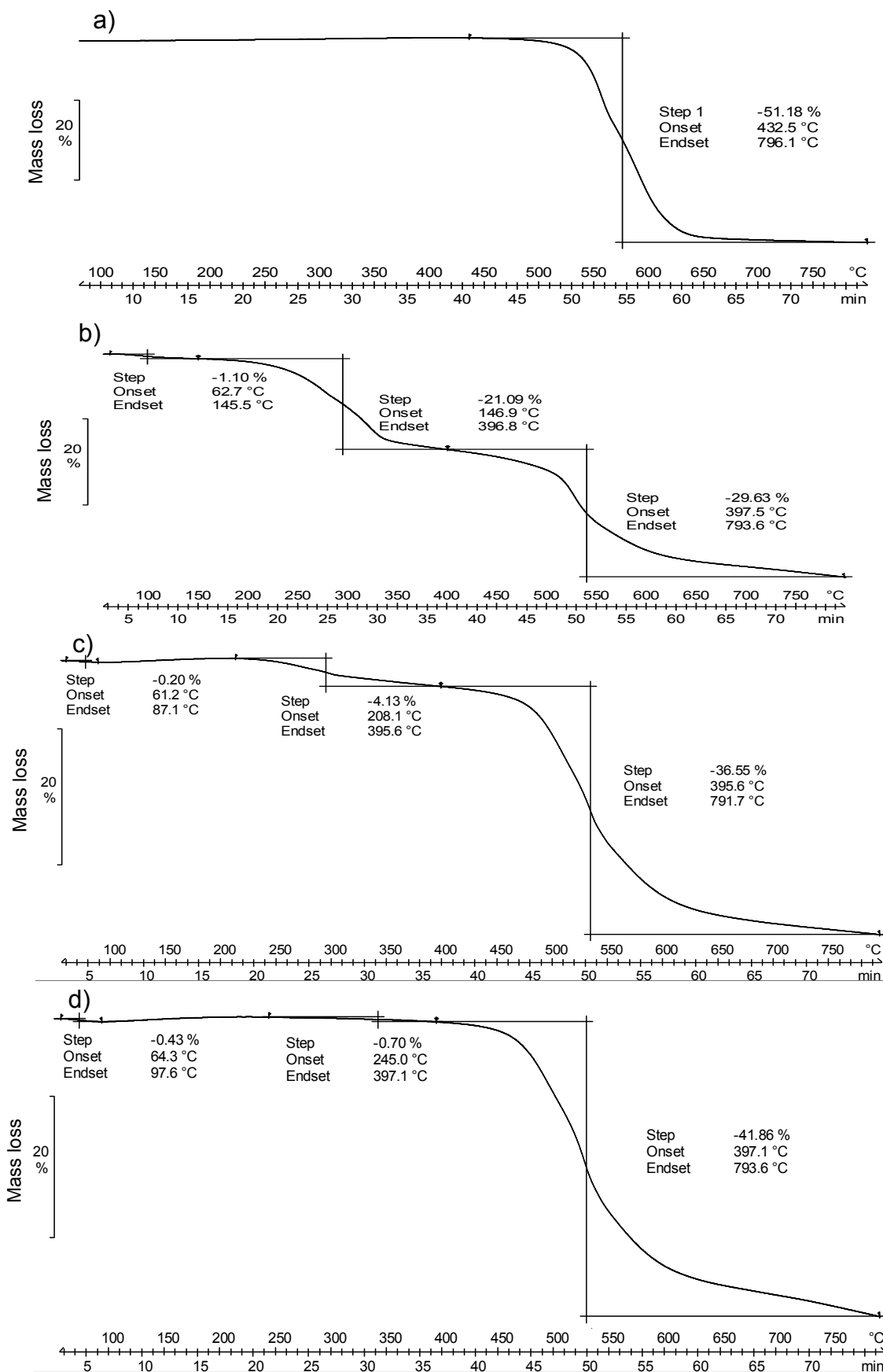**Spectrum 10: ^{1}H NMR of a) FcCONH-MIL-53(Al)-1h-as, b) FcCONH-MIL-53(Al)-1h-vac, c) FcCONH-MIL-53(Al)-5h-as and d) FcCONH-MIL-53(Al)-5h-vac.**

a)

b)

c)

d)
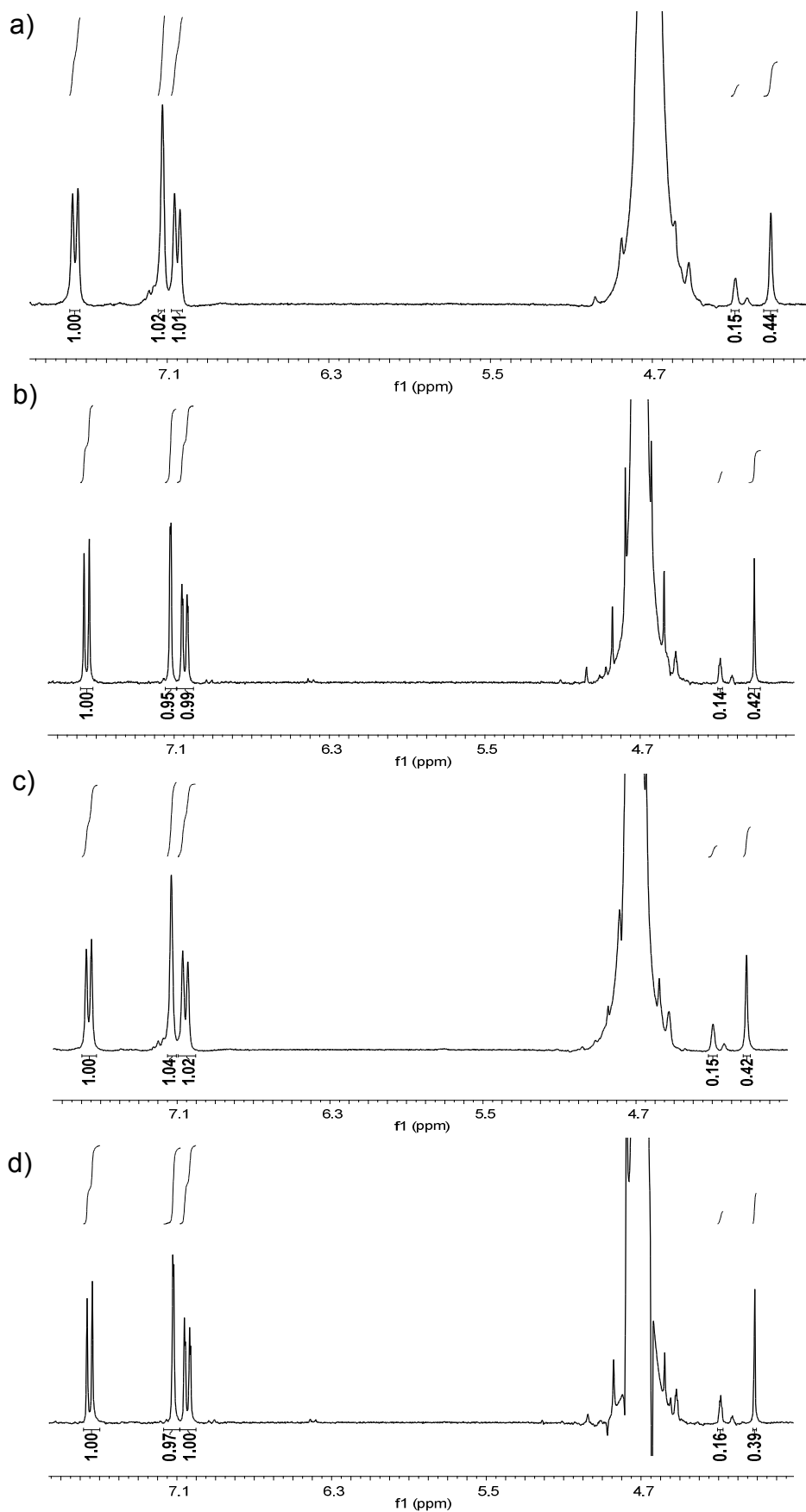
Spectrum 11: ^{1}**H NMRs of a) FcCONH-MIL-53(Al)-24h-as, b) FcCONH-MIL-53(Al)-24h-vac, c) FcCONH-MIL-53(Al)-48h-as and d) FcCONH-MIL-53(Al)-48h-vac.**

Thermogravimetric Analysis (TGA)

a)

Step 1	-51.18 %
Onset	432.5 °C
Endset	796.1 °C

b)

Step	-1.10 %
Onset	62.7 °C
Endset	145.5 °C

Step	-21.09 %
Onset	146.9 °C
Endset	396.8 °C

Step	-29.63 %
Onset	397.5 °C
Endset	793.6 °C

c)

Step	-0.20 %
Onset	61.2 °C
Endset	87.1 °C

Step	-4.13 %
Onset	208.1 °C
Endset	395.6 °C

Step	-36.55 %
Onset	395.6 °C
Endset	791.7 °C

d)

Step	-0.43 %
Onset	64.3 °C
Endset	97.6 °C

Step	-0.70 %
Onset	245.0 °C
Endset	397.1 °C

Step	-41.86 %
Onset	397.1 °C
Endset	793.6 °C

Spectrum 12: TGAs of a) commercial MIL-53(Al)-lt, b) HCONH-MIL-53(Al)-as, c) CH_3CONH-MIL-53(Al)-as and d) CH_3CH_2CONH-MIL-53(Al)-as.
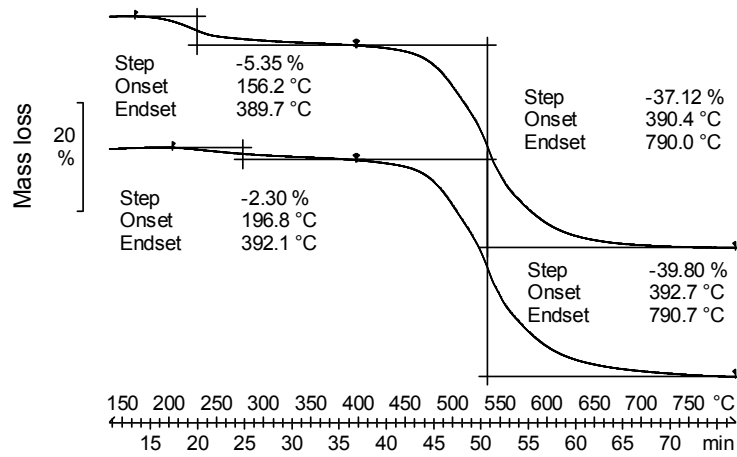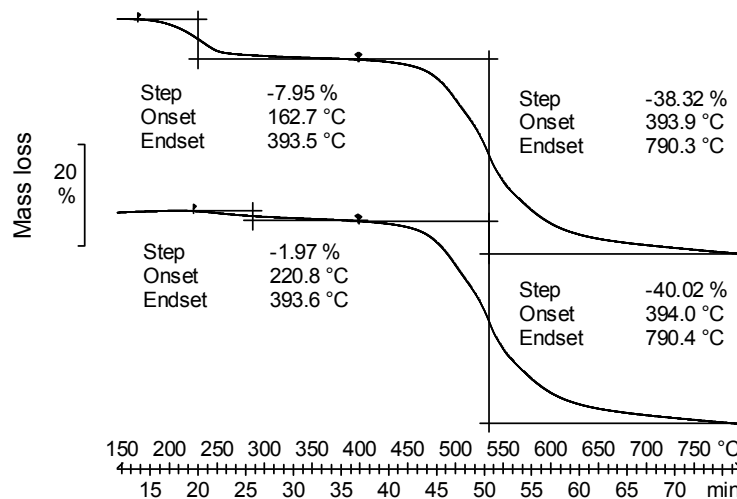
Spectrum 13: TG analysis of a) CH$_3$(CH$_2$)$_2$CONH-MIL-53(Al)-1h-as and b) CH$_3$(CH$_2$)$_2$CONH-MIL-53(Al)-1h-vac.
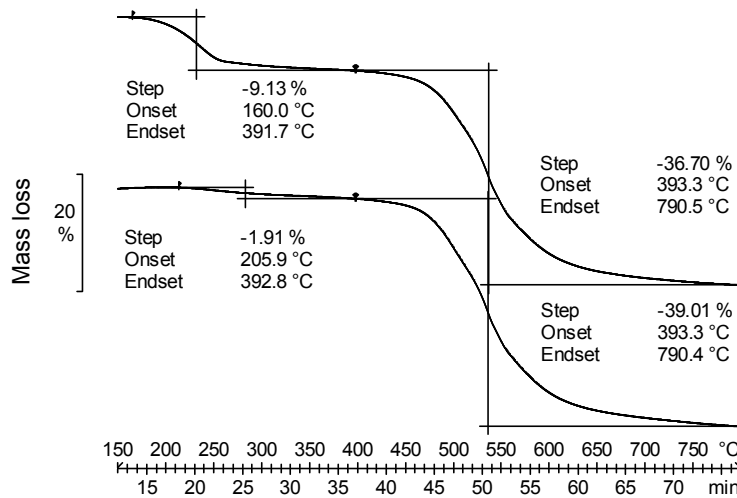
Spectrum 14: TG analysis of a) CH$_3$(CH$_2$)$_2$CONH-MIL-53(Al)-5h-as and b) CH$_3$(CH$_2$)$_2$CONH-MIL-53(Al)-5h-vac.

Spectrum 15: TG analysis of a) CH$_3$(CH$_2$)$_2$CONH-MIL-53(Al)-24h-as and b) CH$_3$(CH$_2$)$_2$CONH-MIL-53(Al)-24h-vac.

Step	-7.88 %
Onset	167.4 °C
Endset	394.1 °C

Step	-38.04 %
Onset	394.1 °C
Endset	790.7 °C

Step	-1.72 %
Onset	210.4 °C
Endset	393.5 °C

Step	-40.42 %
Onset	394.0 °C
Endset	790.2 °C
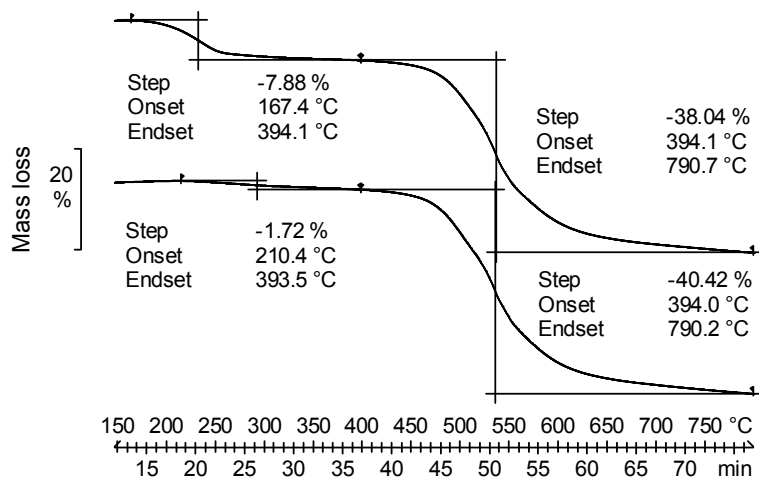
Spectrum 16: TG analysis of a) $CH_3(CH_2)_2CONH$-MIL-53(Al)-48h-as and b) $CH_3(CH_2)_2CONH$-MIL-53(Al)-48h-vac.

Step	-12.75 %
Onset	82.6 °C
Endset	394.1 °C

Step	-47.55 %
Onset	398.8 °C
Endset	793.9 °C

Step	-6.53 %
Onset	183.0 °C
Endset	395.3 °C

Step	-45.82 %
Onset	398.3 °C
Endset	794.0 °C
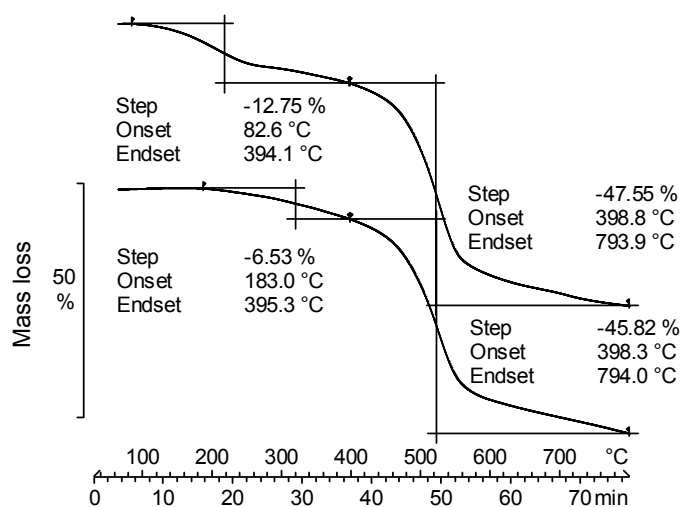
Spectrum 17: TG analysis of a) FcCONH-MIL-53(Al)-1h-as and b) FcCONH-MIL-53(Al)-1h-vac.

Step	-13.17 %
Onset	91.6 °C
Endset	397.2 °C

Step	-39.79 %
Onset	397.4 °C
Endset	794.2 °C

Step	-6.00 %
Onset	183.7 °C
Endset	398.1 °C

Step	-45.10 %
Onset	398.1 °C
Endset	795.0 °C
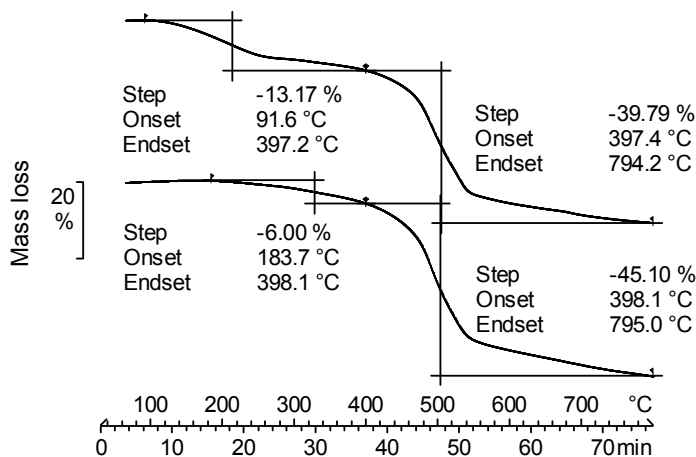
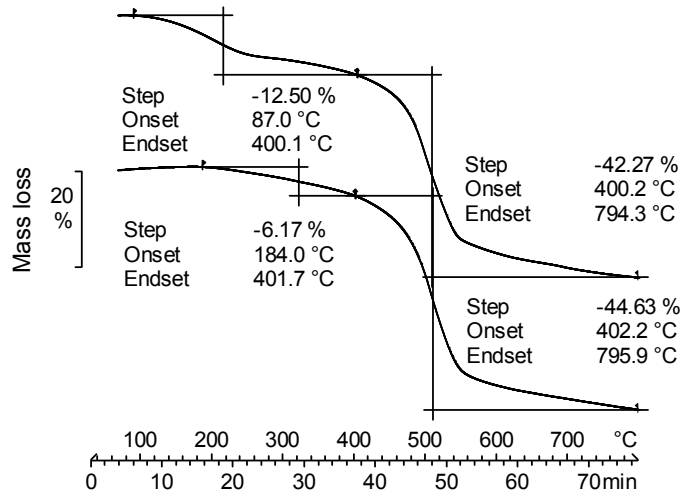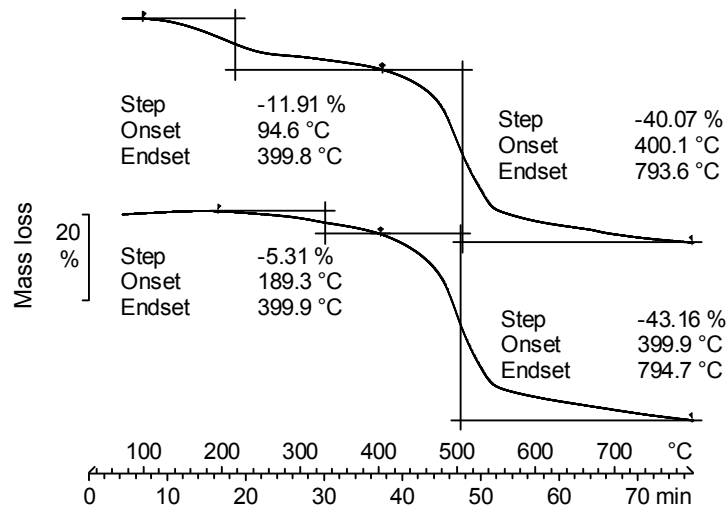**Spectrum 18:** TG analysis of a) FcCONH-MIL-53(Al)-5h-as and b) FcCONH-MIL-53(Al)-5h-vac.
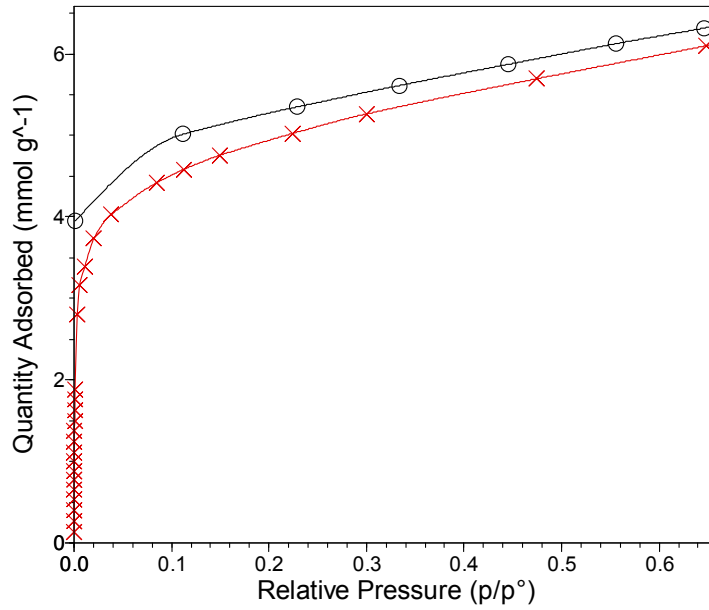
Spectrum 19: TG analysis of a) FcCONH-MIL-53(Al)-24h-as and b) FcCONH-MIL-53(Al)-24h-vac.
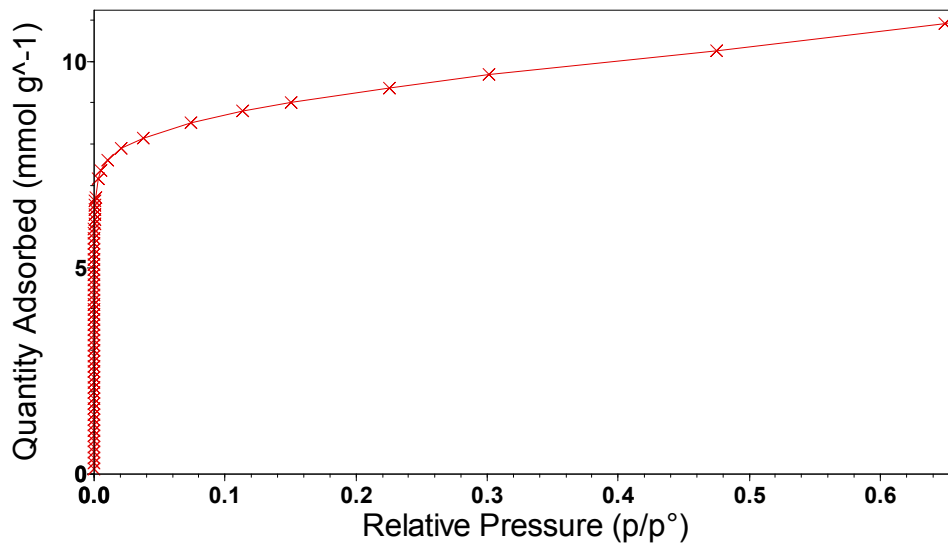

Spectrum 20: TG analysis of a) FcCONH-MIL-53(Al)-48h-as and b) FcCONH-MIL-53(Al)-48h-vac.

A-13

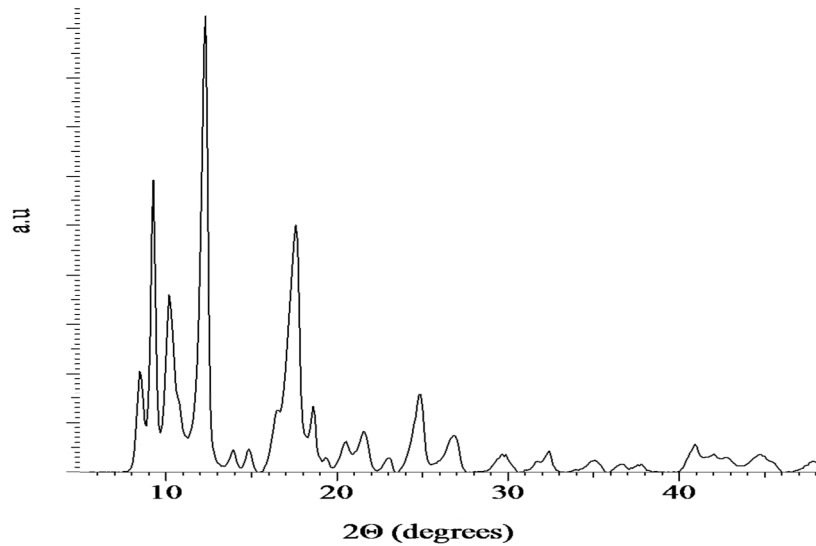# Accelerated Surface Area Porosity Measurements (ASAP)

Spectrum 21: Nitrogen adsorption (crosses) and desorption (circles) isotherms of MIL-53-lt synthesised with method 1.
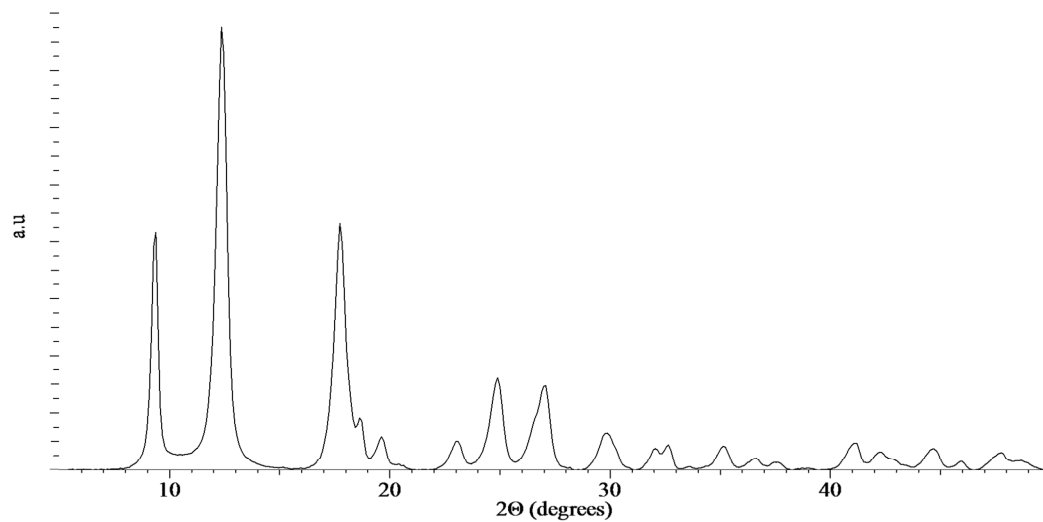

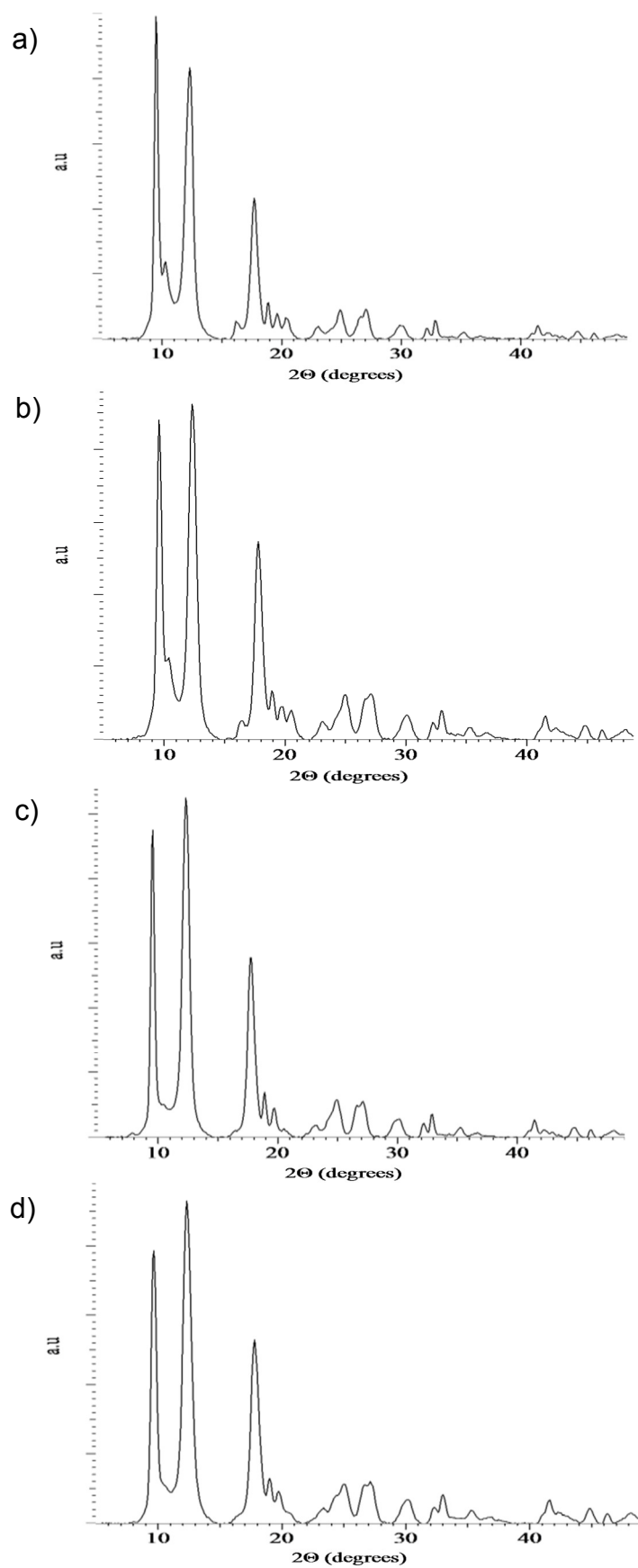**Spectrum 22: Nitrogen adsorption isotherm of commercial MIL-53-lt.**

Powder X-Ray Diffraction (PXRD)

Spectrum 23: PXRD of MIL-53(Al)-lt synthesised with method 1.

Spectrum 24: PXRD of amino-MIL-53(Al)-lt synthesised with method 1.

Spectrum 25: PXRDs of a) CH$_3$(CH$_2$)$_2$CONH-MIL-53(Al)-1h-vac, b) CH$_3$(CH$_2$)$_2$CONH-MIL-53(Al)-5h-vac, c) CH$_3$(CH$_2$)$_2$CONH-MIL-53(Al)-24h-vac and d) CH$_3$(CH$_2$)$_2$CONH-MIL-53(Al)-48h-vac.
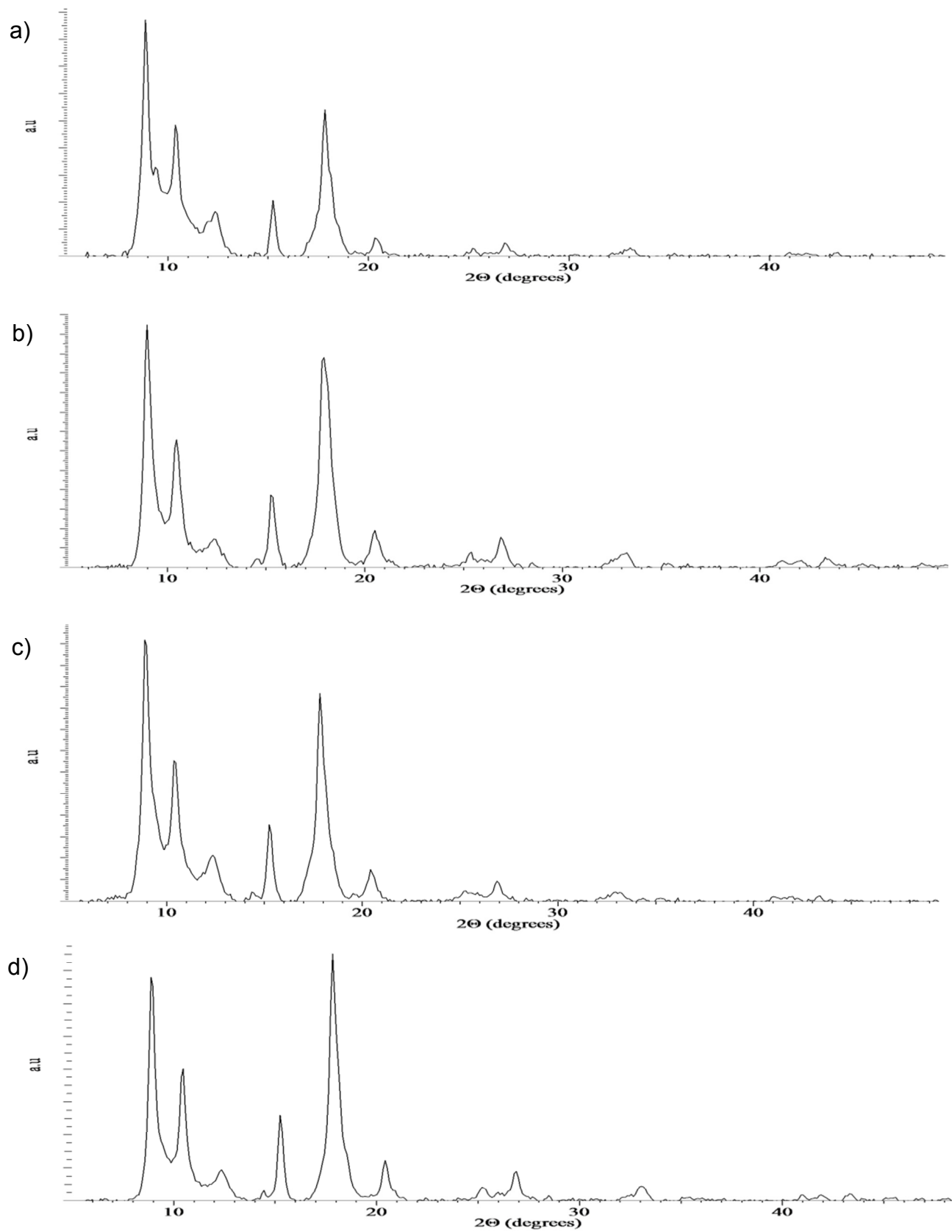
Spectrum 26: PXRDs of a) FcCONH-MIL-53(Al)-1h-vac, b) FcCONH-MIL-53(Al)-5h-vac, c) FcCONH-MIL-53(Al)-24h-as and d) FcCONH-MIL-53(Al)-48h-vac.

Abstract

The Metal Organic Framework (MOF), MIL-53(Al) and its amine functionalised analogue, amino-MIL-53(Al) were synthesized in good yields (57 - 87%) and were employed as solid, porous support systems for the intrusion of ferrocene (Fc), ferrocenecarboxylic acid (FcCOOH) and a series of carboxylic acids with increasing chain length. The intrusion of HCOOH, CH_3COOH, CH_3CH_2COOH, $CH_3(CH_2)_2COOH$ and Fc into MIL-53(Al) was done by a newly developed Incipient Wetness Impregnation (IWI) method: after evacuation of the porous MOF, the high-vacuum was maintained while covering the MOF with the impregnation solution, where after the vacuum was relieved and the solution allowed to intrude into evacuated the pores of the material under atmospheric pressure. The effectiveness of this IWI method was demonstrated by the maximum load of 0.80 HCOOH molecules per unit cell, achieved for HCOOH@MIL-53(Al). Time-resolved intrusion studies, using $CH_3(CH_2)_2COOH$ and FcCOOH, both showed that a maximum load of impregnated material was reached after 16 h of intrusion into amino-MIL-53(Al). An amidation reaction after intrusion resulted in covalent attachment of the acids to the framework structure. In the cases of $CH_3(CH_2)_2COOH$ and FcCOOH, a maximum of 20% and 12% (w.r.t. the total number of available amine groups in amino-MIL-53(Al)) respectively, were covalently bound through amide bonds to the amino-MIL-53(Al) structure, to give $CH_3(CH_2)_2CONH$-MIL-53(Al) and FcCONH-MIL-53(Al). Using a 16 h intrusion period, high loadings of ferrocene, 7.59 mass% in Fc@MIL-53(Al) and 11.02 mass% in Fc@amino-MIL-53(Al), were achieved during IWI, as determined with TGA.

A newly developed solid state Cyclic Voltammetry technique, performed on the Fc-containing framework structures, Fc@MIL-53(Al) as well as Fc@amino-MIL-53(Al) and FcCONH-MIL-53(Al) showed well defined redox couples at $E^{0'}$ = 1, -13 and -71 mV (vs. Fc/Fc^+) respectively. Chemically bound Fc (in FcCONH-MIL-53(Al)) is thus easier to oxidise than free Fc in the channels of the framework structure. Electrochemical reversibility was found in the cases of Fc@amino-MIL-53(Al) and FcCONH-MIL-53(Al), with ΔE_p = 57 and 21 mV respectively, whereas Fc@MIL-53(Al) (ΔE_p = 77 mV) showed quasi-reversibility. All three compounds showed limited chemical reversibility ($0.6 \leq i_{pc}/i_{pa} \leq 0.7$), due to ionic material leaving the analyte during measurement.

Keywords: Metal organic frameworks, amine functionality, incipient wetness impregnation, time-resolved intrusion, carboxylic acids, amidation reaction, solid state cyclic voltammetry.

Opsomming

Die Metaal Organiese Netwerk (MOF), MIL-53(Al) en sy amiengefunksionaliseerde analoog, amino-MIL-53(Al), is met goeie opbrengste (57 - 87%) gesintetiseer en is gebruik as vaste, poreuse draersisteme vir die intrusie van ferroseen (Fc), ferroseenkarboksielsuur (FcCOOH) en 'n reeks karboksielsure met toenemende kettinglengte. Die intrusie van HCOOH, CH$_3$COOH, CH$_3$CH$_2$COOH, CH$_3$(CH$_2$)$_2$COOH en Fc in MIL-53(Al) is met 'n nuutontwikkelde vloeistofimpregneringsmetode (Incipient Wetness Impregnation, IWI) gedoen: na evakuering van die poreuse MOF is die sterk vakuum behou, terwyl die MOF bedek is met die impregneringsoplossing, waarna die vakuum verlig is, en die oplossing toegelaat is om die geëvakueerde porieë van die materiaal binne te dring onder atmosferiese druk. Die doeltreffendheid van dié IWI metode is getoon deur die maksimum lading van 0.8 HCOOH molekule per eenheidsel wat vir HCOOH@MIL-53(Al) behaal is. Tydsveranderlike intrusiestudies, met CH$_3$(CH$_2$)$_2$COOH en FcCOOH, het beide getoon dat 'n maksimum lading geïmpregneerde materiaal bereik word na 'n 16 h intrusie van amino-MIL-53(Al). 'n Amidasiereaksie na intrusie, het kovalente binding van die sure aan die netwerkstruktuur tot gevolg gehad. In die geval van CH$_3$(CH$_2$)$_2$COOH en FcCOOH, is 'n maksimum van 20% en 12% (t.o.v. die totale aantal beskikbare amiengroepe in amino-MIL-53(Al)) onderskeidelik, kovalent deur amiedbindings aan die amino-MIL-53(Al) struktuur gebind, om CH$_3$(CH$_2$)$_2$CONH-MIL-53(Al) en FcCONH-MIL-53(Al) te gee. Met 'n 16 h intrusietydperk is hoë ladings van ferroseen, 7.59 massa% in Fc@MIL-53(Al) en 11.02 massa% in Fc@amino-MIL-53(Al), behaal tydens IWI, soos bepaal met TGA.

'n Nuutontwikkelde vastetoestand Sikliese Voltammetrietegniek, toegepas op die Fc-bevattende netwerkstrukture, Fc@MIL-53(Al) sowel as Fc@amino-MIL-53(Al) en FcCONH-MIL-53(Al), het duidelike redokskoppels by E$^{0\prime}$ = 1, -13 en -71 mV (*vs.* Fc/Fc$^+$) onderskeidelik getoon. Chemies gebonde Fc (in FcCONH-MIL-53(Al)) is dus makliker oksideerbaar as vry Fc in die kanale van die netwerkstruktuur. Elektrochemiese omkeerbaarheid is bepaal in die geval van Fc@amino-MIL-53(Al) en FcCONH-MIL-53(Al), met ΔE_p = 57 en 21 mV onderskeidelik, terwyl Fc@MIL-53(Al) (ΔE_p = 77 mV) kwasi-omkeerbaarheid getoon het. Al drie verbindings het beperkte chemiese omkeerbaarheid (0.6 ≤ i_{pc}/i_{pa} ≤ 0.7) getoon, weens ioniese materiaal wat die analiet tydens meting verlaat het.

Sleutelwoorde: Metaal organiese raamwerke, amienfunksionaliteit, vloeistofimpregnering, tydsveranderlike intrusie, karboksielsure, amidasiereaksie, vastetoestand sikliese voltammetrie.

I, Frederick Hermanus Peens declare that the dissertation hereby submitted by me for the degree, Magister Scientiae at the University of the Free State is my own independent work and has not previously been submitted by me at another university/faculty. I further more cede copyright of the dissertation in favour of the University of the Free State.

Signed:..   Date:..

2014/05/30